ISSN 2096-7071 (Print)
ISSN 2096-3101 (Online)
CN 10-1629/R1

CHINA CDC WEEKLY

Vol. 7 No. 46 Nov. 14, 2025

中国疾病预防控制中心周报

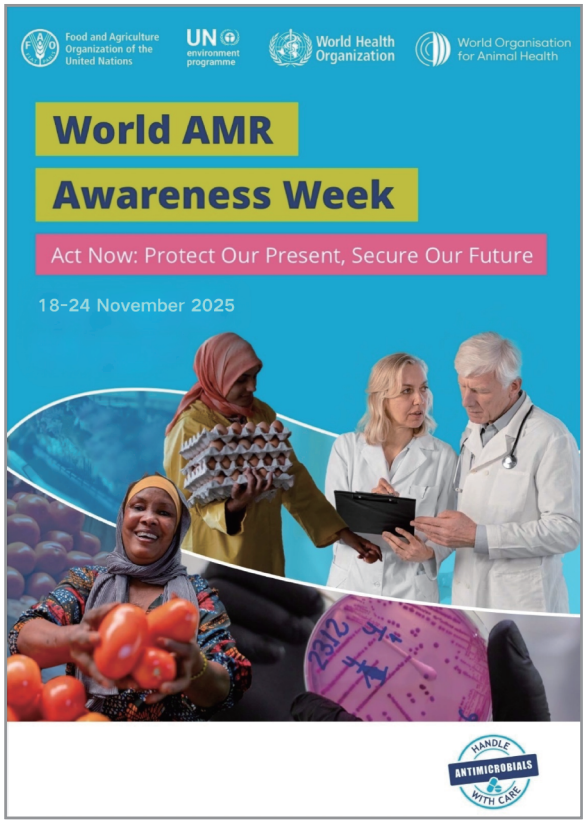

WORLD ANTIBIOTIC AWARENESS WEEK ISSUE

Foreword

World Antimicrobial Awareness Week 2025 — Act Now: Protect Our Present, Secure Our Future 1429

Vital Surveillances

Comparative Analysis of Antibiotic Resistance and Genomic Characteristics of *Enterococcus faecium* and *Enterococcus lactis* Along the Food Chain — 5 PLADs, China, 2015–2024 1434

Antibiotic Susceptibility of *Nocardia* Clinical Isolates Collected from Chinese Patients — China, 2014–2024 1441

Characteristics and Influencing Factors of Antimicrobial Resistance in *Salmonella* Isolated from Asymptomatic Workers — Yulin City, Guangxi Zhuang Autonomous Region, China, 2013–2024 1449

Preplanned Studies

High Prevalence and Genomic Characterization of Extended-Spectrum β-Lactamase-Producing *Escherichia coli* in the Yellow River and Source Water from A One Health Perspective — Henan Province, China, 2023–2024 1457

Genomic Surveillance of *Salmonella* London and Rissen Reveals International Transmission Patterns and Expanding Antimicrobial Resistance — Shanghai Municipality, China, 2020–2024 1465

ISSN 2096-7071

Cover Image: adapted from the World Health Organization, https://www.who.int/publications/m/item/world-amr-awareness-week-2025---campaign-guide.
This week's issue was organized by Guest Editor Yongning Wu.

Foreword

World Antimicrobial Awareness Week 2025 — Act Now: Protect Our Present, Secure Our Future

Zhemin Zhou[1]; Di Wu[2,#]; Yongning Wu[3,#]

Antimicrobial resistance (AMR) threatens to reverse a century of medical progress, representing a silent pandemic in the 21st century driven by the relentless evolution of bacteria against antimicrobials and the looming prospect of a post-antibiotic era. This existential threat directly challenges human health, environmental integrity, food security, and economic stability worldwide (*1*). To address this crisis, the One Health Quadripartite Joint Plan of Action (2022–2026) was launched to combat health threats across humans, animals, plants, and the environment. The plan focuses on strengthening health system capacities, addressing emerging and re-emerging zoonotic epidemics, endemic zoonotic diseases, neglected tropical and vector-borne diseases, food safety risks, antimicrobial resistance, and environmental health. The Quadripartite organizations — the Food and Agriculture Organization of the United Nations (FAO), the United Nations Environment Programme (UNEP), the World Health Organization (WHO), and the World Organisation for Animal Health (WOAH, founded as OIE) — have announced "Act Now: Protect Our Present, Secure Our Future" as the theme for World Antimicrobial Awareness Week (WAAW) 2025 (*2*).

BACKGROUND

As *Science* magazine highlighted in its 125th-anniversary issue, overcoming antibiotic resistance remains one of the most pressing scientific challenges of our time (*3*). China has mounted a comprehensive national response to address this challenge. Building on the success of the National Action Plan to Contain Bacterial Resistance (2016–2020) and guided by the Biosecurity Law, China escalated its policy framework through the "National Action Plan to Contain Antimicrobial Resistance (2022–2025)" (*4*). Jointly issued by 13 ministries, this pivotal document marks a strategic expansion from "bacterial" to "microbial" resistance, representing a concerted national effort to strengthen governance across all sectors affected by AMR. Through implementing this expanded plan and generating evidence spanning the One Health spectrum — from clinical settings to environmental reservoirs — China demonstrates its commitment to combating this pervasive global threat.

China has launched several major AMR research initiatives under the National Research and Development Programme during the 14th Five-year Plan period. These include research on the evolution and transmission mechanisms of multidrug resistance (MDR) in the human-animal-environment system (2024YFE0106300 and UK Research and Innovation MR/Y015223/1), multidrug-resistant foodborne pathogen tracing and resistance gene transmission warning (2022YFC2303900), and livestock pathogen drug resistance generation and transmission mechanisms (2022YFD1800400). Selection for AMR occurs across One Health microbiomes; however, the relative contribution of selection in each compartment to the emergence of AMR in human pathogens, and the transmission dynamics between ecosystem compartments, remain poorly understood. One promising approach involves developing and applying machine learning methods to investigate the relationship between resistance gene carriage and MDR phenotypes in microbiomes and pangenomes.

This issue integrates five Chinese studies to present a comprehensive view of the AMR crisis across its critical domains (Figure 1). The clinical domain reveals narrowing therapeutic options for pathogens such as *Nocardia*, highlighting neglected reservoirs of resistance. Environmental pathways — exemplified by the Yellow River — silently disseminate key resistance genes (e.g., $bla_{\text{CTX-M}}$) from agricultural sources to waterways. The food chain functions as an amplifier, where species like *Enterococcus faecium* pose escalating public health risks. Community reservoirs, illuminated through surveillance of asymptomatic food workers, demonstrate rising MDR *Salmonella* and tigecycline resistance in parallel with socioeconomic development. Finally, global trade networks serve as powerful

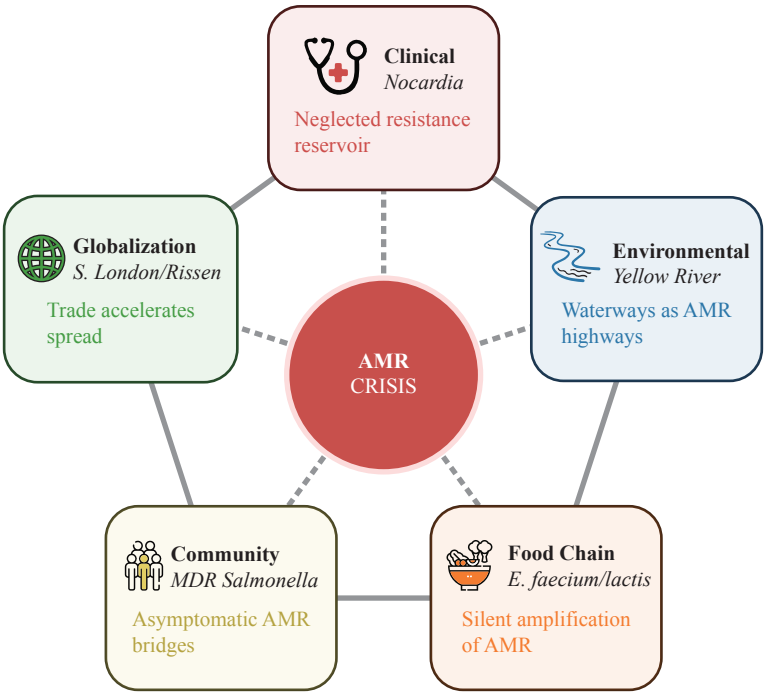

FIGURE 1. The AMR crisis intensifies across interconnected systems. Each frontline simultaneously generates and amplifies resistance, establishing a self-reinforcing cycle that necessitates coordinated, multisectoral intervention across all five domains.
Abbreviation: AMR=antimicrobial resistance; MDR=multidrug resistance.

accelerators, disseminating pathogens such as *Salmonella* London worldwide on plasmids carrying multiple antimicrobial resistance genes.

Evidence synthesized from clinical, environmental, food chain, community, and global surveillance within China's policy framework converges on an inescapable conclusion: AMR represents a metastasizing emergency that compounds in severity across interconnected biological and social systems. This body of evidence establishes a scientific imperative for the decisive action championed by the WAAW 2025 theme, "Act Now: Protect Our Present, Secure Our Future." These findings align with China's strategic commitments under its National Action Plan, demanding an urgent transition from awareness-building to accountable, coordinated multisectoral intervention.

THE EXPANDING AMR CHALLENGE: EVIDENCE FROM FRONTLINES

Clinical Frontline: Neglected Reservoirs of Resistance

Analysis of *Nocardia* clinical isolates collected between 2014 and 2024 demonstrates that this environmental commensal has emerged as a significant AMR reservoir. Although linezolid and amikacin maintain therapeutic efficacy, the pathogen exhibits adaptive capacity by developing resistance to first-line trimethoprim-sulfamethoxazole while harboring established resistance to multiple additional antimicrobial agents. *Nocardia* species now function as repositories of diverse resistance mechanisms, continuously accumulating and diversifying resistance determinants. These findings emphasize the critical need for ongoing antimicrobial susceptibility surveillance and enhanced stewardship programs to prevent the amplification and transmission of resistance across interconnected biological systems.

Environmental Frontline: Waterways as AMR Transmission Highways

Surveillance of the Yellow River system (2023–2024) reveals aquatic environments functioning as natural reservoirs and transmission pathways for AMR. Clinically significant $bla_{\text{CTX-M}}$ genes demonstrated widespread

presence with markedly higher abundance during dry seasons. Genomic analysis identified *Escherichia coli* ST6802 carrying $bla_{\text{CTX-M-14}}$ as the dominant strain, coexisting with numerous resistance genes and virulence factors. Phylogenetic evidence confirmed that these aquatic isolates shared close genetic relationships with strains from pig manure treatment systems, tracing the flow of animal-origin resistance into river ecosystems. These findings illuminate the silent journey of resistance genes through water networks and emphasize the need to monitor these natural pathways while intervening at contamination sources.

Food Chain Frontline: Silent AMR Amplifiers in Microbial Ecosystems

Comprehensive analysis of *Enterococcus faecium* and *E. lactis* isolates from China's food chain (2015–2024) demonstrates how microbial ecosystems serve as reservoirs that accumulate and diversify antimicrobial resistance traits. Following recent taxonomic reclassification, *E. faecium* demonstrates significantly elevated multidrug resistance rates and harbors more extensive resistance genetic elements compared to *E. lactis*, despite both species maintaining comparable virulence gene profiles. This divergence in resistance capacity alongside conserved pathogenic potential reveals a critical evolutionary pathway through which AMR propagates within food production systems. These observations underscore the necessity for sustained surveillance programs and targeted intervention strategies that incorporate both ecological dynamics and genetic adaptability to effectively limit AMR transmission through the food chain.

Community Frontline: The Asymptomatic AMR Bridge of Human Populations

Twelve-year surveillance conducted in Yulin (2013–2024) demonstrates that asymptomatic food workers serve as persistent reservoirs for AMR within community settings. This transmission pathway, though clinically silent, exhibits a pronounced evolutionary trajectory: multidrug-resistant *Salmonella* carriage increased to 41.9%, while tigecycline resistance emerged and escalated from undetectable levels to 24.4%. Notably, resistance patterns correlate strongly with regional socioeconomic development, as expanding healthcare infrastructure and economic growth inadvertently establish selective pressures that favor resistant strains. These findings reveal the complex relationship between human development and microbial adaptation, demonstrating that community environments function as dynamic sites for resistance evolution requiring integrated surveillance and intervention approaches.

Globalization Frontline: Trade Networks as Evolutionary Accelerators for AMR

Genomic investigation of *Salmonella* London and Rissen isolates collected in Shanghai (2020–2024) demonstrates how international trade networks function as evolutionary conduits that accelerate antimicrobial resistance dissemination across continents. While *S.* London displays historical segregation into geographically distinct clades reflecting limited intercontinental transmission, *S.* Rissen exhibits extensive contemporary gene flow, with Thailand identified as a primary source population. This global connectivity enables the widespread distribution of high-risk plasmids harboring up to 15 resistance genes, with Chinese isolates demonstrating the highest resistance burden among analyzed populations. These observations reveal the profound influence of modern commerce on pathogen evolution and underscore the urgent need for integrated global surveillance systems that span human health, animal agriculture, and international food trade to effectively prevent the emergence and spread of pan-drug-resistant pathogens.

CHINA'S COMPREHENSIVE AMR GOVERNANCE STRATEGY FOR A POST-ANTIBIOTIC ERA

Compelling evidence from multisectoral frontline studies aligns with China's National Action Plan to Contain Antimicrobial Resistance (2022–2025) within the One Health governance framework (Figure 2). This strategic alignment demonstrates how empirical findings from clinical, environmental, food chain, community, and global surveillance inform policy development and implementation.

China is strengthening antimicrobial efficacy through a comprehensive system of coordinated interventions. Prevention-centered approaches address infections at their source through healthcare controls, environmental sanitation, and vaccine expansion. Public education initiatives build health literacy across urban-rural populations

FIGURE 2. China's National Action Plan (2022–2025) exemplifies the translation of World Antimicrobial Awareness Week (WAAW) 2025's "Act Now" imperative into accountable, measurable interventions characterized by specific targets and sustained investment.

and schools. Antimicrobial stewardship is being implemented comprehensively across medical and agricultural sectors, effectively safeguarding last-resort antibiotics. Surveillance systems have evolved from passive data collection into proactive early-warning networks that seamlessly integrate human health, animal health, and environmental monitoring. Sustained investment in scientific innovation spans novel antimicrobials, diagnostics, and molecular epidemiology studies. International cooperation facilitates knowledge exchange and technical assistance globally. This multidimensional strategy, backed by inter-ministerial coordination and evaluation mechanisms, exemplifies translating the "Act Now" imperative into accountable, cross-sectoral interventions that safeguard health security and ensure a healthier future.

ACT NOW, SECURE OUR FUTURE TOGETHER

The World AMR Awareness Week 2025 theme, "Act Now: Protect Our Present, Secure Our Future," functions as both an urgent warning and a global call to action. Building on the momentum generated by the 2024 United Nations General Assembly High-Level Meeting on AMR, this imperative urges all stakeholders — including governments, civil society organizations, healthcare providers, veterinarians, agricultural producers, environmental advocates, and the public — to transform political commitments into tangible, accountable, life-saving interventions.

China has demonstrated its commitment through the implementation of the National Action Plan, establishing comprehensive surveillance systems and promoting the One Health approach across all sectors. These concrete measures represent significant progress in containing AMR within a complex, interconnected system. We call upon all nations to strengthen their AMR containment efforts through coordinated global action, including the sharing of best practices, alignment of policies, and fostering of multilateral cooperation. Together, we can preserve antimicrobial efficacy and create a healthier, more sustainable world for generations to come.

doi: 10.46234/ccdcw2025.240

[#] Corresponding authors: Di Wu, d.wu@qub.ac.uk; Yongning Wu, wuyongning@cfsa.net.cn.

[1] Department of Clinical Laboratory, The Second Affiliated Hospital of Soochow University, Cancer Institute, Suzhou Medical College, Soochow University, Suzhou City, Jiangsu Province, China; [2] Institute for Global Food Security, Queen's University of Belfast, Belfast, United Kingdom; [3] NHC Key Laboratory of Food Safety Risk Assessment, Chinese Academy of Medical Science Research Unit (2019RU014 Food Safety), China National Center for Food Safety Risk Assessment, Beijing, China.

Submitted: November 09, 2025
Accepted: November 10, 2025
Issued: November 14, 2025

REFERENCES

1. Naddaf M. 40 million deaths by 2050: toll of drug-resistant infections to rise by 70%. Nature 2024;633(8031):747 – 8. https://doi.org/10.1038/d41586-

024-03033-w.
2. WHO. World AMR Awareness Week 2025. 2025. https://www.who.int/campaigns/world-amr-awareness-week/2025. [2025-11-9]
3. Science/AAAS Custom Publishing Office. 125 Questions: Exploration and Discovery. 2021. https://www.science.org/doi/10.1126/resource.2499249. [2025-11-9].
4. WHO. China: Second national action plan for containing antimicrobial resistance 2022-2025. 2022. https://www.who.int/publications/m/item/china-second-amr-national-action-plan-2022-2025.[2025-11-9]

Di Wu, PhD
Newton International Fellow of Royal Society, London, UK
Institute for Global Food Security, Queen's University of Belfast, Belfast, UK
School of Biological Sciences, Queen's University of Belfast, Belfast, UK

Yongning Wu, PhD, MD
Chief Scientist and Professor, China National Center for Food Safety Risk Assessment, Beijing, China
Director of NHC Key Laboratory of Food Safety Risk Assessment and Chinese Academy of Medical Science Research Unit (2019RU014 Food Safety), Beijing, China
Member of the WHO Strategic and Technical Advisory Group for Antimicrobial Resistance (STAG-AMR 2019-2020)

Vital Surveillances

Comparative Analysis of Antibiotic Resistance and Genomic Characteristics of *Enterococcus faecium* and *Enterococcus lactis* Along the Food Chain — 5 PLADs, China, 2015–2024

Wenbin Chen[1,2,3]; Xiaoyi Zheng[3]; Hao Wu[3]; Yiwen Jing[4]; Zehong Ye[2]; Zixin Peng[1,2,#]; Shaofu Qiu[3,#]

ABSTRACT

Introduction: Foodborne antibiotic-resistant enterococci pose significant risks to One Health and clinical antimicrobial efficacy through food chain transmission. Following the taxonomic reclassification of *Enterococcus faecium* (*E. faecium*), comprehensive long-term surveillance data on antibiotic resistance (ABR) patterns and genomic characteristics of *E. faecium* and *Enterococcus lactis* (*E. lactis*) across food animals, environmental sources, and human populations remain limited.

Methods: A total of 2,233 samples were collected from multiple nodes along the food chain across 5 Chinese provincial-level administrative divisions (PLADs) during 2015–2019 and 2023–2024. *E. faecium* (87 isolates) and *E. lactis* (153 isolates) were identified through whole-genome sequencing and average nucleotide identity analysis. Antimicrobial susceptibility testing, comprehensive genomic content analysis, and pan-genome-wide association studies were performed.

Results: *E. faecium* demonstrated significantly higher resistance rates to 12 antimicrobials compared with *E. lactis* (P<0.05). Conversely, *E. lactis* exhibited a higher resistance rate to erythromycin than *E. faecium* (P<0.01). The multidrug-resistant (MDR) rate of *E. faecium* (43/87, 49.4%) substantially exceeded that of *E. lactis* (16/153, 10.5%) (P<0.001). Genomic analysis revealed that *E. faecium* harbors significantly more antibiotic resistance genes, mobile genetic elements, and plasmid replicons than *E. lactis*. No significant interspecies differences were observed in virulence gene profiles associated with adhesion, immune modulation, biofilm formation, and exotoxin production.

Conclusions: *E. faecium* presents substantially greater ABR risks than *E. lactis* within the Chinese food chain, necessitating enhanced species-specific surveillance programs. Future interventions should prioritize targeted control strategies tailored to each species to effectively mitigate One Health threats.

Foodborne antibiotic-resistant enterococci represent a critical surveillance priority within the "Human-Animal-Environment" One Health framework (*1*). *Enterococcus faecium* (*E. faecium*) exhibits a dual nature: it serves as a beneficial probiotic in fermented foods and dietary supplements while simultaneously acting as an opportunistic pathogen capable of causing antibiotic-resistant infections, including endocarditis and sepsis (*2*). In contrast, *Enterococcus lactis* (*E. lactis*) strains are generally regarded as non-pathogenic probiotic bacteria (*3*). Historically, phylogenetic analyses classified *E. faecium* into two distinct clades: Clade A, comprising clinical and animal isolates, and Clade B, consisting of strains from healthy humans (*4*). However, recent genomic studies demonstrated that Clade B isolates share >97% average nucleotide identity (ANI) with *E. lactis*, exceeding the 95% species delineation threshold and prompting their reclassification as *E. lactis* (*5*). Despite this taxonomic revision, comprehensive long-term surveillance data characterizing the antibiotic resistance (ABR) profiles and genomic features of redefined *E. faecium* and *E. lactis* populations within the Chinese food chain remain limited.

In this study, we collected samples from multiple nodes along the food chain across five provincial-level administrative divisions (PLADs) in China during 2015–2019 and 2023–2024. We conducted a comparative analysis of ABR phenotypes and genomic content between *E. faecium* and *E. lactis* isolates. This investigation aimed to elucidate the distinct ABR risks posed by these two species within the Chinese food chain and provide evidence-based data to support risk assessment and control strategies for foodborne antibiotic-resistant enterococci.

METHODS

Sample Collection and *Enterococcus* Detection and Identification

During 2015–2019, 694 samples were collected from Beijing, Henan, Hubei, and Jilin PLADs. From 2023–2024, 1,539 samples were collected from Beijing, Henan, Hubei, Jilin, and Hebei PLADs (Supplementary Table S1, available at https://weekly.chinacdc.cn/). Samples were obtained from multiple sites and sources across the food chain, including food animals, food products, environmental surfaces, and human specimens, to capture the diversity of enterococcal populations. Sample collection, *Enterococcus* detection, and identification procedures followed previously established methods (*1*).

Whole-genome Sequencing (WGS), Genome Assembly, and ANI Analysis

Whole-genome sequencing of *Enterococcus* isolates was performed using the Illumina HiSeq platform (Illumina Inc., United States). Paired-end libraries (2×150 bp) were prepared with the Nextera DNA Sample Preparation Kit (Illumina Inc., United States) according to the manufacturer's protocol. High-quality paired-end reads were processed using Shovill v1.1.0 (https://github.com/tseemann/shovill), and *de novo* genome assemblies were generated with SPAdes (version 3.15.5; Algorithmic Biology Lab, St. Petersburg, Russia), yielding contigs (*6*). ANI values were calculated for all assembled *Enterococcus* genomes using FastANI (version 1.3.3; Atlanta, USA), with a species delineation threshold of 95%(*7*).

Antimicrobial Susceptibility Testing (AST)

Antimicrobial susceptibility of *E. faecium* and *E. lactis* isolates was determined by broth microdilution and interpreted according to Clinical & Laboratory Standards Institute (CLSI) interpretive criteria. Minimum inhibitory concentrations (MICs) were determined for 13 antibacterial compounds: ampicillin and penicillin (β-lactams), erythromycin (a macrolide), enrofloxacin and ciprofloxacin (quinolones), daptomycin and vancomycin (glycopeptides), tetracycline and doxycycline (tetracyclines), chloramphenicol (a phenicol), high-level gentamicin (HLGA) and high-level streptomycin (HLSA) (aminoglycosides), and linezolid (an oxazolidinone). An isolate was classified as multidrug-resistant (MDR) if it exhibited resistance to three or more antibacterial compounds from different classes.

Bioinformatics Analysis

Antibacterial resistance genes (ARGs), virulence factor encoding genes (VFs), mobile genetic elements (MGEs), and plasmid replicons were identified using ABRicate (https://github.com/tseemann/abricate) against the following databases: the Comprehensive Antimicrobial Resistance Database for ARGs (*8*), the Virulence Factors Database for VFs (*9*), the Mobile Orthologous Groups Database for MGEs (*10*), and PlasmidFinder (*11*) for plasmid replicons. Detection thresholds of 80% minimum coverage and 80% minimum identity were uniformly applied across all analyses.

To construct the core genome single nucleotide polymorphism (SNP)-based phylogenetic tree, the following bioinformatic pipeline was employed: Snippy v4.6.0 (https://github.com/tseemann/snippy) was used for core genome alignment and variant calling. Core genome alignment was reconstructed using Gubbins (version 2.4.1; Hinxton, UK) (*12*). A maximum likelihood phylogenetic tree was then inferred from non-repetitive core SNPs using FastTree (version 2.1.11; Berkeley, USA) with the GTR+CAT substitution model (*13*).

Roary (version 3.6.1; Exeter, UK) (*14*) was used to identify core genes and pan-genes. Pan-genome-wide association study (Pan-GWAS) was performed using Scoary (version 1.6.16; Oslo, Norway) (*15*). Species-specific genes were defined as those present in more than 80% of isolates from one species but absent in the other species. Clusters of Orthologous Groups (COG) classification of significantly associated genes was performed by mapping to the COG function database using BLAST.

Statistical Analysis

Statistical analyses were conducted using SPSS Statistics for Windows, version 17.0 (SPSS Inc., Chicago, IL, USA). Categorical variables were compared using Pearson's chi-squared test and Fisher's exact test. Correlation analyses between dichotomous categorical variables were performed using the Phi coefficient. Statistical significance was defined as $P<0.05$.

RESULTS

Prevalence of *E. faecium* and *E. lactis* in Food Chain

As shown in Supplementary Table S2 (available at https://weekly.chinacdc.cn/), *E. lactis* exhibited a

significantly higher prevalence rate (6.9%, 153/2,233) in the food chain compared to *E. faecium* (3.9%, 87/2,233) (P<0.001). Additionally, *E. lactis* demonstrated significantly higher prevalence rates than *E. faecium* in both food and livestock samples (P<0.05). This pattern was particularly pronounced during 2023–2024, when *E. lactis* prevalence significantly exceeded that of *E. faecium* (P<0.001). Temporal analysis revealed that neither species exhibited significant changes in prevalence rates when comparing the 2015–2019 period to the 2023–2024 period (P>0.05).

ABR and ARGs of *E. faecium* and *E. lactis*

E. faecium isolates demonstrated significantly higher resistance rates to 12 antimicrobials compared with *E. lactis* (P<0.05) (Figure 1). In contrast, *E. lactis* exhibited a significantly higher resistance rate to erythromycin than *E. faecium* (P<0.01). Specifically, *E. faecium* showed elevated resistance to erythromycin (58/87, 66.7%), tetracycline (51/87, 58.6%), and enrofloxacin (48/87, 55.2%), while displaying minimal resistance to daptomycin (3/87, 3.4%), vancomycin (6/87, 6.9%), and linezolid (6/87, 6.9%). *E. lactis* exhibited the highest resistance rates to erythromycin (127/153, 83.0%), tetracycline (29/153, 19.0%), and ciprofloxacin (18/153, 11.8%), but demonstrated negligible resistance to vancomycin (0%), daptomycin (1/153, 0.7%), and ampicillin (1/153, 0.7%). The MDR rate of *E. faecium* (43/87, 49.4%) significantly exceeded that of *E. lactis* (16/153, 10.5%) (P<0.001). Among MDR *E. faecium* isolates, the largest proportion originated from hospital patients (19/43, 44.2%), whereas among MDR *E. lactis* isolates, the largest proportion was food-derived (7/16, 43.8%). The most common resistance profile in *E. faecium* was ciprofloxacin-enrofloxacin co-resistance (5/87, 5.7%), while *E. lactis* most frequently exhibited tetracycline-erythromycin co-resistance (10/153, 6.5%).

A total of 20 distinct ARG types belonging to 8 functional categories were detected across *E. faecium* and *E. lactis* genomes (Figure 2A). *E. faecium* carried significantly more ARGs than *E. lactis* (P<0.001). Furthermore, the *tetM*, *tetL*, *ermB*, and *fexA* genes in *E. faecium* showed significant associations with resistance phenotypes to their corresponding antimicrobials (tetracycline, erythromycin, and chloramphenicol) (Figure 2B). Notably, the macrolide resistance gene *ermT* in *E. faecium* demonstrated a significant association with resistance phenotypes to the two β-lactam antibacterials (ampicillin and penicillin). In *E. lactis*, the tetracycline resistance genes (*tetL* and *tetM*) exhibited significant correlations with resistance to both tetracycline antibacterials tested (doxycycline and tetracycline) (Figure 2C).

Genomic content of *E. faecium* and *E. lactis*

Core genome-based SNP phylogenetic analysis demonstrated distinct separation between *E. faecium*

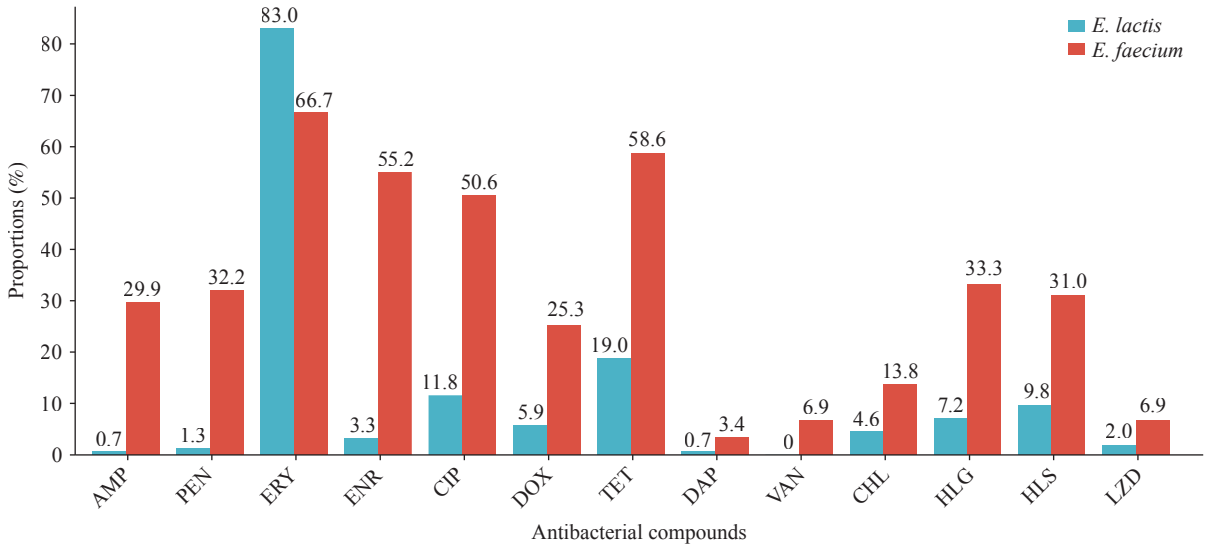

FIGURE 1. Enterococcal resistance profiles against a panel of 13 antibacterial compounds.
Abbreviation: AMP=ampicillin; PEN=penicillin; ERY=erythromycin; ENR=enrofloxacin; CIP=ciprofloxacin; DOX=doxycycline; TET=tetracycline; DAP=daptomycin; VAN=vancomycin; CHL=chloramphenicol; HLGA=high-level gentamicin; HLSA=high-level streptomycin; LZD=linezolid; *E. faecium=Enterococcus faecium*; *E. lactis=Enterococcus lactis*.

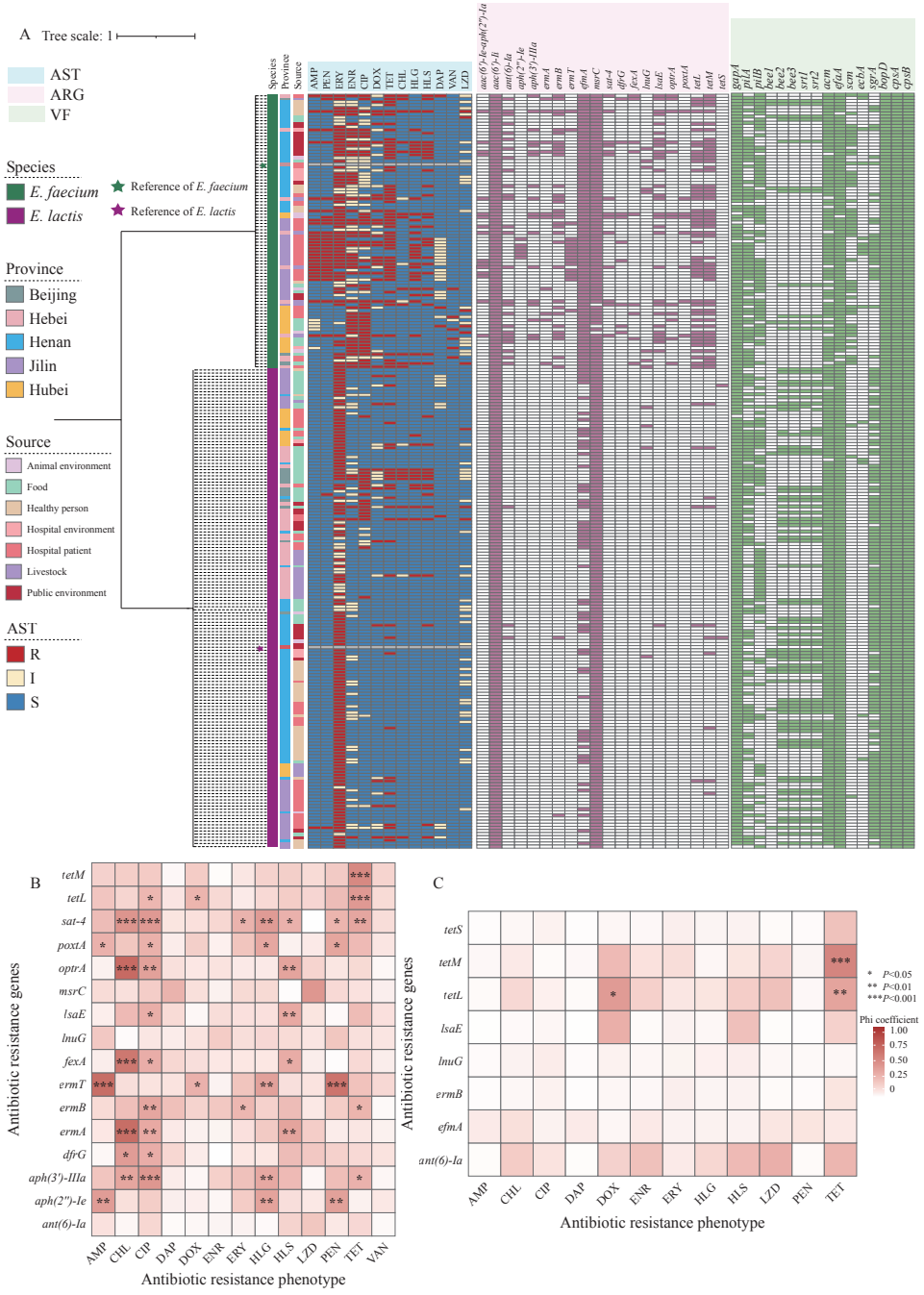

FIGURE 2. Phylogenetic relationships of *E. faecium* and *E. lactis* and correlation analysis between ARGs and ABR phenotypes. (A) Midpoint-rooted maximum likelihood phylogenetic tree constructed from 87 *E. faecium* genomes and 153 *E. lactis* genomes. (B) Correlation heatmap between ARGs and ABR phenotypes in *E. faecium*. (C) Correlation heatmap between ARGs and ABR phenotypes in *E. lactis*.

Note: For (A), reference strains used were SRR24 (accession number: GCA_009734005.2) for *E. faecium* and CX262 (accession number: GCA_019343125.1) for *E. lactis*. Colored bands on the right display genomic information for *Enterococcus* isolates. The first heatmap presents antibacterial susceptibility testing results for *Enterococcus*. The second heatmap illustrates the distribution of antibacterial resistance genes (ARGs) across *Enterococcus* isolates. The third heatmap depicts the distribution of virulence factor encoding genes in *Enterococcus*.

Abbreviation: ABR=antibacterial resistance; AMP=ampicillin; PEN=penicillin; ERY=erythromycin; ENR=enrofloxacin; CIP=ciprofloxacin; DOX=doxycycline; TET=tetracycline; DAP=daptomycin; VAN=vancomycin; CHL=chloramphenicol; HLGA=high-level gentamicin; HLSA=high-level streptomycin; LZD=linezolid; S=susceptible; I=intermediate; R=resistant; AST=antibacterial susceptibility testing; ARG=antibacterial resistance gene; *E. faecium=Enterococcus faecium*; *E. lactis=Enterococcus lactis*.

and *E. lactis* (Figure 2A). The two species carried comparable numbers of virulence factor genes, with no significant difference observed (P>0.05). We identified 25 unique VFs across four functional categories — adhesion, immune modulation, biofilm formation, and exotoxin production — in both *E. faecium* and *E. lactis* genomes. Adhesion genes predominated (18/26, 69.2%), followed by immune modulation factors (*galE*, *cpsA*, *cpsB*, and *cpsD*), biofilm formation genes (*bopD* and *papR*), and a single exotoxin gene (*nheB*). Three VFs — *bopD* (biofilm formation), *cpsA*, and *cpsB* (immune modulation) — were universally present across all isolates. The most prevalent adhesion genes were *efaA* (236/240, 98.3%), *gapA* (234/240, 97.5%), and *acm* (223/240, 92.9%). Notably, the adhesion gene *sgrA* exhibited differential distribution, appearing in 67.7% (20/30) of *E. faecium* isolates from hospital patients versus 83.0% (127/153) of *E. lactis* isolates. Comparative genomic analysis revealed that *E. faecium* harbored significantly higher numbers of ARGs, MGEs, and plasmid replicons compared to *E. lactis* (P<0.05) (Figure 3).

Pan-GWAS analysis identified 267 species-specific genes in *E. lactis* and 222 in *E. faecium* (Figure 4A). COG functional classification demonstrated that species-specific genes from both enterococcal species were significantly enriched in three major categories: metabolism, cellular processes and signaling, and information storage and processing (Figure 4B).

DISCUSSION

The distinct ABR and genomic characteristics of *E. lactis* and *E. faecium* pose different food safety risks. *E. faecium* demonstrated significantly higher resistance to 12 antimicrobials, a substantially elevated MDR rate, and greater abundance of ARGs, MGEs, and plasmid replicons compared to *E. lactis*. These genetic elements increase the potential for ABR transmission throughout the food chain, with specific gene-phenotype correlations providing mechanistic explanations for the observed resistance patterns. The unexpected correlation between *ermT* and β-lactam resistance in *E. faecium* warrants further investigation to elucidate the underlying mechanisms. Although *E. lactis* exhibited overall lower ABR, it showed notably higher erythromycin resistance than *E. faecium*. This elevated resistance is likely attributable to the

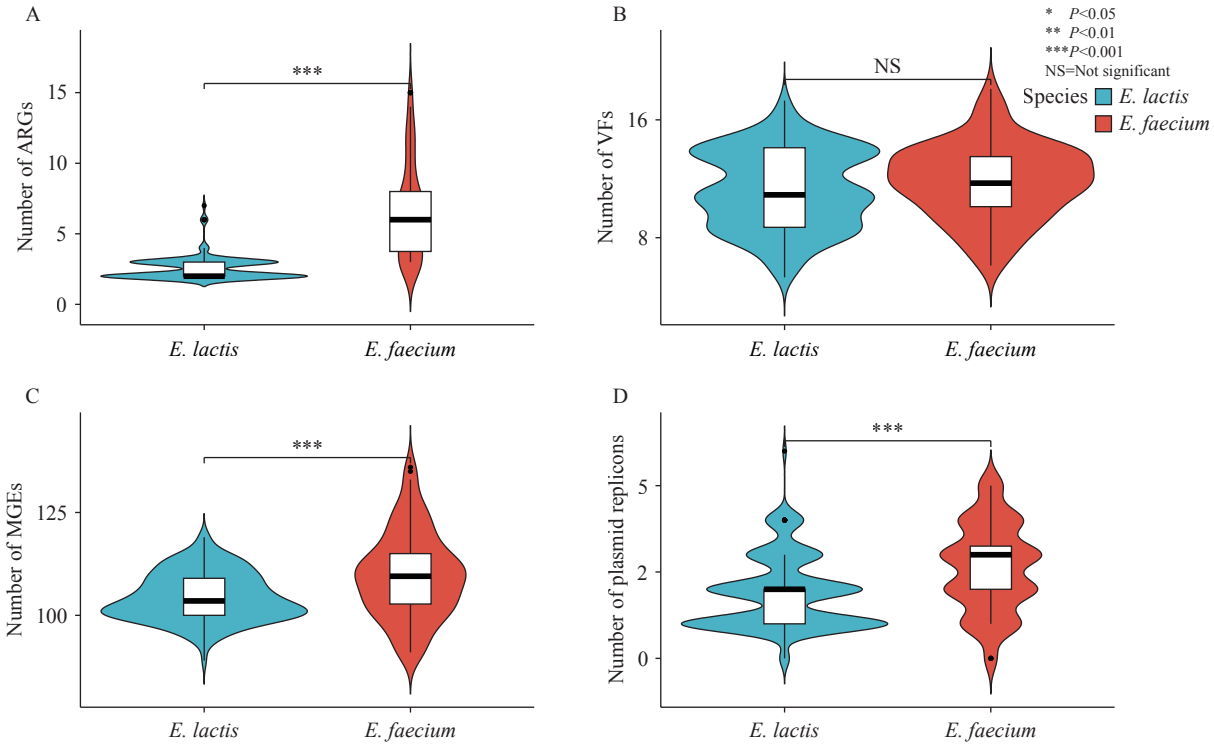

FIGURE 3. Comparative analysis of *E. faecium* and *E. lactis* genomic content. (A) Antibacterial resistance genes, (B) Virulence factor encoding genes, (C) Mobile genetic elements; (D) Plasmid replicons.
Abbreviation: ARG=antibacterial resistance gene; VF=virulence factor encoding gene; MGE=mobile genetic element; *E. faecium=Enterococcus faecium*; *E. lactis=Enterococcus lactis*.

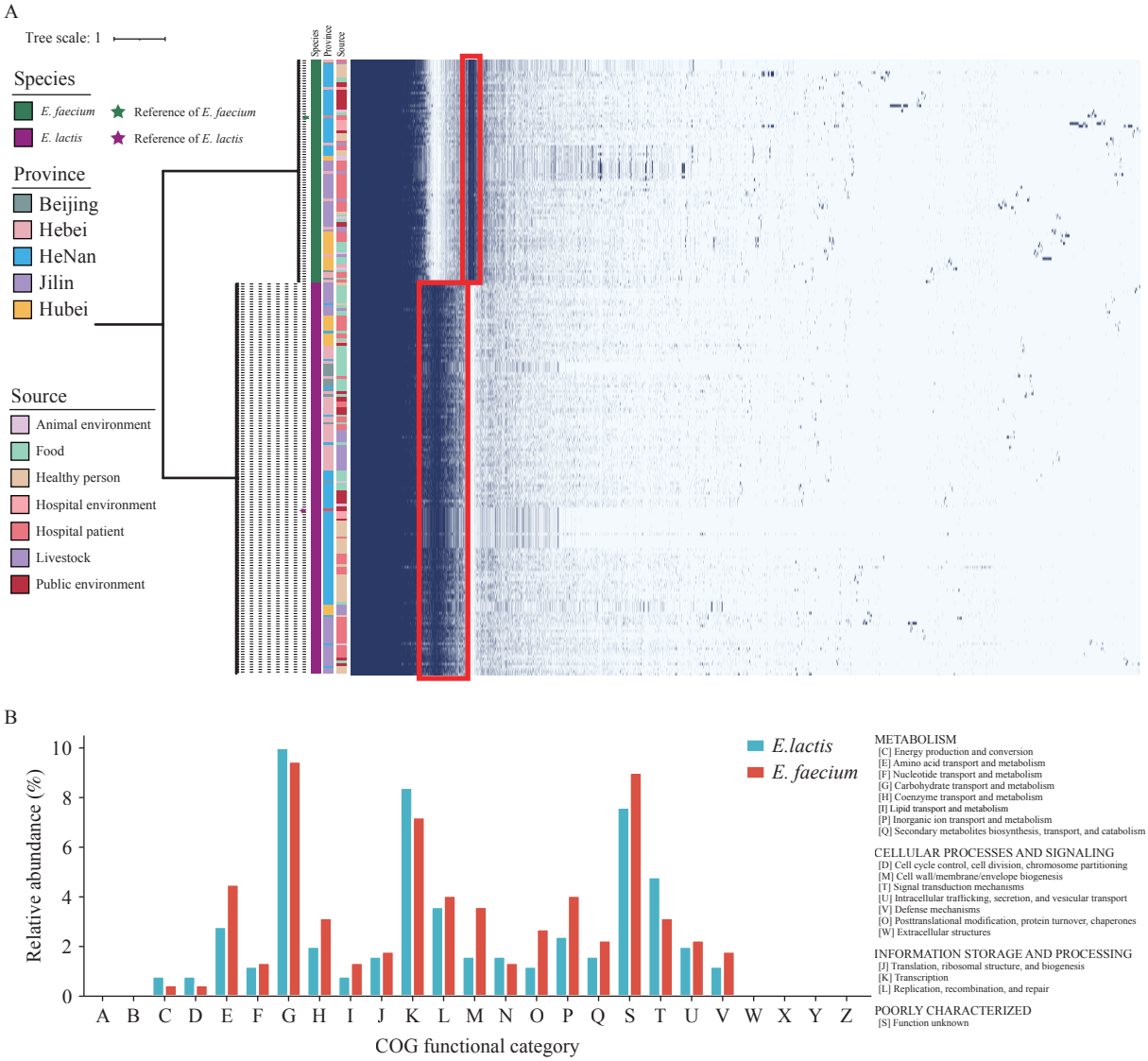

FIGURE 4. Pan-genome-wide association study of *E. faecium* and *E. lactis*. (A) Species-specific differential genes are highlighted in the red box. (B) Relative abundance of differential genes between *E. lactis* and *E. faecium* across distinct Clusters of Orthologous Groups functional categories.
Note: For (A), the colored bands on the right side of the phylogenetic tree represent genomic information for *Enterococcus* isolates. For (B), functional category explanations are provided on the right side of the figure.
Abbreviation: *E. faecium=Enterococcus faecium*; *E. lactis=Enterococcus lactis*.

macrolide resistance gene *msrC*, which is chromosomally encoded and therefore presents limited risk for horizontal gene transfer to other bacterial species (*16*).

The widespread distribution of adhesion genes likely contributes substantially to colonization capacity and virulence expression of both *E. faecium* and *E. lactis* within the food chain. Previous research has demonstrated that *sgrA* plays a critical role in bacterial adherence during hospital-associated infections by facilitating biofilm formation in *E. faecium* (*17*). The high prevalence of *sgrA* among *E. lactis* isolates suggests that this species may harbor underappreciated clinical virulence potential, warranting enhanced surveillance of its pathogenic characteristics throughout food production and distribution systems.

Pan-GWAS analysis revealed substantial inter-species variation in gene content between *E. faecium* and *E. lactis*, while their functional gene distributions demonstrated remarkable conservation. This pattern suggests that despite divergent evolutionary trajectories involving species-specific gene acquisition and loss events, both species have maintained similar functional capabilities in essential biological processes (*3*).

Several limitations should be acknowledged. The absence of sampling data from 2020–2022 and the restriction to five PLADs may limit the generalizability of these findings to other time periods and geographic regions. Future surveillance efforts should expand temporal and spatial coverage while implementing species-specific monitoring strategies to comprehensively assess the evolving ABR landscape of enterococci in food production systems.

This research provides valuable insights for addressing antimicrobial resistance risks in the food chain, a central priority within the One Health framework. By characterizing the distinct ABR profiles and genomic features of *E. faecium* and *E. lactis*, this study addresses critical knowledge gaps in species-specific risk assessments of enterococci in Chinese food systems. These findings facilitate the integration of food safety, animal health, and public health perspectives, supporting the development of targeted interventions to prevent ABR transmission across food-animal-human interfaces.

Conflicts of interest: No conflicts of interest.

Ethical statement: Approved by the Ethics Committee of the State Key Laboratory of the China National Centre for Food Safety Risk Assessment (CFSA).

Funding: Supported by the National Natural Science Foundation of China (32172314) and the National Key Research and Development Program of China (2023YFD1801004).

doi: 10.46234/ccdcw2025.241

[#] Corresponding authors: Zixin Peng, pengzixin@cfsa.net.cn; Shaofu Qiu, qiushf0613@hotmail.com.

[1] School of Public Health, Southern Medical University, Guangzhou City, Guangdong Province, China; [2] NHC Key Laboratory of Food Safety Risk Assessment, Chinese Academy of Medical Science Research Unit (2019RU014), China National Center for Food Safety Risk Assessment, Beijing, China; [3] Center for Disease Control and Prevention of Chinese PLA, Beijing, China; [4] Fengjie County Center for Disease Control and Prevention, Chongqing, China.

Submitted: September 26, 2025
Accepted: November 06, 2025
Issued: November 14, 2025

REFERENCES

1. Peng ZX, Hu Y, Ye ZH, Deng J, Yang DJ, Xu J, et al. One health approach of enterococcal population structure and antibacterial resistance along the food chain — four PLADs, China, 2015-2022. China CDC Wkly 2024;6(47):1223 – 31. https://doi.org/10.46234/ccdcw2024.246.
2. Cattoir V. The multifaceted lifestyle of enterococci: genetic diversity, ecology and risks for public health. Curr Opin Microbiol 2022;65:73 – 80. https://doi.org/10.1016/j.mib.2021.10.013.
3. Choi DG, Baek JH, Han DM, Khan SA, Jeon CO. Comparative pangenome analysis of *Enterococcus faecium* and *Enterococcus lactis* provides new insights into the adaptive evolution by horizontal gene acquisitions. BMC Genomics 2024;25(1):28. https://doi.org/10.1186/s12864-023-09945-7.
4. Lebreton F, van Schaik W, McGuire AM, Godfrey P, Griggs A, Mazumdar V, et al. Emergence of epidemic multidrug-resistant *Enterococcus faecium* from animal and commensal strains. mBio 2013;4(4):e00534 – 13. https://doi.org/10.1128/mBio.00534-13.
5. Belloso Daza MV, Cortimiglia C, Bassi D, Cocconcelli PS. Genome-based studies indicate that the *Enterococcus faecium* clade b strains belong to *Enterococcus lactis* species and lack of the hospital infection associated markers. Int J Syst Evol Microbiol 2021;71(8):004948. https://doi.org/10.1099/ijsem.0.004948.
6. Prjibelski A, Antipov D, Meleshko D, Lapidus A, Korobeynikov A. Using SPAdes de novo assembler. Curr Protoc Bioinformatics 2020;70(1):e102. https://doi.org/10.1002/cpbi.102.
7. Jain C, Rodriguez-R LM, Phillippy AM, Konstantinidis KT, Aluru S. High throughput ANI analysis of 90K prokaryotic genomes reveals clear species boundaries. Nat Commun 2018;9(1):5114. https://doi.org/10.1038/s41467-018-07641-9.
8. McArthur AG, Waglechner N, Nizam F, Yan A, Azad MA, Baylay AJ, et al. The comprehensive antibiotic resistance database. Antimicrob Agents Chemother 2013;57(7):3348 – 57. https://doi.org/10.1128/AAC.00419-13.
9. Chen LH, Yang J, Yu J, Yao ZJ, Sun LL, Shen Y, et al. VFDB: a reference database for bacterial virulence factors. Nucleic Acids Res 2005;33(Database issue):D325-8. http://dx.doi.org/10.1093/nar/gki008.
10. Johansson MHK, Bortolaia V, Tansirichaiya S, Aarestrup FM, Roberts AP, Petersen TN. Detection of mobile genetic elements associated with antibiotic resistance in *Salmonella enterica* using a newly developed web tool: MobileElementFinder. J Antimicrob Chemother 2021;76(1):101 – 9. https://doi.org/10.1093/jac/dkaa390.
11. Carattoli A, Hasman H. PlasmidFinder and in silico pMLST: identification and typing of plasmid replicons in whole-genome sequencing (WGS). In: de la Cruz F, editor. Horizontal gene transfer: methods and protocols. New York: Humana. 2020; p. 285-94. http://dx.doi.org/10.1007/978-1-4939-9877-7_20.
12. Croucher NJ, Page AJ, Connor TR, Delaney AJ, Keane JA, Bentley SD, et al. Rapid phylogenetic analysis of large samples of recombinant bacterial whole genome sequences using Gubbins. Nucleic Acids Res 2015;43(3):e15. https://doi.org/10.1093/nar/gku1196.
13. Price MN, Dehal PS, Arkin AP. FastTree 2 – approximately maximum-likelihood trees for large alignments. PLoS One 2010;5(3):e9490. https://doi.org/10.1371/journal.pone.0009490.
14. Page AJ, Cummins CA, Hunt M, Wong VK, Reuter S, Holden MTG, et al. Roary: rapid large-scale prokaryote pan genome analysis. Bioinformatics 2015;31(22):3691 – 3. https://doi.org/10.1093/bioinformatics/btv421.
15. Brynildsrud O, Bohlin J, Scheffer L, Eldholm V. Rapid scoring of genes in microbial pan-genome-wide association studies with Scoary. Genome Biol 2016;17(1):238. https://doi.org/10.1186/s13059-016-1108-8.
16. Kim E, Yang SM, Kim HJ, Kim HY. Differentiating between *Enterococcusfaecium* and *Enterococcuslactis* by matrix-assisted laser desorption ionization time-of-flight mass spectrometry. Foods 2022;11(7):1046. https://doi.org/10.3390/foods11071046.
17. Nagarajan R, Hendrickx APA, Ponnuraj K. Cloning, expression, purification, crystallization and preliminary crystallographic analysis of the N-terminal domain of serine glutamate repeat A (SgrA) protein from *Enterococcus faecium*. Acta Crystallogr Sect F Struct Biol Cryst Commun 2013;69(Pt 4):441-4. http://dx.doi.org/10.1107/S1744309113005745.

SUPPLEMENTARY MATERIAL

SUPPLEMENTARY TABLE S1. Geographic prevalence of *Enterococcus faecium* and *Enterococcus lactis* in samples.

PLADs	No. of samples	No. of *E. faecium* samples	Prevalence of *E. faecium* (%)	No. of *E. lactis* samples	Prevalence of *E. lactis* (%)
Beijing	405	3	0.7	12	3.0
Hebei	404	10	2.5	34	8.4
Henan	425	33	7.8	60	14.1
Hubei	503	16	3.2	15	3.0
Jilin	496	25	5.0	32	6.5
Total	2,233	87	3.9	153	6.9

Abbreviation: PLAD=provincial-level administrative division; *E. faecium*=*Enterococcus faecium*; *E. lactis*=*Enterococcus lactis*.

SUPPLEMENTARY TABLE S2. Distribution and prevalence rates of *Enterococcus faecium* and *Enterococcus lactis* across sampling sources.

Sample category	No. of samples	No. of *E. faecium* samples	Prevalence of *E. faecium* (%)	No. of *E. lactis* samples	Prevalence of *E. lactis* (%)	χ^2	*P*
Environment	**521**	**24**	**4.6**	**23**	**4.4**	**0**	***P*>0.05**
Public environment	234	13	5.6	16	6.8	0.2	*P*>0.05
Hospital environment	119	6	5.0	4	3.4	0.1	*P*>0.05
Animal environment	168	5	3.0	3	1.8	Fisher's exact test	*P*>0.05
Food	**701**	**14**	**2.0**	**42**	**6.0**	**13.6**	***P*<0.001**
Poultry	**70**	**1**	**1.4**	**0**	**0.0**	**Fisher's Exact Test**	***P*>0.05**
Livestock	**323**	**7**	**2.2**	**20**	**6.2**	**5.6**	***P*<0.05**
Human	**618**	**41**	**6.6**	**38**	**6.1**	**0.1**	***P*>0.05**
Periods							
2015–2019	694	30	4.3	37	5.3	0.6	*P*>0.05
2023–2024	1,539	57	3.7	116	7.5	20.6	*P*<0.001
Total	**2,233**	**87**	**3.9**	**153**	**6.9**	**18.6**	***P*<0.001**

Vital Surveillances

Antibiotic Susceptibility of *Nocardia* Clinical Isolates Collected from Chinese Patients — China, 2014–2024

Pan Zhao[1,2]; Shuai Xu[1]; Min Yuan[1]; Zhiguo Liu[1]; Xiaotong Qiu[1]; Zhenjun Li[1,#]

ABSTRACT

Introduction: *Nocardia* species are found worldwide in soil rich in organic matter and can cause nocardiosis in humans. Trimethoprim-sulfamethoxazole has long been the first-line treatment for *Nocardia* infections; however, resistance to this therapy has recently been reported.

Methods: Sixty-three clinical *Nocardia* isolates collected in China were tested against 32 antimicrobial agents using the broth microdilution method. Phylogenetic analysis of the 16S rRNA gene was performed to identify the species.

Results: Three sequences from samples collected in Hainan Province did not match any known *Nocardia* species, suggesting significant genetic diversity among *Nocardia* isolates. *Nocardia* strains generally exhibited high resistance to clarithromycin, clindamycin, and isoniazid. Clinical and reference strains of *N. farcinica* and *N. otitidiscaviarum* were susceptible to amikacin and linezolid. Amoxicillin-clavulanate and imipenem were effective against all clinical and reference strains of *N. farcinica*, whereas gentamicin was effective against all clinical and reference strains of *N. otitidiscaviarum*.

Conclusions: Linezolid and amikacin were the most consistently active drugs among the analyzed species. Variability of antimicrobial susceptibility was observed among clinical isolates of the same species and between clinical and reference isolates of the same species. Overall, this study highlights the need for better assessment of the burden of nocardiosis in China and for continuous monitoring of antimicrobial resistance among *Nocardia* isolates.

Nocardia species are found worldwide in soil rich in organic matter (*1*). As of April 2025, 252 *Nocardia* species have been identified, and approximately 50 of them are considered human pathogens (https://www.bacterio.net/) (*2–3*). Most *Nocardia* infections are acquired through inhalation or traumatic inoculation (*4–7*). Infections are often seen in immunocompromised hosts, such as patients with AIDS, autoimmune diseases, malignancies, diabetes mellitus, or organ transplants (*8–10*). Infection with Mycobacterium tuberculosis (TB) is associated with chronic lung disease, and the similarity in the diagnosis and clinical manifestations of nocardiosis and TB may lead to misdiagnosis (*11*). The treatment of choice for tuberculosis is ineffective against nocardiosis, underscoring the importance of accurate diagnosis for effective therapy. The antimicrobial susceptibility of *Nocardia* is highly variable and depends on the species. Several studies have raised concerns about increasing resistance among *Nocardia* isolates, particularly to trimethoprim-sulfamethoxazole (SXT). Similarly, breakthrough infections have been reported in immunocompromised individuals receiving SXT prophylaxis (*12*).

The present study is an extension of a previous investigation (*13*), focusing on 63 clinical *Nocardia* isolates collected from 11 provincial-level administrative divisions (PLADs) across 6 of the 7 administrative regions of China. Variability in antimicrobial susceptibility was observed among isolates of the same species. Overall, this study highlights the need for better assessment of the burden of nocardiosis in China and for continuous monitoring of antimicrobial resistance among *Nocardia* isolates.

METHODS

We collected 305 clinical samples, 63 of which were identified as *Nocardia* strains. These isolates were obtained from patients across 11 PLADs in China, representing 6 of the 7 administrative regions. Phylogenetic analysis of the 16S rRNA gene was conducted to determine the species. Antimicrobial susceptibility to 32 antibiotics was determined using the broth microdilution method in accordance with the Clinical and Laboratory Standards Institute (CLSI)

guidelines (*14*). The Alamar Blue assay was used as the visual endpoint indicator, as previously described (*13*). The minimum inhibitory concentration (MIC) was defined as the lowest drug concentration that inhibited visible growth of the tested isolates. Cluster analyses of samples and antibiotics were performed using SPSS Statistics (version 22.0; IBM, Armonk, New York, USA), and both antibiotic and sample clusters were analyzed through hierarchical cluster analysis.

RESULTS

The sample sources were diverse, including eye secretions, sputum, abscesses, blood, bronchoalveolar lavage fluid, cerebrospinal fluid, and lung or liver biopsies. The most represented species was *N. farcinica* (23; 36.5%), followed by *N. cyriacigeorgica* (17; 27.0%). Three species were marginally represented in the dataset: *N. brasiliensis* (6; 9.5%), *N. otitidiscaviarum* (5; 7.9%), and *N. beijingensis* (4; 6.3%). Four species were rarely represented: *N. asiatica*, *N. terpenica*, *N. veterana,* and *N. abscessus* (Supplementary Table S1, available at https://weekly.chinacdc.cn/). One sequence (159) showed 98.4% identity with *N. nova* based on BLASTn analysis, while two sequences (153 and 160) did not match any of the established *Nocardia* species (Supplementary Figure S1, available at https://weekly.chinacdc.cn/).

Antibiotic Resistance Patterns of the 63 Strains

MIC values were determined for 32 antibiotics from 13 drug classes, with β-lactam antibiotics (9 drugs) (Figure 1). The resulting heatmap was analyzed in two ways: based on MIC values themselves and based on breakpoint values determined for each antibiotic by CLSI. To identify trends between strains and antibiotics, cluster analysis was performed on both the strains and the drugs (Figure 1). As mentioned earlier, phylogenetic analysis of the 16S rRNA gene identified 10 groups — nine corresponding to known species and one containing the two undetermined sequences, 153 and 160. A cluster analysis was performed using 12 clusters, considering that strains 153 and 160 were genetically distinct. Overall, the cluster analysis did not correspond to species determination. For example, the 23 *N. farcinica* strains were distributed across six clusters, with cluster 1 containing 17 of these strains. The six remaining strains (170, 158, 178, 165, 176, and 335) showed significantly different MIC patterns. Strain 170 in cluster 4 and strains 158 and 178 in cluster 2 exhibited strong resistance to cefotaxime (CTX) (MIC 256 mg/L) compared with other *N. farcinica* strains. Strain 165 in cluster 5 showed an intermediate MIC value for isoniazid (INH) (8 mg/L). Strain 176 in cluster 3 showed strong resistance to gentamicin (GEN) (MIC 256 mg/L). Finally, strain 335 in cluster 6 showed strong resistance to cefmetazole (CMZ), ceftriaxone (CRO), cefotaxime (CTX), cefoxitin (FOX), ethambutol (ETH), streptomycin (STR), clofazimine (CLO), and kanamycin (KAN) (256 mg/L). A discrepancy between species determination and cluster analysis was observed for all species except *N. brasiliensis* and *N. asiatica*, which were found in clusters 1 and 7, respectively. *N. cyriacigeorgica* strains were found in clusters 1 and 4, *N. otitidiscaviarum* in clusters 11 and 12, and *N. beijingensis* in clusters 1 and 7, respectively. The 63 strains showed intermediate MIC values for clindamycin (CLI) (8–64 mg/L). All strains except one (165) showed high MIC values for INH (256 mg/L). Although the strains were initially divided into 12 clusters, these clusters could be grouped into two mega groups: A (clusters 1–5 and 7) and B (clusters 6 and 8–12). The main difference between these two mega groups involved CMZ, with group A showing a lower average MIC (27.1 mg/L) and group B showing a higher average MIC (243.2 mg/L). In group A, cluster 7 was characterized by high ciprofloxacin (CIP) and levofloxacin (LVX) (128–256 mg/L), whereas cluster 3 was characterized by high GEN (256 mg/L). In group B, cluster 6 was characterized by high GEN values (32–256 mg/L) compared with other strains in group B (average, 0.8 mg/L).

Cluster analysis was performed based on the drugs. The 32 drugs belonged to 13 drug classes. The most represented class was β-lactam antibiotics, comprising nine drugs that were distributed across three different clusters (1, 2 and 3). Five of these drugs were found in cluster 1. The drugs were further grouped into two mega groups, I and II, with three clusters (clusters 6–8) forming the mega group II. Overall, group I showed low MIC values, whereas group II was characterized by high MIC values and included INH, RIF, and VAN. The clusters differed in their overall MIC values, with cluster 1 showing the lowest and cluster 7 the highest.

The average MIC value was calculated for each drug across all 63 clinical samples. Three antibiotics (linezolid, amikacin, and meropenem) had mean MIC

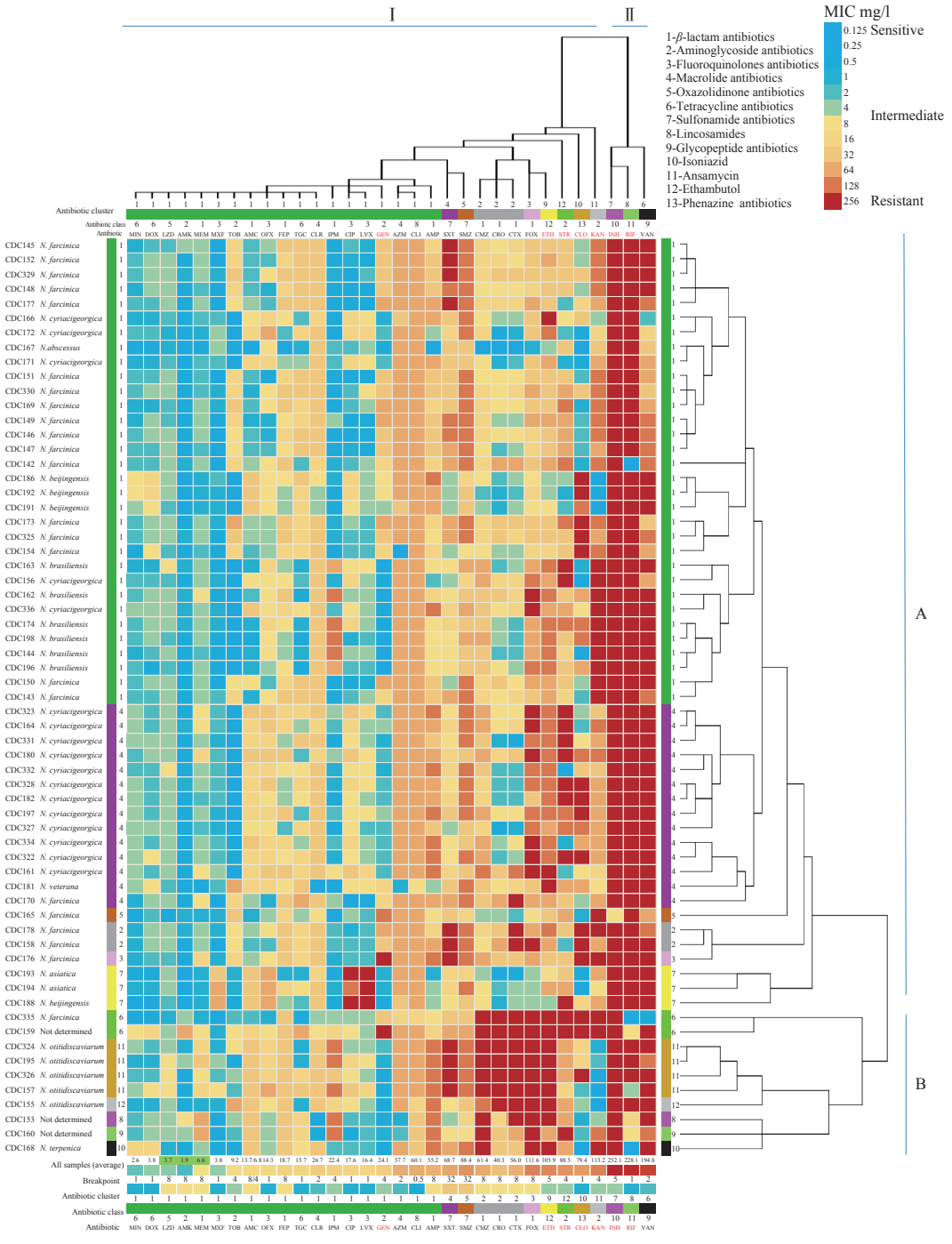

FIGURE 1. Heatmap showing MIC values of 63 *Nocardia* clinical isolates for 32 antimicrobial drugs.

Note: Drugs used to treat TB are shown in red font. Isolate species were determined by phylogenetic analysis of the 16S rRNA gene. MIC data were clustered by strains as well as drugs. Trees based on cluster analyses are shown on the right for the strains and at the top for the drugs. In both cases, 12 clusters were identified and are color-coded and numbered. Drug classes are indicated by a number. MIC values were also color-coded, from blue (MIC of 0.125 mg/L) for a susceptible strain to red (MIC of 256 mg/L) for a resistant strain. Clusters based on the strains were organized into two mega groups, labeled A and B. Similarly, clusters based on drugs were organized into two mega groups, labeled I and II. The average MIC value for each drug is shown at the bottom and is color-coded. Breakpoint values for each drug are also shown at the bottom. Average MIC values below the breakpoint are highlighted in green.

Abbreviation: MIC=minimum inhibitory concentration; TB=tuberculosis; AMK=amikacin; AMC=amoxicillin-clavulanate; AMP=ampicillin; AZM=azithromycin; FEP=cefepime; CMZ=cefmetazole; CTX=cefotaxime; FOX=cefoxitin; CRO=ceftriaxone; CIP=ciprofloxacin; CLR=clarithromycin; CLI=clindamycin; CLO=clofazimine; DOX=doxycycline; ETH=ethambutol.

values below their respective breakpoints, suggesting that these antibiotics were likely effective against all clinical isolates analyzed. However, variations were observed both between and within species. For example, *N. otidiscavarium* strains 155 and 324 had intermediate MIC values for tobramycin (TOB) (8–64 mg/L), whereas the other three *N. otidiscavarium* strains had MIC values below the TOB breakpoint value (4 mg/L). Three antibiotics — minocycline (MIN), doxycycline (DOX), and moxifloxacin (MXF) — had average MIC values (2.6, 3.8, and 3.8 mg/L, respectively) that were close to their breakpoint values (1 mg/L for all three) and might also be considered effective against most *Nocardia* species.

Antibiotic Resistance in Five Species

The previous analysis did not reveal any significant trend in antibiotic resistance across species. The next step was to assess whether any resistance pattern was consistent among all clinical strains of the same species. Although nine species were reported in this study, only five were analyzed because the remaining species were represented by only one or two clinical strains. Only the drugs for which MIC values exceeded the breakpoint value for each clinical isolate are listed in Table 1. Six resistance patterns were identified among the antibiotics and *Nocardia* species. Lincosamides (CLI) and INH were ineffective against all clinical isolates of the five *Nocardia* species. Six additional drug classes — ETH, ansamycin (rifampin, RIF), glycopeptides (vancomycin), tetracyclines (tigecycline), phenazine (clofazimine), and sulfonamides (sulfamethoxazole) — were ineffective against at least two species. Among macrolides, clarithromycin (CLR) was ineffective against all five species, whereas azithromycin (AZM) was ineffective against four of the five analyzed species. The effectiveness of *β-lactams* and fluoroquinolones varied by both drug and species. GEN was ineffective against *N. farcinica*, whereas KAN and STR were ineffective against two species. The last category concerned oxazolidinone (linezolid, LZD), which is not listed in Table 1, indicating that this drug might be effective against at least one clinical isolate from each of the five analyzed species. Consistent susceptibility to both amikacin (AMK) and LZD was observed across all five *Nocardia* species, while complete resistance was observed against CLR, CLI, and INH (Tables 2–3).

TABLE 1. List of antibiotics ineffective against all clinical isolates of the five *Nocardia* species.

Antibiotic class	Species†					Category
	N. farcinica (23)	*N. cyriacigeorgica* (17)	*N. brasiliensis* (6)	*N. otitidiscaviarum* (5)	*N. beijingensis* (4)	
Lincosamides (1)*	CLI §	CLI	CLI	CLI	CLI	1
Isoniazid (1)	INH	INH	INH	INH	INH	1
Ethambutol (1)	ETH	ETH	ETH	ETH		2
Ansamycin (1)		RIF	RIF	RIF	RIF	2
Glycopeptide (1)			VAN	VAN	VAN	2
Tetracyclines (3)		TGC			TGC	2
Sulfonamides (2)			SMZ	SMZ		2
Phenazine (1)				CLO	CLO	2
Macrolides (2)	CLR	CLR, AZM	CLR, AZM	CLR, AZM	CLR, AZM	3
β-lactams (9)		FOX	FOX, CMZ, IPM	AMP, AMC, FEP, CTX, FOX, CMZ, CRO, IPM	AMC	4
Fluoroquinolones (4)		CIP, LVX, OFX	LVX, OFX	CIP, LVX, OFX	CIP, LVX, OFX	4
Aminoglycosides (5)	GEN, KAN		KAN, STR	STR		5
Oxazolidinone (1)						6

Abbreviation: AMK=amikacin; AMC=amoxicillin-clavulanate; AMP=ampicillin; AZM=azithromycin; FEP=cefepime; CMZ=cefmetazole; CTX=cefotaxime; FOX=cefoxitin; CRO=ceftriaxone; CIP=ciprofloxacin; CLR=clarithromycin; CLI=clindamycin; CLO=clofazimine; DOX=doxycycline; ETH=ethambutol; GEN=gentamicin; IPM=imipenem; INH=isoniazid; KAN=kanamycin; LVX=levofloxacin; LZD=linezolid; MEM=meropenem; MIN=minocycline; MXF=moxifloxacin; OFX=ofloxacin; RIF=rifampicin; STR=streptomycin; SMZ=sulfamethoxazole; TGC=tigecycline; TOB=tobramycin; SXT=trimethoprim-sulfamethoxazole; VAN=vancomycin.

* Antibiotic classes were sorted based on the category column. The number of drugs in each class is indicated in parentheses.

† The number of clinical isolates for each species is indicated in parentheses.

§ Only drugs that were ineffective, i.e., with MIC values greater than breakpoint values for all clinical isolates of the analyzed species, are listed.

TABLE 2. Antibiotic categories based on the effectiveness of clinical and reference strains of the same *Nocardia* species.

Species*	Category	Antibiotic	
		Name	Class
N. farcinica, *N. otitidiscaviarum*	Antibiotics effective on all clinical and reference strains	AMK	Aminoglycoside
		LZD	Oxazolidinone
	Antibiotics effective on all reference strains	MXF	Fluoroquinolone
		SXT	Sulfonamide
N. farcinica	Antibiotics effective on all clinical and reference strains	AMC, IPM	β-lactam
	Antibiotics effective on all reference strains	MEM	β-lactam
N. otitidiscaviarum	Antibiotics effective on all clinical and reference strains	GEN	Aminoglycoside
	Antibiotics effective on all clinical strains	KAN	Aminoglycoside

* Only two *Nocardia* species were analyzed, as the remaining species were represented by fewer than four clinical or reference strains.

Overall, this analysis demonstrated that *Nocardia* species can exhibit variable responses to different antibiotics.

Comparison with *Nocardia* Standards

The present study identified different MIC patterns among strains of the same species as well as within the same antibiotic class. Comparison with the MIC patterns of *Nocardia* reference strains was necessary (Figure 2). The number of strains of each species with MIC values lower than or equal to the breakpoint value is shown for the 63 clinical strains (C) and the 26 reference strains (S). Some antibiotics had the same effect on all strains (clinical or/and reference) of the same species and are labeled as "100" in Figure 2. Only species with four or more strains (clinical or reference) were included in the comparison.

Overall, four categories of antibiotics were identified based on their effectiveness in both clinical and reference strains (Table 2). First, AMK and LZD were effective against all clinical and reference strains of *N. farcinica* and *N. otitidiscaviarum* (labeled with "100" in green in Figure 2). Second, amoxicillin-clavulanate (AMC), imipenem (IPM), and GEN were effective against all clinical and reference strains of one species. AMC and IPM were effective against all the clinical and reference strains of *N. farcinica,* whereas GEN was effective against all the clinical and reference strains of *N. otitidiscaviarum*. Third, MXF, SXT, and meropenem (MEM) were effective against all 10 *N. farcinica* reference strains, whereas lower effectiveness was observed among the 23 *N. farcinica* clinical strains. Finally, KAN was effective against all five *N. otitidiscaviarum* clinical strains, whereas one *N. otitidiscaviarum* reference strain was highly resistant (MIC value 256 mg/L; breakpoint 4 mg/L). None of the drug classes used in this study were consistently effective against all clinical strains of the analyzed species. Among the seven TB drugs, resistance to INH was observed in the clinical strains of all analyzed species. GEN and KAN were the only drugs used to treat TB that showed some effectiveness against all *Nocardia* strains. Other TB drugs, including STR, RIF, ETH, and CLO, were effective against only a few *Nocardia* clinical strains (Table 3).

DISCUSSION

The present study focused on the antibiotic susceptibility patterns of 63 clinical *Nocardia* strains collected in China. Recent studies identified *N. farcinica* and *N. otitidiscaviarum* as the most prevalent species, confirming the present findings (*4*,*13*,*15*). Although this study, which included 63 clinical isolates and nine known *Nocardia* species, extends a previous study that featured only 14 clinical isolates and three species, it is worth noting some limitations. Although clinical isolates from nine species were reported in the present study, only two species (*N. farcinica and N. cyriacigeorgica)* were represented by more than 10 strains. Another limitation concerned the number of reference strains for each species. Only three species (*N. farcinica, N. otitidiscaviarum*, and *N. veterana)* were represented by four or more standard strains. Geographic distribution was also a limitation, as one administrative region — Dongbei — was not represented in the present study. The reported strains were collected from 11 PLADs with relatively developed economies in China. Despite these limitations, the present study identified important trends that should be further confirmed by additional research.

The present study identified antibiotics based on their efficiency against *Nocardia* species, revealing that two drugs, LZD and AMK, were effective against all analyzed *N. farcinica, N. otitidiscaviarum* species.

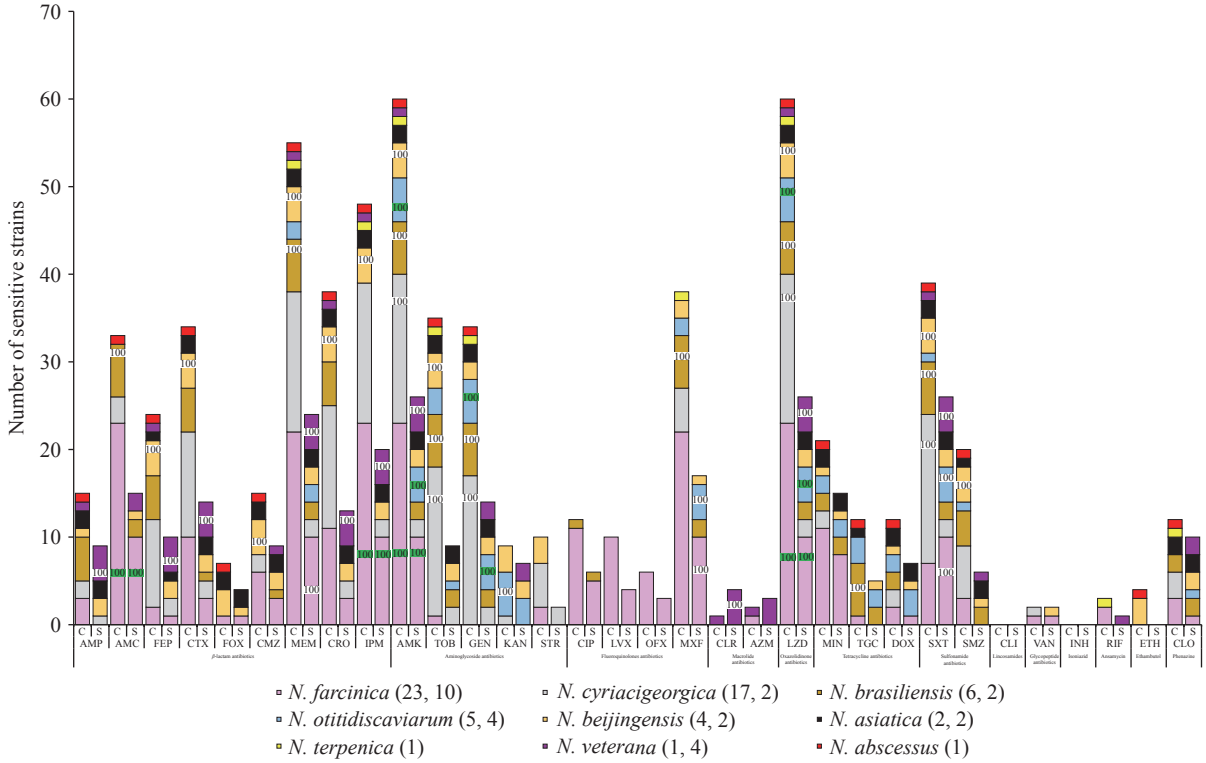

FIGURE 2. Number of susceptible strains for each antibiotic.

Note: The number of strains with MIC values lower than the breakpoint value for each antibiotic is shown. Clinical (C) and reference (S) strains were analyzed. Species are color-coded according to the legend at the bottom. The number of clinical and reference strains is indicated in parentheses. Species for which all clinical and/or reference strains were susceptible to an antibiotic are labeled with "100". Only species with four or more strains were included. Species for which all clinical and reference strains were susceptible to an antibiotic are shown with a green "100", and the results are summarized in Table 2.

Abbreviation: AMK=amikacin; AMC=amoxicillin-clavulanate; AMP=ampicillin; AZM=azithromycin; FEP=cefepime; CMZ=cefmetazole; CTX=cefotaxime; FOX=cefoxitin; CRO=ceftriaxone; CIP=ciprofloxacin; CLR=clarithromycin; CLI=clindamycin; CLO=clofazimine; DOX=doxycycline; ETH=ethambutol; GEN=gentamicin; IPM=imipenem; INH=isoniazid; KAN=kanamycin; LVX=levofloxacin; LZD=linezolid; MEM=meropenem; MIN=minocycline; MXF=moxifloxacin; OFX=ofloxacin; RIF=rifampicin; STR=streptomycin; SMZ=sulfamethoxazole; TGC=tigecycline; TOB=tobramycin; SXT=trimethoprim-sulfamethoxazole; VAN=vancomycin; MIC=minimum inhibitory concentration.

These antibiotics were also effective against all analyzed strains in studies conducted in Henan and Shandong provinces (*4*,*10*,*15*). Our recent systematic review of antimicrobial susceptibility data from *Nocardia* clinical isolates in China (as of 2024) revealed relatively low overall resistance rates to three antibiotics: LZD (0.30%, 1/336), AMK (3.87%, 13/336), and SXT (3.87%, 13/336) (in press, Disease Surveillance).

The present study revealed differences in antibiotic susceptibility among the same *Nocardia* species. Strains of the same species were not all sensitive to the same antibiotics. Moreover, antibiotics belonging to the same drug class did not exhibit equal effectiveness against *Nocardia* strains. The most consistent drug class was the aminoglycosides, which showed some degree of effectiveness, with variations observed among *Nocardia* strains. A previous study reported similar findings, with AMK being effective against six of seven tested species (*10*).

In summary, the present study revealed potential genetic diversity among *Nocardia* strains, at least based on the 16S rRNA gene, which resulted in incomplete species identification. Moreover, differences in antibiotic susceptibility were observed among strains of the same species. Finally, a comprehensive analysis of *Nocardia* strains in China would be beneficial for monitoring the potential emergence of antibiotic resistance.

Conflicts of interest: No conflicts of interest.

Funding: Supported by National Natural Science Foundation of China (82073624) and Hangzhou Medical and Health Technology Project (A20230270).

doi: 10.46234/ccdcw2025.242

TABLE 3. Species-specific antimicrobial susceptibility of *Nocardia* strains.

Antibiotic class*	*N. farcinica* (23)†	*N. cyriacigeorgica* (17)	*N. brasiliensis* (6)	*N. otitidiscaviarum* (5)	*N. beijingensis* (4)
β-lactams (9)	AMP, FEP, CTX, FOX, CMZ, CRO, MEM	FOX§	FOX, CMZ, IPM	AMP, AMC, FEP, CTX, FOX, CMZ, CRO, IPM	AMC
		AMP, AMC, FEP, CTX, CMZ, CRO, IPM, MEM	AMP, FEP, CTX, CRO	MEM	AMP, FOX
	AMC, IPM		AMC, MEM		FEP, CTX, CMZ, MEM, CRO, IPM
Aminoglycosides (5)	GEN, KAN		KAN, STR	STR	
	TOB, STR	KAN, STR		TOB	GEN, KAN, STR
	AMK	AMK, TOB, GEN	AMK, TOB, GEN	AMK, GEN, KAN	AMK, TOB
Fluoroquinolones (4)	CIP, LVX, OFX, MXF,	CIP, LVX, OFX MXF,	LVX, OFX CIP, MXF	CIP, LVX, OFX, MXF	CIP, LVX, OFX, MXF
Macrolides (2)	CLR AZM	CLR, AZM	CLR, AZM	CLR, AZM	CLR, AZM
Oxazolidinone (1)	LZD	LZD	LZD	LZD	LZD
Tetracyclines (3)	MIN, TGC, DOX	TGC MIN, DOX	MIN, DOX TGC	MIN, TGC, DOX	TGC MIN, DOX
Sulfonamides (2)	SXT, SMZ	SMZ SXT	SMZ SXT	SMZ SXT	SXT, SMZ
Phenazine (1)	CLO	CLO	CLO	CLO	CLO
Lincosamides (1)	CLI	CLI	CLI	CLI	CLI
Glycopeptide (1)	VAN	VAN	VAN	VAN	VAN
Isoniazid (1)	INH	INH	INH	INH	INH
Ansamycin (1)	RIF	RIF	RIF	RIF	RIF
Ethambutol (1)	ETH	ETH	ETH	ETH	ETH

Abbreviation: AMK=amikacin; AMC=amoxicillin-clavulanate; AMP=ampicillin; AZM=azithromycin; FEP=cefepime; CMZ=cefmetazole; CTX=cefotaxime; FOX=cefoxitin; CRO=ceftriaxone; CIP=ciprofloxacin; CLR=clarithromycin; CLI=clindamycin; CLO=clofazimine; DOX=doxycycline; ETH=ethambutol; GEN=gentamicin; IPM=imipenem; INH=isoniazid; KAN=kanamycin; LVX=levofloxacin; LZD=linezolid; MEM=meropenem; MIN=minocycline; MXF=moxifloxacin; OFX=ofloxacin; RIF=rifampicin; STR=streptomycin; SMZ=sulfamethoxazole; TGC=tigecycline; TOB=tobramycin; SXT=trimethoprim-sulfamethoxazole; VAN=vancomycin.

* The number of drugs in each class is indicated in parentheses.

† The number of clinical isolates for each species is indicated in parentheses.

§ Antimicrobial susceptibility of *Nocardia* species is color-coded as follows: red (resistant; MIC value greater than the breakpoint value for all clinical isolates of the analyzed species), blue (susceptible; MIC value less than or equal to the breakpoint value for all clinical isolates of the analyzed species), and yellow (intermediate).

Corresponding author: Zhenjun Li, lizhenjun@icdc.cn.

[1] National Key Laboratory of Intelligent Tracking and Forecasting for Infectious Diseases, National Institute for Communicable Disease Control and Prevention, Chinese Center for Disease Control and Prevention, Beijing, China; [2] Microbiology Laboratory, Hangzhou Center for Disease Control and Prevention (Hangzhou Health Supervision Institution), Hangzhou, Zhejiang, China.

Submitted: September 02, 2025
Accepted: October 21, 2025
Issued: November 14, 2025

REFERENCES

1. Gupta S, Grant LM, Powers HR, Kimes KE, Hamdi A, Butterfield RJ, et al. Invasive *Nocardia* infections across distinct geographic regions, United States. Emerg Infect Dis 2023;29(12):2417 – 25. https://doi.org/10.3201/eid2912.230673.
2. Parte AC, Sardà Carbasse J, Meier-Kolthoff JP, Reimer LC, Göker M. List of prokaryotic names with standing in nomenclature (LPSN) moves to the DSMZ. Int J Syst Evol Microbiol 2020;70(11):5607 – 12. https://doi.org/10.1099/ijsem.0.004332.
3. Conville PS, Brown-Elliott BA, Smith T, Zelazny AM. The complexities of *Nocardia* taxonomy and identification. J Clin Microbiol 2018;56(1):e01419 – 17. https://doi.org/10.1128/JCM.01419-17.
4. Han YG, Cheng MJ, Li Z, Chen HH, Xia S, Zhao Y, et al. Clinical characteristics and drug resistance of *Nocardia* in Henan, China, 2017-2023. Ann Clin Microbiol Antimicrob 2024;23(1):23. https://doi.org/10.1186/s12941-024-00677-4.
5. Mehta HH, Shamoo Y. Pathogenic *Nocardia*: a diverse genus of emerging pathogens or just poorly recognized? PLoS Pathog 2020;16(3):e1008280. http://dx.doi.org/10.1371/journal.ppat.1008280.
6. Huang L, Chen XC, Xu HP, Sun LY, Li C, Guo WC, et al. Clinical features, identification, antimicrobial resistance patterns of *Nocardia* species in China: 2009-2017. Diagn Microbiol Infect Dis 2019;94(2):165 – 72. https://doi.org/10.1016/j.diagmicrobio.2018.12.007.
7. Tan YE, Chen SCA, Halliday CL. Antimicrobial susceptibility profiles and species distribution of medically relevant *Nocardia* species: results from a large tertiary laboratory in Australia. J Glob Antimicrob Resist 2020;20:110 – 7. https://doi.org/10.1016/j.jgar.2019.06.018.
8. Rathish B, Zito PM. Nocardia. Treasure Island (FL): StatPearls. 2025. https://pubmed.ncbi.nlm.nih.gov/32809707/.
9. Yang J, Ren HT, Wang J, Dong AY, Chen YL, Hu DX, et al. Clinical characteristics, susceptibility profiles, and treatment of nocardiosis: a multicenter retrospective study in 2015-2021. Int J Infect Dis 2023;130:136 – 43. https://doi.org/10.1016/j.ijid.2023.02.023.
10. Lu SH, Qian ZW, Mou PP, Xie L. Clinical *Nocardia* species: identification, clinical characteristics, and antimicrobial susceptibility in Shandong, China. Bosn J Basic Med Sci 2020;20(4):531 – 8. https://doi.org/10.17305/bjbms.2020.4764.
11. Duggal SD, Chugh TD. Nocardiosis: a neglected disease. Med Princ Pract 2020;29(6):514 – 23. https://doi.org/10.1159/000508717.
12. Wang H, Zhu Y, Cui QZ, Wu WM, Li G, Chen DK, et al. Epidemiology and antimicrobial resistance profiles of the *Nocardia* species in China, 2009 to 2021. Microbiol Spectr 2022;10(2):e0156021 – 21. https://doi.org/10.1128/spectrum.01560-21.
13. Zhao P, Zhang XJ, Du PC, Li GL, Li LX, Li ZJ. Susceptibility profiles of *Nocardia* spp. to antimicrobial and antituberculotic agents detected by a microplate Alamar Blue assay. Sci Rep 2017;7:43660. https://doi.org/10.1038/srep43660.
14. Clinical and Laboratory Standards Institute. Performance standards for susceptibility testing of mycobacteria, *Nocardia* spp., and other aerobic actinomycetes. 2nd ed. Wayne: Clinical and Laboratory Standards Institute. 2023. https://clsi.org/shop/standards/m24s/.
15. Yi ML, Wang LP, Xu WH, Sheng L, Jiang LH, Yang FZ, et al. Species distribution and antibiotic susceptibility of *Nocardia* isolates from Yantai, China. Infect Drug Resist 2019;12:3653 – 61. https://doi.org/10.2147/IDR.S232098.

SUPPLEMENTARY MATERIALS

SUPPLEMENTARY TABLE S1. List of clinical *Nocardia* strains analyzed in this study.

Strain ID	GB-ID	Species	Cluster	Year	PLAD	Administrative region	Sex	Age	Sample source
CDC193	MW563821	*N. asiatica*	7	2015	Beijing	Huabei	–	–	Sputum
CDC194	MW563822	*N. asiatica*	7	2016	Guangxi	Huanan	–	–	Cerebrum
CDC186	MW563817	*N. beijingensis*	1	2015	Chongqing	Xinan	–	–	Sputum
CDC191	MW563819	*N. beijingensis*	1	2015	Chongqing	Xinan	–	–	Sputum
CDC192	MW563820	*N. beijingensis*	1	2015	Chongqing	Xinan	–	–	Sputum
CDC188	MW563818	*N. beijingensis*	7	2015	Unknown	–	–	–	Sputum
CDC162	MW563798	*N. brasiliensis*	1	2015	Beijing	Huabei	–	–	–
CDC196	MW563824	*N. brasiliensis*	1	2016	Zhejiang	Huadong	–	–	Hand abscess
CDC198	MW563826	*N. brasiliensis*	1	2016	Zhejiang	Huadong	–	–	Hand abscess
CDC144	MW563780	*N. brasiliensis*	1	2015	Sichuan	Xinan	–	–	–
CDC163	MW563799	*N. brasiliensis*	1	2015	Hunan	Huazhong	–	–	Abscess
CDC174	MW563810	*N. brasiliensis*	1	2015	Unknown	–	–	–	–
CDC156	MW563792	*N. cyriacigeorgica*	1	2015	Beijing	Huabei	–	–	Sputum
CDC166	MW563802	*N. cyriacigeorgica*	1	2015	Beijing	Huabei	–	–	Sputum
CDC171	MW563807	*N. cyriacigeorgica*	1	2015	Beijing	Huabei	–	–	Sputum
CDC172	MW563808	*N. cyriacigeorgica*	1	2015	Beijing	Huabei	–	–	Sputum
CDC336	MW563840	*N. cyriacigeorgica*	1	2016	Ningxia	Xibei	Female	53	Sputum
CDC161	MW563797	*N. cyriacigeorgica*	4	2015	Beijing	Huabei	–	–	–
CDC164	MW563800	*N. cyriacigeorgica*	4	2015	Beijing	Huabei	–	–	Sputum
CDC182	MW563816	*N. cyriacigeorgica*	4	2015	Inner Mongolia	Huabei	–	–	Sputum
CDC197	MW563825	*N. cyriacigeorgica*	4	2016	Zhejiang	Huadong	–	–	Lung
CDC322	MW563827	*N. cyriacigeorgica*	4	2016	Ningxia	Xibei	Female	48	Purulent secretion
CDC323	MW563828	*N. cyriacigeorgica*	4	2016	Ningxia	Xibei	Female	52	–
CDC327	MW563832	*N. cyriacigeorgica*	4	2016	Ningxia	Xibei	Male	80	Sputum
CDC328	MW563833	*N. cyriacigeorgica*	4	2016	Ningxia	Xibei	Male	48	Sputum
CDC331	MW563836	*N. cyriacigeorgica*	4	2016	Ningxia	Xibei	Male	64	Sputum
CDC332	MW563837	*N. cyriacigeorgica*	4	2016	Ningxia	Xibei	Male	40	Bronchoalveolar lavage fluid
CDC334	MW563838	*N. cyriacigeorgica*	4	2016	Ningxia	Xibei	Female	53	Sputum
CDC180	MW563814	*N. cyriacigeorgica*	4	2015	Unknown	–	–	–	–
CDC154	MW563790	*N. farcinica*	1	2015	Beijing	Huabei	–	–	Sputum
CDC169	MW563805	*N. farcinica*	1	2015	Beijing	Huabei	–	–	–
CDC173	MW563809	*N. farcinica*	1	2015	Beijing	Huabei	–	–	Facial pustules
CDC177	MW563812	*N. farcinica*	1	2015	Beijing	Huabei	–	–	Sputum
CDC325	MW563830	*N. farcinica*	1	2016	Ningxia	Xibei	Female	53	Venous blood
CDC329	MW563834	*N. farcinica*	1	2016	Ningxia	Xibei	Female	71	Venous blood
CDC330	MW563835	*N. farcinica*	1	2016	Ningxia	Xibei	Male	51	Puncture fluid
CDC142	MW563778	*N. farcinica*	1	2015	Sichuan	Xinan	–	–	–
CDC143	MW563779	*N. farcinica*	1	2015	Sichuan	Xinan	–	–	–
CDC145	MW563781	*N. farcinica*	1	2015	Sichuan	Xinan	–	–	–
CDC146	MW563782	*N. farcinica*	1	2015	Guangdong	Huanan	–	–	–

Continued

Strain ID	GB-ID	Species	Cluster	Year	PLAD	Administrative region	Sex	Age	Sample source
CDC147	MW563783	*N. farcinica*	1	2015	Guangdong	Huanan	–	–	–
CDC148	MW563784	*N. farcinica*	1	2015	Guangdong	Huanan	–	–	–
CDC149	MW563785	*N. farcinica*	1	2015	Guangdong	Huanan	–	–	–
CDC150	MW563786	*N. farcinica*	1	2015	Guangdong	Huanan	–	–	–
CDC151	MW563787	*N. farcinica*	1	2015	Guangdong	Huanan	–	–	–
CDC152	MW563788	*N. farcinica*	1	2015	Guangdong	Huanan	–	–	–
CDC158	MW563794	*N. farcinica*	2	2015	Beijing	Huabei	–	–	–
CDC178	MW563813	*N. farcinica*	2	2015	Beijing	Huabei	–	–	Facial pustules
CDC176	MW563811	*N. farcinica*	3	2015	Guangdong	Huanan	–	–	–
CDC170	MW563806	*N. farcinica*	4	2015	Beijing	Huabei	–	–	Blood
CDC165	MW563801	*N. farcinica*	5	2015	Beijing	Huabei	–	–	Sputum
CDC335	MW563839	*N. farcinica*	6	2016	Ningxia	Xibei	Female	38	Cerebrospinal fluid
CDC157	MW563793	*N. otitidiscaviarum*	11	2015	Inner Mongolia	Huabei	–	–	Liver biopsy material
CDC324	MW563829	*N. otitidiscaviarum*	11	2016	Ningxia	Xibei	Male	33	Dialysate
CDC326	MW563831	*N. otitidiscaviarum*	11	2016	Ningxia	Xibei	Male	57	Sputum
CDC195	MW563823	*N. otitidiscaviarum*	11	2016	Guangxi	Huanan	–	–	Lung
CDC155	MW563791	*N. otitidiscaviarum*	12	2015	Hebei	Huabei	–	–	Sputum
CDC168	MW563804	*N. terpenica*	10	2015	Hunan	Huazhong	–	–	Sputum
CDC181	MW563815	*N. veterana*	4	2015	Inner Mongolia	Huabei	–	–	Alveolar lavage fluid
CDC167	MW563803	*N. abscessus*	1	2015	Beijing	Huabei	–	–	Sputum
CDC159	MW563795	N/D	6	2015	Hainan	Huanan	–	–	–
CDC153	MW563789	N/D	8	2015	Hainan	Huanan	–	–	Eye secretions
CDC160	MW563796	N/D	9	2015	Hainan	Huanan	–	–	–

Note: "-" means missing data.
Abbreviation: PLAD=provincial-level administrative division; GB-ID =GenBank ID.

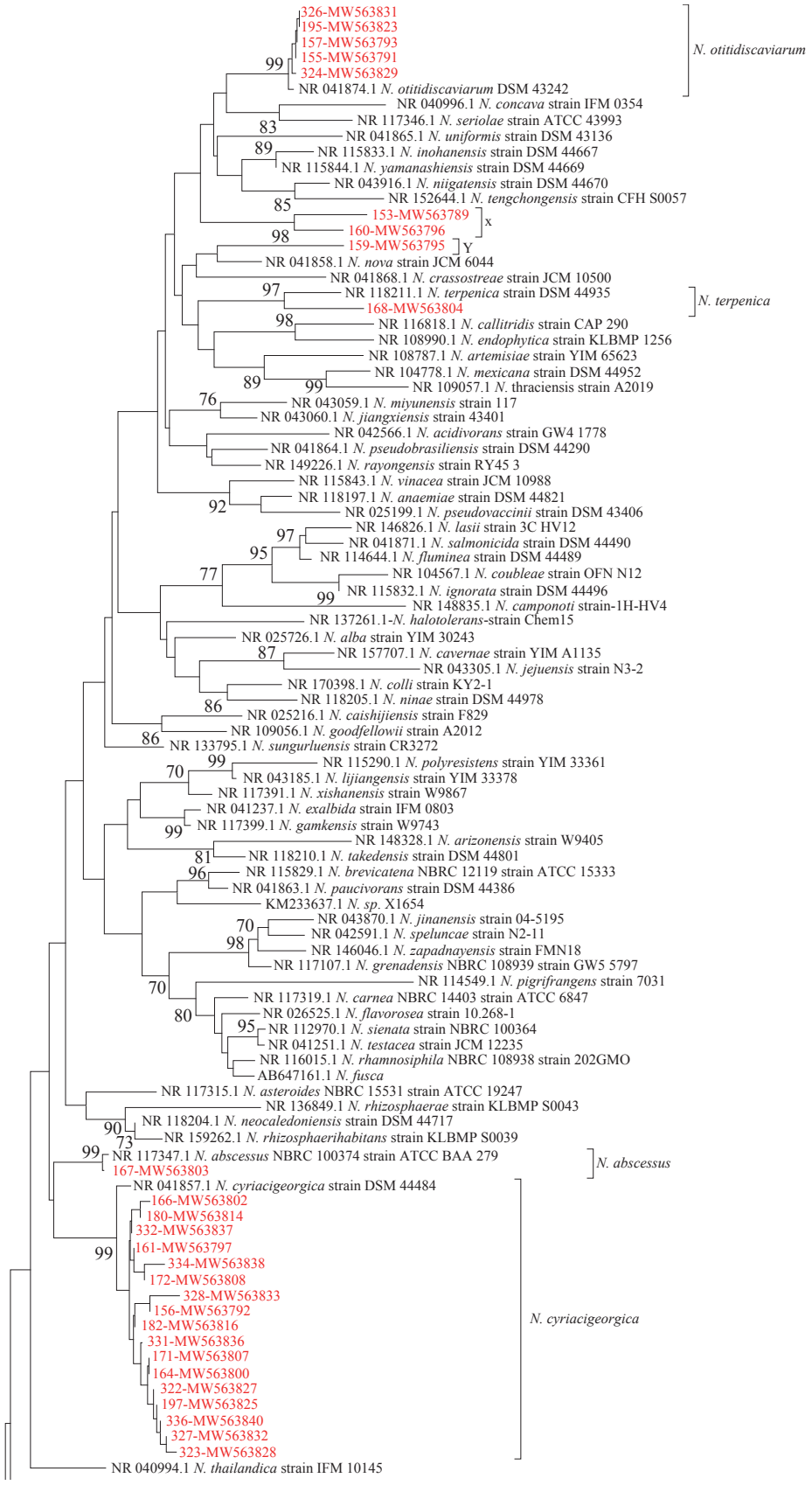
326-MW563831
195-MW563823
157-MW563793
155-MW563791
324-MW563829
99
NR 041874.1 N. otitidiscaviarum DSM 43242
N. otitidiscaviarum
NR 040996.1 N. concava strain IFM 0354
NR 117346.1 N. seriolae strain ATCC 43993
83
NR 041865.1 N. uniformis strain DSM 43136
89
NR 115833.1 N. inohanensis strain DSM 44667
NR 115844.1 N. yamanashiensis strain DSM 44669
NR 043916.1 N. niigatensis strain DSM 44670
85
NR 152644.1 N. tengchongensis strain CFH S0057
153-MW563789
x
98
160-MW563796
159-MW563795
Y
NR 041858.1 N. nova strain JCM 6044
NR 041868.1 N. crassostreae strain JCM 10500
97
NR 118211.1 N. terpenica strain DSM 44935
N. terpenica
168-MW563804
98
NR 116818.1 N. callitridis strain CAP 290
NR 108990.1 N. endophytica strain KLBMP 1256
NR 108787.1 N. artemisiae strain YIM 65623
89
NR 104778.1 N. mexicana strain DSM 44952
99
NR 109057.1 N. thraciensis strain A2019
76
NR 043059.1 N. miyunensis strain 117
NR 043060.1 N. jiangxiensis strain 43401
NR 042566.1 N. acidivorans strain GW4 1778
NR 041864.1 N. pseudobrasiliensis strain DSM 44290
NR 149226.1 N. rayongensis strain RY45 3
NR 115843.1 N. vinacea strain JCM 10988
92
NR 118197.1 N. anaemiae strain DSM 44821
NR 025199.1 N. pseudovaccinii strain DSM 43406
97
NR 146826.1 N. lasii strain 3C HV12
95
NR 041871.1 N. salmonicida strain DSM 44490
NR 114644.1 N. fluminea strain DSM 44489
77
NR 104567.1 N. coubleae strain OFN N12
99
NR 115832.1 N. ignorata strain DSM 44496
NR 148835.1 N. camponoti strain-1H-HV4
NR 137261.1-N. halotolerans-strain Chem15
NR 025726.1 N. alba strain YIM 30243
87
NR 157707.1 N. cavernae strain YIM A1135
NR 043305.1 N. jejuensis strain N3-2
NR 170398.1 N. colli strain KY2-1
86
NR 118205.1 N. ninae strain DSM 44978
NR 025216.1 N. caishijiensis strain F829
NR 109056.1 N. goodfellowii strain A2012
86
NR 133795.1 N. sungurluensis strain CR3272
99
NR 115290.1 N. polyresistens strain YIM 33361
70
NR 043185.1 N. lijiangensis strain YIM 33378
NR 117391.1 N. xishanensis strain W9867
NR 041237.1 N. exalbida strain IFM 0803
99
NR 117399.1 N. gamkensis strain W9743
NR 148328.1 N. arizonensis strain W9405
81
NR 118210.1 N. takedensis strain DSM 44801
96
NR 115829.1 N. brevicatena NBRC 12119 strain ATCC 15333
NR 041863.1 N. paucivorans strain DSM 44386
KM233637.1 N. sp. X1654
70
NR 043870.1 N. jinanensis strain 04-5195
98
NR 042591.1 N. speluncae strain N2-11
NR 146046.1 N. zapadnayensis strain FMN18
NR 117107.1 N. grenadensis NBRC 108939 strain GW5 5797
70
NR 114549.1 N. pigrifrangens strain 7031
NR 117319.1 N. carnea NBRC 14403 strain ATCC 6847
80
NR 026525.1 N. flavorosea strain 10.268-1
95
NR 112970.1 N. sienata strain NBRC 100364
NR 041251.1 N. testacea strain JCM 12235
NR 116015.1 N. rhamnosiphila NBRC 108938 strain 202GMO
AB647161.1 N. fusca
NR 117315.1 N. asteroides NBRC 15531 strain ATCC 19247
NR 136849.1 N. rhizosphaerae strain KLBMP S0043
90
NR 118204.1 N. neocaledoniensis strain DSM 44717
73
NR 159262.1 N. rhizosphaerihabitans strain KLBMP S0039
99
NR 117347.1 N. abscessus NBRC 100374 strain ATCC BAA 279
N. abscessus
167-MW563803
NR 041857.1 N. cyriacigeorgica strain DSM 44484
166-MW563802
180-MW563814
332-MW563837
99
161-MW563797
334-MW563838
172-MW563808
328-MW563833
156-MW563792
182-MW563816
331-MW563836
171-MW563807
164-MW563800
322-MW563827
197-MW563825
336-MW563840
327-MW563832
323-MW563828
N. cyriacigeorgica
NR 040994.1 N. thailandica strain IFM 10145

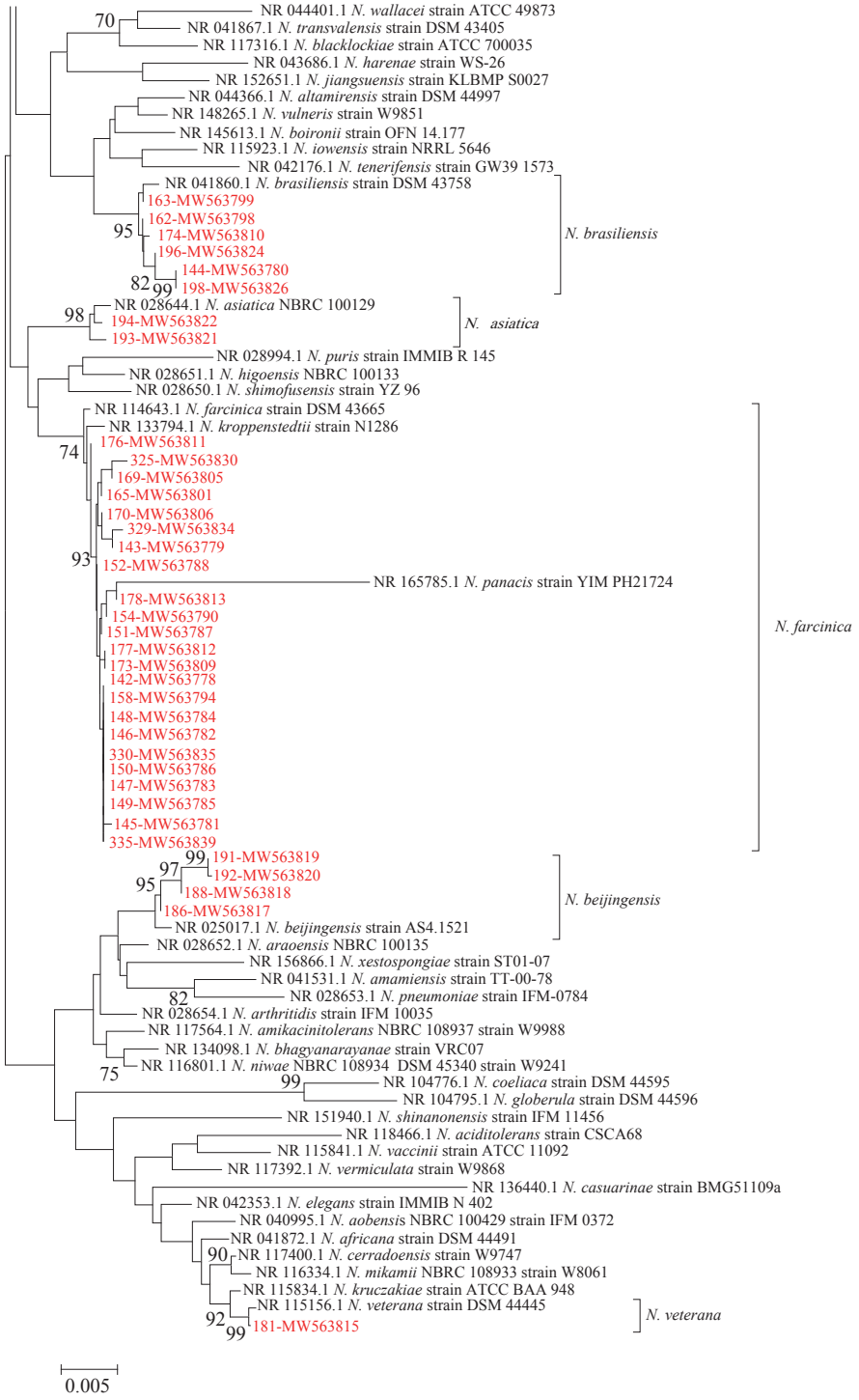

SUPPLEMENTARY FIGURE S1. NJ phylogenetic tree of 16S rRNA sequences from 63 clinical isolates in the context of *Nocardia* reference strains.

Note: *De novo* 16S rRNA sequences are shown in red and identified by both laboratory ID and GenBank ID. Clinical strains are listed in Supplementary Table S1. Reference strains were selected based on (3). Bootstrap values >70% are indicated. *De novo* sequences clustered with nine known species, indicated in brackets. Three strains did not match any known species. Strains 153 and 160 formed cluster X, while strain 159 was considered an outlier and is identified as Y. Abbreviation: NJ=Neighbor-joining.

Vital Surveillances

Characteristics and Influencing Factors of Antimicrobial Resistance in *Salmonella* Isolated from Asymptomatic Workers — Yulin City, Guangxi Zhuang Autonomous Region, China, 2013–2024

Yao Peng[1,2,&]; Ming Luo[3,&]; Ziyu Liu[2,4]; Changyu Zhou[3]; Hongqun Zhao[2]; Zhenpeng Li[2,4]; Biao Kan[1,2,#]; Ning Jiang[3,#]; Xin Lu[4,#]

ABSTRACT

Introduction: Asymptomatic carriers of antibiotic-resistant *Salmonella* constitute a significant yet frequently overlooked public health threat. This study aimed to characterize antimicrobial resistance (AMR) patterns in *Salmonella* isolated from asymptomatic workers in Yulin, China, over a 12-year period (2013–2024) and to identify the potential influence of natural and socioeconomic factors.

Methods: Antimicrobial susceptibility testing was performed against 11 antimicrobial agents. We analyzed temporal trends in AMR rates using the Mann-Kendall test and assessed associations between AMR rates and natural or socioeconomic variables using Spearman's rank correlation, Principal Component Regression (PCR), and Least Absolute Shrinkage and Selection Operator (LASSO) regression. An Autoregressive Integrated Moving Average (ARIMA) model was employed to forecast future resistance trends.

Results: Resistance to tetracycline (TET) was most prevalent (mean rate: 66.2%). The overall multidrug resistance (MDR) rate was 41.9%, exhibiting a significant increasing trend (P<0.05). Most alarmingly, the tigecycline (TGC) resistance rate surged from 0% to 24.4% by 2024. PCR model analysis revealed that a composite "Socioeconomic and Healthcare Development Index" served as the primary predictor of this increase, explaining 54.9% of the variance in TGC resistance rates. The ARIMA model forecasted a continued upward trajectory for TGC resistance through 2025–2026.

Conclusion: Our findings demonstrate a significant rise in MDR *Salmonella* among asymptomatic workers in Yulin, establishing them as important reservoirs of antibiotic-resistant *Salmonella*. The emergence and rapid escalation of TGC resistance is strongly associated with regional socioeconomic and healthcare development. These results underscore the urgent need for integrated surveillance within the One Health framework to effectively address AMR transmission.

Salmonella represents a leading cause of diarrheal disease worldwide and constitutes a major pathogen in foodborne outbreaks throughout China (*1–2*). The emergence of antimicrobial resistance (AMR) in *Salmonella* has substantially intensified this public health challenge. An alarming global increase in multidrug-resistant strains has been documented, particularly among isolates resistant to critically important antibiotics such as fluoroquinolones and third-generation cephalosporins, thereby elevating the risk of treatment failure (*3–4*).

Although clinically based surveillance systems for AMR are well established, they frequently overlook a critical transmission reservoir: asymptomatic carriers. These individuals, particularly food workers (FWs), function as silent reservoirs and play a pivotal role in disseminating resistant pathogens throughout the food supply chain. Food workers may acquire asymptomatic carriage through exposure to contaminated food products, subsequently transmitting these pathogens to additional food items and consumer populations, potentially causing disease in susceptible individuals (*5–7*).

The One Health framework provides an essential paradigm for addressing AMR by recognizing the intricate interconnections among human, animal, and environmental health. Multiple factors — including antimicrobial use in livestock production, environmental contamination, climatic conditions, and socioeconomic development — collectively shape the complex epidemiology of AMR (*8–9*). However, the

specific influence of these macro-level determinants on long-term AMR trends remains poorly characterized, particularly within asymptomatic carrier populations.

This study conducted 12-year (2013–2024) longitudinal surveillance of asymptomatic individuals in Yulin, China, to investigate the dynamic influence of natural and socioeconomic factors on *Salmonella* antimicrobial resistance. By integrating antimicrobial resistance data with environmental and socioeconomic variables, we aimed to develop evidence-based strategies for containing AMR transmission within the One Health framework.

METHODS

Sample Collection and Isolate Identification

Between January 2013 and December 2024, we collected 488,409 fecal samples from asymptomatic workers (aged 18–65 years) in Yulin, China. Samples were cultured for *Salmonella* spp. according to established protocols (*10*). Species identification was confirmed using Matrix-Assisted Laser Desorption/ Ionization Time-of-Flight Mass Spectrometry (MALDI-TOF MS), and confirmed isolates were stored at −80 °C for subsequent analysis.

Antimicrobial Susceptibility Testing

Antimicrobial susceptibility testing was performed on all *Salmonella* isolates using the Phoenix NMIC803 panel (Becton, Dickinson Co., Franklin Lakes, NJ, USA) on the BD Phoenix^{TM} automated system. Minimum inhibitory concentrations (MICs) were determined for 11 antimicrobial agents: amikacin (AMK), ceftazidime (CAZ), chloramphenicol (CHL), ciprofloxacin (CIP), colistin (COL), ertapenem (ETP), meropenem (MEM), ampicillin-sulbactam (SAM), tetracycline (TET), tigecycline (TGC), and trimethoprim-sulfamethoxazole (SXT). Resistance profiles were interpreted according to the Clinical and Laboratory Standards Institute (CLSI) M100 guidelines (30th Edition) (*11*). *Escherichia coli* ATCC 25922 served as the quality control strain. Multidrug resistance (MDR) was defined as acquired non-susceptibility to at least one agent in three or more antimicrobial categories (*12*).

Collection of Data on Natural and Socioeconomic Factors

To identify potential drivers of temporal changes in *Salmonella* antimicrobial resistance rates, we collected data on environmental conditions and socioeconomic variables. Monthly meteorological data, including mean temperature (℃) and precipitation (mm), were obtained from the China Meteorological Data Service Center. Annual economic and public health indicators from 2013 to 2023 were sourced from the Guangxi Zhuang Autonomous Region Bureau of Statistics (http://tjj.gxzf.gov.cn). This dataset encompassed gross domestic product (GDP), per capita GDP, urbanization rate, number of hospitals, number of hospital beds, number of public toilets, water consumption, and the production and consumption of pork and poultry. Additionally, national antibiotic consumption data were acquired from the One Health Trust's ResistanceMap platform (https://resistancemap.onehealthtrust.org/AntibioticUse.php).

Statistical Analysis

All statistical analyses were performed using R software (version 4.3.3, R Foundation for Statistical Computing, Vienna, Austria). Temporal trends in annual antimicrobial resistance rates were evaluated using the Mann-Kendall test. Associations between antimicrobial resistance rates and natural or socioeconomic variables were assessed through Spearman's rank correlation analysis. To address multicollinearity among predictor variables, particularly when modeling annual tigecycline resistance rates, we employed two complementary regression approaches: Principal Component Regression (PCR) and Least Absolute Shrinkage and Selection Operator (LASSO) regression. Subsequently, an Autoregressive Integrated Moving Average (ARIMA) model was constructed to project future trends in tigecycline resistance. Statistical significance was defined as a two-sided $P<0.05$ for all analyses.

RESULTS

Overall Antimicrobial Resistance Trend

According to our previous study (*13*), between 2013 and 2024, a total of 9,276 non-duplicate *Salmonella* strains were isolated from 488,409 fecal samples collected from asymptomatic workers in Yulin. Antimicrobial susceptibility testing revealed substantial and rising resistance rates across several key antimicrobial agents (Figure 1A). Resistance to TET was the most prevalent, with a mean rate of 66.2% across the study period. Resistance rates for CHL

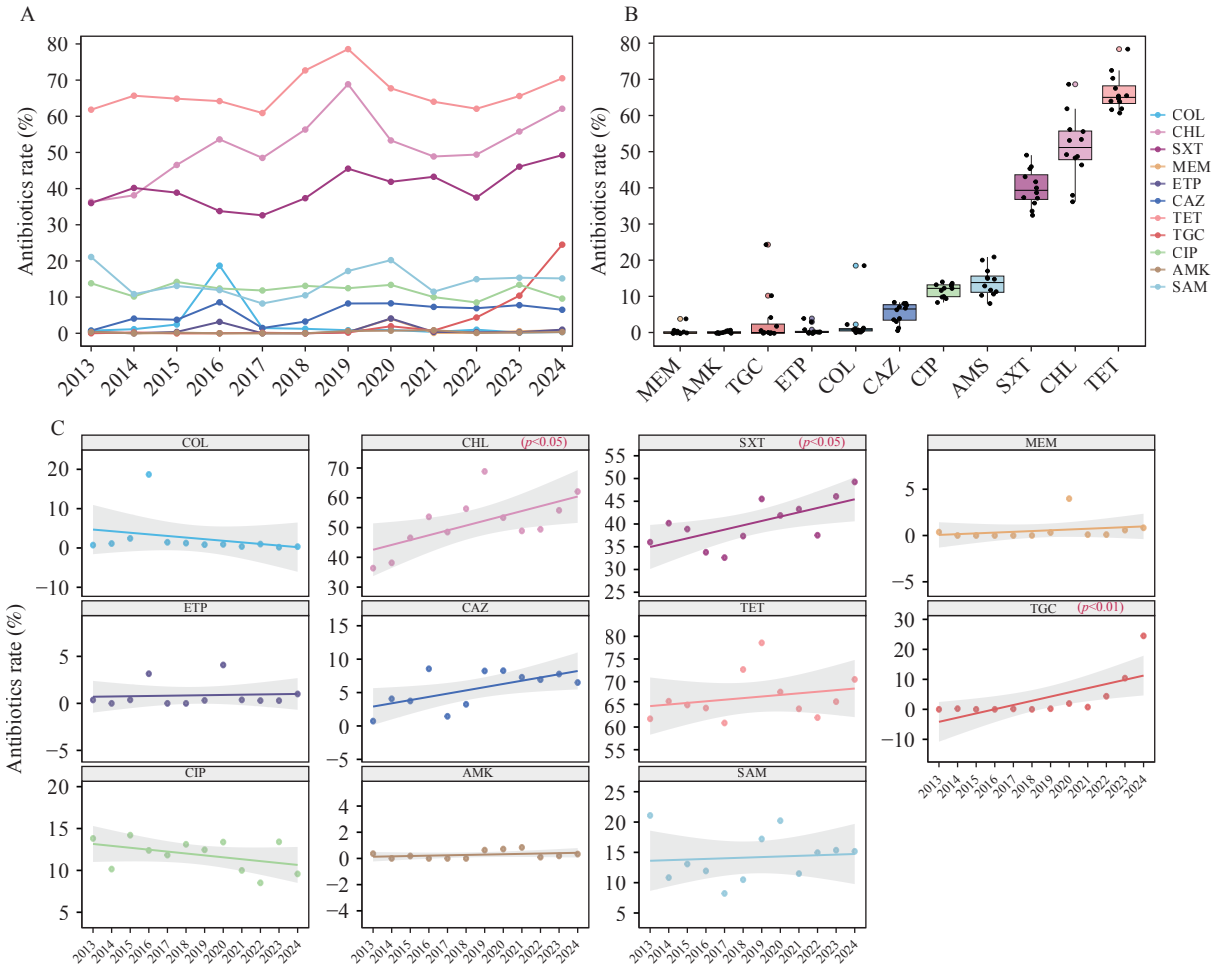

FIGURE 1. Temporal trends and overall rates of antimicrobial resistance (2013–2024). (A) Line chart illustrating the annual resistance rates (%) for 11 different antimicrobials over the 12-year study period. (B) Overall distribution of resistance rates for each antimicrobial over the 12-year period, showing the median (line), interquartile range (box), and annual values (dots). (C) Linear regression plots showing resistance trends over time.
Note: For (A), Each colored line represents a specific antimicrobial agent. For (C), The shaded area is the 95% confidence interval. *P* values indicate a significant increasing trend of the annual resistance rates for CHL, SXT, and TGC.
Abbreviation: CHL=chloramphenicol; SXT=trimethoprim-sulfamethoxazole; TGC=tigecycline; AMK=amikacin; CAZ=ceftazidime; CIP=ciprofloxacin; COL=colistin; ETP=ertapenem; MEM=meropenem; SAM=ampicillin-sulbactam, TET=tetracycline.

(mean 49.6%) and SXT (mean 38.9%) were also substantial and demonstrated significant upward trends (P<0.05 for both). Although resistance to carbapenems (MEM and ETP) and COL remained comparatively low (0.8% and 2.6%, respectively), their detection indicates that the efficacy of last-line antibiotics is threatened (Figure 1A).

A critical finding was the rapid increase in TGC resistance from 0% in 2021 to 24.5% in 2024, highlighting a significant and emerging public health concern. In contrast, COL resistance declined significantly after peaking at 17% in 2016 (Figure 1A). This downward trend is potentially attributable to the 2017 governmental regulatory change that banned the use of colistin as an animal growth-promoting feed additive, as implemented by the Ministry of Agriculture of China (*11*).

Trends in Multidrug Resistance

The overall MDR rate was 41.86% (3,883/9,276), demonstrating a significant upward trend (P<0.05) with an 11.8% increase over the decade. The MDR rate remained relatively stable through 2018, then surged to 49.5% in 2019, followed by a slight decline from 2020 to 2022, before rising again to exceed 45% from 2023 to 2024. This pattern suggests an exacerbation of the resistance burden in recent years (Figure 2A).

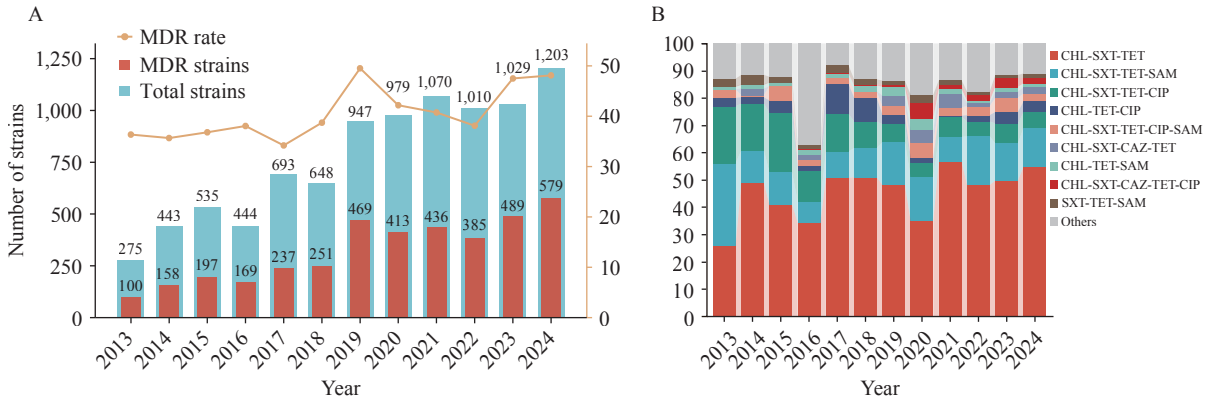

FIGURE 2. Trends in multidrug-resistant *Salmonella* isolations and MDR profiles in Yulin City, 2013–2024. (A) Annual trends of multidrug-resistant *Salmonella* isolates. (B) Temporal distribution of major MDR profiles among the resistant isolates.
Note: For (A), the bar chart displays the total number of isolates (light blue) and the subset of multidrug-resistant isolates (red) collected each year (left y-axis). The orange line indicates the corresponding annual MDR rate (%, right y-axis). For (B), the 100% stacked area chart illustrates the relative annual proportion of different resistance patterns. The dominant CHL-SXT-TET profile is highlighted in red. The "Others" category includes all other less frequent MDR combinations.
Abbreviation: MDR=multidrug resistance; CHL=chloramphenicol; SXT=trimethoprim-sulfamethoxazole; TET=tetracycline; CAZ=ceftazidime; CIP=ciprofloxacin; SAM=ampicillin-sulbactam; TET=tetracycline.

Analysis of resistance patterns revealed that CHL-SXT-TET was the most dominant MDR profile, accounting for 47.7% of all MDR isolates. The next most prevalent profiles were CHL-SXT-TET-SAM (13.7%) and CHL-SXT-TET-CIP (8.8%). Notably, the prevalence of the CHL-SXT-TET-CIP pattern exhibited a downward trend (Figure 2B). Seventeen isolates demonstrated resistance to both quinolones and third-generation cephalosporins. More alarmingly, eight of these isolates were also resistant to carbapenems and colistin, representing a critical threat to last-resort treatment options.

Correlations Between Resistance Rates and Natural and Socioeconomic Factors

Spearman's rank correlation analysis identified significant associations between AMR patterns and both natural and socioeconomic variables. Among natural factors, resistance rates to CHL, TET, AMK, and SAM exhibited weak positive correlations with temperature (r= 0.244–0.262). To investigate temporal dynamics, we conducted a time-lag analysis examining temperature effects on resistance rates. The strongest associations occurred when comparing resistance rates with concurrent monthly temperatures (0-month lag). These correlations diminished rapidly when temperature values were lagged by one or two months prior to resistance measurement (1-month lag/2-month lag), with only the AMK resistance rate maintaining significance at a 1-month lag (Supplementary Table S1, available at https://weekly.chinacdc.cn/). Regarding precipitation, only the SAM resistance rate demonstrated a significant correlation with rainfall patterns.

TGC resistance rates exhibited particularly strong positive correlations with multiple socioeconomic indicators, including GDP (r=0.805), per capita GDP (r=0.805), urbanization rate (r=0.791), number of hospitals (r=0.840), number of hospital beds (r=0.833), and agricultural water usage (r=0.819). Additionally, meropenem resistance rates correlated positively with poultry production in Yulin (r=0.801), while the overall MDR rate showed positive correlations with both poultry production and consumption (Figure 3A).

Identifying Influencing Factors of Tigecycline Resistance

Five socioeconomic factors demonstrated significant associations with TGC resistance rates. To address the substantial multicollinearity among these variables, we employed both PCR and LASSO regression models. The PCR analysis identified a single principal component, designated the "Socioeconomic and Healthcare Development Index (SHDI)", which accounted for 89.5% of the total variance across the original factors. This composite index exhibited a strong positive correlation with TGC resistance rates, explaining 54.9% of the observed variance. Component loading analysis revealed that all six variables contributed positively to this index. The primary drivers of the SHDI were the number of

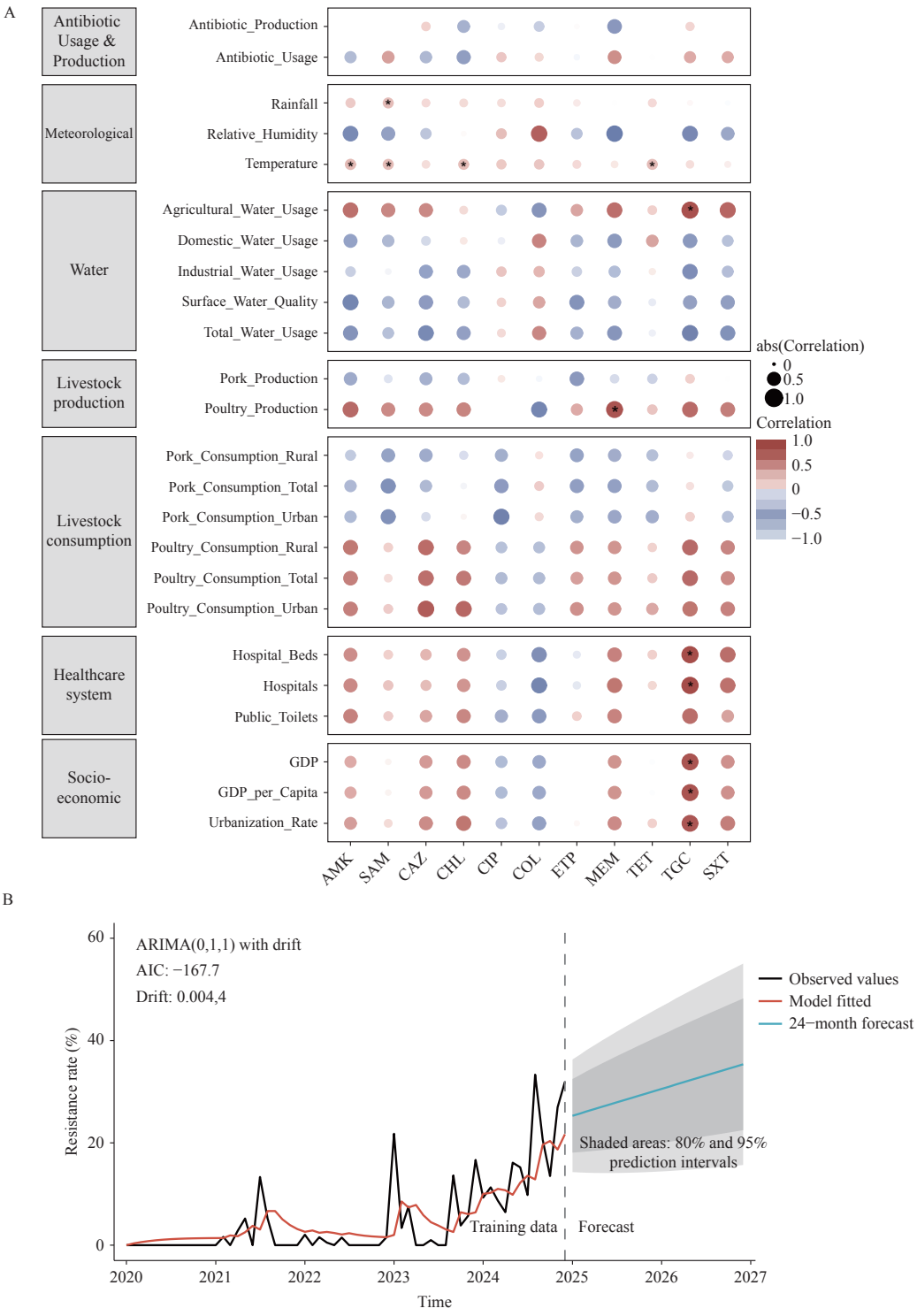

FIGURE 3. Correlation between the resistance rates to 11 antibiotics and natural/socioeconomic factors, and forecasting of TGC resistance. (A) Spearman correlation matrix between potential influencing factors and antimicrobial resistance rates. (B) Time-series forecast for TGC resistance based on an ARIMA (0,1,1) model with drift.

Note: For (A), the color and size of the circles represent the direction and magnitude of the correlation, respectively. For (B), the black line shows actual data, while the blue line and shaded areas show the point forecast with 80% and 95% prediction intervals.

Abbreviation: CHL=chloramphenicol; SXT=trimethoprim-sulfamethoxazole; TGC=tigecycline; AMK=amikacin; CAZ=ceftazidime; CIP=ciprofloxacin; COL=colistin; ETP=ertapenem; MEM=meropenem; SAM=ampicillin-sulbactam, TET=tetracycline; abs=absolute value; ARIMA= Autoregressive Integrated Moving Average; AIC=Akaike Information Criterion.

* Significance (P<0.05).

hospital beds (loading=0.425), GDP (0.417), GDP per capita (0.416), urbanization rate (0.415), number of hospitals (0.402), and agricultural water usage (0.373). This composition confirms that the index effectively captures the convergent trends of economic growth, urbanization, and healthcare infrastructure expansion. In contrast, the LASSO regression penalized all individual factor coefficients to zero, indicating that no single variable independently predicted resistance when accounting for multicollinearity. The combined results from both analytical approaches strongly indicate that the rise in TGC resistance rates is driven by an integrated set of underlying socioeconomic factors rather than any single determinant.

Forecasting Tigecycline Resistance Rate

The resistance rate to TGC has demonstrated a significant upward trajectory in recent years, prompting the development of an ARIMA model to forecast potential future threats. Initial modeling using TGC resistance data from January 2013 to December 2024 yielded a significant Ljung-Box test result (P=0.03), indicating residual autocorrelation. Given that TGC resistance rates were negligible before 2020, we refined the model using only data from January 2020 to December 2024. The optimal model specification, determined by the Akaike Information Criterion (AIC=−167.74), was ARIMA (0,1,1) with a drift term of 0.004. This refined model produced a non-significant Ljung-Box test result (P=0.08), confirming the absence of substantial residual autocorrelation and indicating that residuals approximated white noise. The model demonstrated strong predictive performance, with a Root Mean Square Error (RMSE) of 0.05 and a Mean Absolute Error (MAE) of 0.04, supporting its utility for trend identification and informing targeted public health interventions, including enhanced surveillance protocols and strategic resource allocation.

DISCUSSION

This 12-year surveillance study of asymptomatic workers revealed a significant increase in the prevalence of MDR *Salmonella*, with the CHL-SXT-TET resistance profile emerging as the most dominant pattern. Notably, our findings demonstrate the emergence of TGC resistance, which is strongly associated with a composite index of regional socioeconomic and healthcare development. The ARIMA model's forecast of continued increases in TGC resistance serves as a critical warning that demands immediate public health attention and intervention.

The persistently high resistance rate to TET (66.2%) and the increasing resistance to CHL align with other studies (*14*–*16*) and are likely attributable to their historical overuse in both agricultural and clinical settings (*17*). Of greater concern is the detection of isolates resistant to TGC, COL, and the carbapenems (ETP and MEM). The emergence of resistance to these last-line agents within a community setting, particularly among food workers, represents a serious public health challenge with implications for treatment options.

Temperature serves as a key driver of AMR dissemination. Higher temperatures have been shown to accelerate the frequency of horizontal gene transfer (HGT), the principal mechanism for the dissemination of resistance genes among bacterial communities, primarily through conjugation (*18*–*19*). Warmer temperatures are also associated with higher insect populations, which contribute to disseminating resistant bacteria (*20*). These mechanisms explain the positive correlations observed between temperature and resistance to CHL, TET, AMK, and SAM in our study. Although a positive relationship was identified for AMK, this result should be interpreted cautiously due to the small sample size of AMK-resistant isolates (n=31), which reduces statistical power and may affect the reliability of the correlation analysis. Despite this limitation, our findings suggest that rising global temperatures may exacerbate the spread of resistant phenotypes. Therefore, increased attention must be directed toward understanding the impact of global warming on AMR dynamics.

The strong positive correlation between the "Socioeconomic and Healthcare Development Index" and TGC resistance rates provides novel insight into the macro-level drivers of AMR. This finding aligns with previous research demonstrating that socioeconomic factors — including health investment, out-of-pocket health costs, access to water, sanitation, and hygiene (WASH) services, and immunization coverage — contribute to the rise of AMR (*21*). Tigecycline, a glycylcycline antibiotic, is often reserved as a last-resort treatment for severe infections caused by MDR pathogens, such as carbapenem-resistant Enterobacteriaceae (CRE) and *Acinetobacter baumannii* (*22*–*23*). Importantly, tigecycline use is prohibited in all food-producing animals (*24*–*25*). This regulatory

context strongly supports our finding that the rise in TGC resistance is linked to the "Socioeconomic and Healthcare Development Index" (which encompasses hospital numbers and bed capacity) and is driven by human healthcare pressures rather than agricultural practices. The positive correlation between MDR rates and poultry production and consumption further reinforces the One Health framework, highlighting the critical role of food chain pathways in disseminating AMR and antibiotic resistance genes (ARGs) from animals to humans, as emphasized in global analyses (*26*).

Several limitations warrant consideration. First, our data originate from a single region, which may limit generalizability to other geographic contexts. Second, we did not perform genomic analyses (e.g., whole-genome sequencing) to trace specific resistance genes or elucidate transmission pathways at the molecular level. Future research should integrate comprehensive genomic surveillance to identify the genetic mechanisms and transmission dynamics underlying the observed resistance trends.

In conclusion, this 12-year surveillance study demonstrates that AMR *Salmonella* isolated from asymptomatic carriers represents a growing public health threat in Yulin, characterized by increasing MDR rates and emerging TGC resistance. These resistance patterns are influenced by both natural and socioeconomic factors. Our findings underscore the urgent need for integrated surveillance and management strategies to contain AMR transmission. Specifically, surveillance programs must address the critical issue of asymptomatic carriage and silent transmission of antibiotic-resistant pathogens in healthy populations, particularly among food handlers who serve as key reservoirs in the transmission chain.

Conflicts of interest: No conflicts of interest.

Acknowledgements: Supported by the National Key Research and Development Program of China (2022YFC2303900) and the major projects of the National Natural Science Foundation of China (22193064).

doi: 10.46234/ccdcw2025.243

[#] Corresponding authors: Ning Jiang, ylcdcjn@163.com; Biao Kan, kanbiao@icdc.cn; Xin Lu, luxin@icdc.cn.

[1] School of Public Health, Nanjing Medical University, Nanjing City, Jiangsu Province, China; [2] National Key Laboratory of Intelligent Tracking and Forecasting for Infectious Diseases, National Institute for Communicable Disease Control and Prevention, Chinese Center for Disease Control and Prevention, Beijing, China; [3] Yulin Center for Disease Control and Prevention, Yulin City, Guangxi Zhuang Autonomous Region, China; [4] Department of Microbiomics, National Institute for Communicable Disease Control and Prevention, Chinese Center for Disease Control and Prevention, Beijing, China.
[&] Joint first authors.

Submitted: October 14, 2025
Accepted: November 06, 2025
Issued: November 14, 2025

REFERENCES

1. Wang LP, Zhou SX, Wang X, Lu QB, Shi LS, Ren X, et al. Etiological, epidemiological, and clinical features of acute diarrhea in China. Nat Commun 2021;12(1):2464. https://doi.org/10.1038/s41467-021-22551-z.
2. Li WW, Pires SM, Liu ZT, Ma XC, Liang JJ, Jiang YY, et al. Surveillance of foodborne disease outbreaks in China, 2003–2017. Food Control 2020;118:107359. https://doi.org/10.1016/j.foodcont.2020.107359.
3. GBD 2021 Antimicrobial Resistance Collaborators. Global burden of bacterial antimicrobial resistance 1990–2021: a systematic analysis with forecasts to 2050. Lancet 2024;404(10459):1199 – 226. https://doi.org/10.1016/S0140-6736(24)01867-1.
4. Antimicrobial Resistance Collaborators. Global burden of bacterial antimicrobial resistance in 2019: a systematic analysis. Lancet 2022;399(10325):629 – 55. https://doi.org/10.1016/S0140-6736(21)02724-0.
5. Ehuwa O, Jaiswal AK, Jaiswal S. *Salmonella*, food safety and food handling practices. Foods 2021;10(5):907. https://doi.org/10.3390/foods10050907.
6. Viana GGF, Cardozo MV, Pereira JG, Rossi GAM. Antimicrobial resistant *Staphylococcus* spp. , Escherichia coli, and Salmonella spp. in food handlers: a global review of persistence, transmission, and mitigation challenges. Pathogens 2025;14(5):496. https://doi.org/10.3390/pathogens14050496.
7. Han RR, Shi QY, Wu S, Yin DD, Peng MJ, Dong D, et al. Dissemination of carbapenemases (KPC, NDM, OXA-48, IMP, and VIM) among carbapenem-resistant *Enterobacteriaceae* isolated from adult and children patients in China. Front Cell Infect Microbiol 2020;10:314. https://doi.org/10.3389/fcimb.2020.00314.
8. Matheou A, Abousetta A, Pascoe AP, Papakostopoulos D, Charalambous L, Panagi S, et al. Antibiotic use in livestock farming: a driver of multidrug resistance? Microorganisms 2025;13(4):779. http://dx.doi.org/10.3390/microorganisms13040779.
9. Zhao WY, Ye CS, Li JG, Yu X. Increased risk of antibiotic resistance in surface water due to global warming. Environ Res 2024;263(Pt 2):120149. http://dx.doi.org/10.1016/j.envres.2024.120149.
10. Im J, Nichols C, Bjerregaard-Andersen M, Sow AG, Løfberg S, Tall A, et al. Prevalence of *Salmonella* excretion in stool: a community survey in 2 sites, Guinea-Bissau and Senegal. Clin Infect Dis 2016;62 Suppl 1 (Suppl 1):S50-5. http://dx.doi.org/10.1093/cid/civ789.
11. Satlin MJ, Lewis II JS, Weinstein MP, Patel J, Humphries RM, Kahlmeter G, et al. Clinical and laboratory standards institute and European Committee on antimicrobial susceptibility testing position statements on polymyxin B and colistin clinical breakpoints. Clin Infect Dis 2020;71(9):e523 – 9. https://doi.org/10.1093/cid/ciaa121.
12. Magiorakos AP, Srinivasan A, Carey RB, Carmeli Y, Falagas ME, Giske CG, et al. Multidrug-resistant, extensively drug-resistant and pandrug-resistant bacteria: an international expert proposal for interim standard definitions for acquired resistance. Clin Microbiol Infect 2012;18(3):268 – 81. https://doi.org/10.1111/j.1469-0691.2011.03570.x.
13. Lu X, Luo M, Wang MY, Zhou ZM, Xu JL, Li ZP, et al. High carriage and possible hidden spread of multidrug-resistant *Salmonella* among asymptomatic workers in Yulin, China. Nat Commun 2024;15(1):

10238. https://doi.org/10.1038/s41467-024-54405-9.
14. Gargano V, Sciortino S, Gambino D, Costa A, Agozzino V, Reale S, et al. Antibiotic susceptibility profile and tetracycline resistance genes detection in *Salmonella* spp. strains isolated from animals and food. Antibiotics (Basel) 2021;10(7):809. https://doi.org/10.3390/antibiotics10070809.
15. Wei B, Shang K, Cha SY, Zhang JF, Jang HK, Kang M. Clonal dissemination of *Salmonella enterica* serovar *albany* with concurrent resistance to ampicillin, chloramphenicol, streptomycin, sulfisoxazole, tetracycline, and nalidixic acid in broiler chicken in Korea. Poult Sci 2021;100(7):101141. https://doi.org/10.1016/j.psj.2021.101141.
16. Ohata N, Noda M, Ohta K, Hatta M, Nakayama T. Prevalence of streptomycin and tetracycline resistance and increased transmissible third-generation cephalosporin resistance in *Salmonella enterica* isolates derived from food handlers in Japan from 2006 to 2021. J Appl Microbiol 2024;135(9):lxae236. https://doi.org/10.1093/jambio/lxae236.
17. Chereau F, Opatowski L, Tourdjman M, Vong S. Risk assessment for antibiotic resistance in South East Asia. BMJ 2017;358:j3393. https://doi.org/10.1136/bmj.j3393.
18. Zhao WY, Zhang BH, Zheng SK, Yan WL, Yu X, Ye CS. High temperatures promote antibiotic resistance genes conjugative transfer under residual chlorine: mechanisms and risks. J Hazard Mater 2025;483:136675. https://doi.org/10.1016/j.jhazmat.2024.136675.
19. Zhao CD, Suyamud B, Yuan Y, Ghosh S, Xu XL, Hu JY. Effect of non-antibiotic factors on conjugative transfer of antibiotic resistance genes in aquaculture water. J Hazard Mater 2025;483:136701. https://doi.org/10.1016/j.jhazmat.2024.136701.
20. Onwugamba FC, Fitzgerald JR, Rochon K, Guardabassi L, Alabi A, Kühne S, et al. The role of 'filth flies' in the spread of antimicrobial resistance. Travel Med Infect Dis 2018;22:8 – 17. https://doi.org/10.1016/j.tmaid.2018.02.007.
21. Li WB, Huang TT, Liu CJ, Wushouer H, Yang XY, Wang RN, et al. Changing climate and socioeconomic factors contribute to global antimicrobial resistance. Nat Med 2025;31(6):1798 – 808. https://doi.org/10.1038/s41591-025-03629-3.
22. Sun CT, Cui MQ, Zhang S, Wang HJ, Song L, Zhang CP, et al. Plasmid-mediated tigecycline-resistant gene *tet*(X4) in *Escherichia coli* from food-producing animals, China, 2008-2018. Emerg Microbes Infect 2019;8(1):1524 – 7. https://doi.org/10.1080/22221751.2019.1678367.
23. Jin X, Chen Q, Shen F, Jiang Y, Wu XQ, Hua XT, et al. Resistance evolution of hypervirulent carbapenem-resistant *Klebsiella pneumoniae* ST11 during treatment with tigecycline and polymyxin. Emerg Microbes Infect 2021;10(1):1129 – 36. https://doi.org/10.1080/22221751.2021.1937327.
24. Lan X, Qin SG, Liu H, Guo MR, Zhang YP, Jin XY, et al. Dual-targeting tigecycline nanoparticles for treating intracranial infections caused by multidrug-resistant *Acinetobacter baumannii*. J Nanobiotechnology 2024;22(1):138. https://doi.org/10.1186/s12951-024-02373-z.
25. He T, Wang R, Liu DJ, Walsh TR, Zhang R, Lv Y, et al. Emergence of plasmid-mediated high-level tigecycline resistance genes in animals and humans. Nat Microbiol 2019;4(9):1450 – 6. https://doi.org/10.1038/s41564-019-0445-2.
26. Allel K, Day L, Hamilton A, Lin LES, Furuya-Kanamori L, Moore CE, et al. Global antimicrobial-resistance drivers: an ecological country-level study at the human–animal interface. Lancet Planet Health 2023;7(4):e291 – 303. https://doi.org/10.1016/S2542-5196(23)00026-8.

SUPPLEMENTARY MATERIAL

SUPPLEMENTARY TABLE S1. Correlation between temperature and antibiotic resistance rates.

Antibiotics	Temperature		Temperature adjustment			
			One-month lag		Two-month lag	
	r	*P*	*r*	*P*	*r*	*P*
AMK	0.2621	0.0133*	0.2497	0.0443*	0.1599	0.3808
SAM	0.2496	0.0133*	0.1942	0.0962	0.0983	0.5846
CAZ	0.1082	0.2869	0.0941	0.4478	0.0705	0.5846
CHL	0.2439	0.0133*	0.1707	0.1411	0.103	0.5846
CIP	0.1956	0.0551	0.0604	0.5423	−0.0375	0.7394
COL	0.2035	0.0524	0.1283	0.3172	0.0755	0.5846
ETP	0.1213	0.2608	0.0837	0.4699	0.0194	0.8264
MEM	0.0723	0.4512	0.0705	0.5180	0.0812	0.5846
SXT	0.0492	0.5756	−0.0475	0.5899	−0.0608	0.6017
TET	0.2476	0.0133 *	0.2182	0.0676	0.1948	0.2899
TIG	0.1041	0.2869	0.1088	0.3963	0.0784	0.5846

*Significance (P<0.05).

Abbreviation: CHL=chloramphenicol; SXT=trimethoprim-sulfamethoxazole; TIG=tigecycline; AMK=amikacin; CAZ=ceftazidime; CIP=ciprofloxacin; COL=colistin; ETP=ertapenem; MEM=meropenem; SAM=ampicillin-sulbactam; TET=tetracycline.

Preplanned Studies

High Prevalence and Genomic Characterization of Extended-Spectrum β-Lactamase-Producing *Escherichia coli* in the Yellow River and Source Water from A One Health Perspective — Henan Province, China, 2023–2024

Tiantian Tian[1,2,3]; Yan Sun[1]; Yunfeng Shi[1]; Shimin Zhang[1]; Shuxia Xu[1]; Jiran Zhang[1]; Xitian Yang[3]; Yu Zhang[2,4,#]

Summary

What is already known about this topic?

The Yellow River serves as a significant conduit for antibiotic resistance transmission from environmental reservoirs to human populations. However, the occurrence and transmission pathways of the clinically relevant extended-spectrum β-lactamase (ESBL) gene *bla*$_{\text{CTX-M-G9}}$ and ESBL-producing *Escherichia coli* (*E. coli*) within the Yellow River remain poorly characterized.

What is added by this report?

This study reveals the widespread prevalence of *bla*$_{\text{CTX-M-G9}}$ throughout the Yellow River and its associated water sources in Henan Province, and demonstrates the environmental dissemination and probable animal origin of the dominant *E. coli* sequence type (ST) 6802 harboring the *bla*$_{\text{CTX-M-14}}$ genotype.

What are the implications for public health practice?

The findings underscore the critical need to strengthen environmental surveillance and implement robust control measures targeting antibiotic resistance of animal origin. Additionally, we advocate for enhanced public awareness and education initiatives regarding antibiotic resistance to foster broader societal engagement and support for mitigation efforts.

ABSTRACT

Introduction: Understanding the prevalence and dissemination pathways of the clinically relevant extended-spectrum β-lactamase (ESBL) genes and ESBL-producing *Escherichia coli* (*E. coli*) within the Yellow River is essential from a One Health perspective to control antibiotic resistance dissemination from environmental reservoirs to human populations.

Methods: Water samples were collected from the Yellow River and two of its major tributaries in Henan Province during 2023 and 2024. TaqMan quantitative polymerase chain reaction (qPCR) was used to quantify the abundance of the ESBL gene *bla*$_{\text{CTX-M-G9}}$. Twenty-three *E. coli* isolates underwent whole-genome sequencing (WGS), and 167 publicly available *E. coli* genomes from diverse sources were incorporated into the comparative phylogenetic analysis.

Results: The *bla*$_{\text{CTX-M-G9}}$ gene was ubiquitous across all sampling sites, exhibiting significantly higher relative abundance during the dry season compared to the flat season. The multidrug-resistant *E. coli* sequence type (ST) 6802 carrying *bla*$_{\text{CTX-M-14}}$ emerged as the predominant clone. Strong positive correlations were observed between *bla*$_{\text{CTX-M-G9}}$ abundance and plasmids carried by *E. coli* ST6802 in the Yellow River, providing evidence for clonal expansion during the dry season. Furthermore, comparative phylogenetic analysis integrating human, animal, and environmental isolates demonstrated that ST6802 strains from this study were closely related to those previously identified in anaerobic digestion systems treating pig manure in China, suggesting an animal-to-environment transmission pathway.

Conclusion: These findings emphasize the urgent need to implement targeted interventions that prevent the transmission of antibiotic resistance from animal sources into aquatic environments, thereby protecting public health and preserving the integrity of critical water resources.

The emergence and spread of extended-spectrum β-lactamase (ESBL)-producing *Escherichia coli* (*E. coli*) poses a substantial threat to public health worldwide. In 2019, antimicrobial resistance accounted for an estimated 145,000 deaths in China, with ESBL-

producing *E. coli* ranking as the third leading cause (8,032 deaths) (*1*). Recognizing this growing concern, the World Health Organization launched the "ESBL *E. coli* tricycle AMR surveillance project" in 2017, which encompasses monitoring across human populations, the food chain, and environmental reservoirs. Environmental surveillance has historically been the weakest component of this integrated approach. However, recent years have witnessed increasing attention to ESBL-producing *E. coli* surveillance in environmental settings (*2*). Among the diverse ESBLs, the cefotaxime from Munich (CTX-M) has emerged as the most prevalent ESBL type globally. In China, *E. coli* strains carrying CTX-M group 9 variants, particularly the CTX-M-14 subtype, predominate, despite CTX-M group 1 subtype CTX-M-15 being the most widespread variant internationally (*3*). Surveillance data from Chinese hospitals revealed a high prevalence (62.8%) of CTX-M group genes in *E. coli* isolated from outpatients. The most common genotype was the CTX-M group 9 subtype $bla_{\text{CTX-M-14}}$ (57.7%), followed by $bla_{\text{CTX-M-55}}$ (23.4%) and $bla_{\text{CTX-M-15}}$ (15.4%) (*4*). Notably, *E. coli* isolates from community-acquired urinary tract infections across various regions demonstrated a high prevalence of $bla_{\text{CTX-M-14}}$ genotype, with an incidence rate of 31.8% (*5*). Our previous research identified $bla_{\text{CTX-M-14}}$ as the dominant genotype in *E. coli* from anaerobic digestion systems treating pig manure (*6*).

The Yellow River, China's second longest river at 5,464 km, plays a critical role in water supply and agricultural irrigation throughout northern China. Flowing through densely populated urban areas and extensive agricultural lands, the river basin receives environmental discharges exceeding 3,000 tons of antibiotics annually (*7*), thereby functioning as both a reservoir and transmission medium for antibiotic resistance genes (ARGs). Understanding the prevalence, transmission dynamics, and potential sources of CTX-M group 9 genes and CTX-M-producing *E. coli* in the Yellow River and its associated source waters is essential from a One Health perspective to effectively control ARG dissemination from environmental reservoirs to human populations. Despite this critical need, the abundance of CTX-M group 9 genes and the dissemination routes of CTX-M-producing *E. coli* in the Yellow River remain poorly characterized.

Henan Province is located in the east-central region of China, encompassing the middle and lower reaches of the Yellow River. Although urban areas have primarily relied on the South-to-North Water Transfer Project since 2014, several regions in Henan continue to utilize water from the Yellow River as their primary or backup source for drinking water, irrigation, and landscaping. In this study, we collected water samples from the Yellow River at six cities in Henan Province (Lingbao, Luoyang, Jiaozuo, Xinxiang, Zhengzhou, and Puyang), an associated water source in Zhengzhou City, and two major tributaries (the Qin River and the Yiluo River) upstream of the water source. Sampling was conducted during three distinct hydrological periods: the wet season (August 2023), the dry season (December 2023), and the flat season (April 2024).

We employed TaqMan quantitative polymerase chain reaction (qPCR) to quantify the abundance of the $bla_{\text{CTX-M-G9}}$ gene and its associated mobile genetic elements (MGEs). The qPCR primers are provided in Supplementary Table S1 (available at https://weekly.chinacdc.cn/). During the dry season, we filtered 100 mL water samples from each sampling point through 0.45 μm microporous membranes for bacterial isolation. The filtered membranes were incubated on fuchsin sodium sulfite medium supplemented with 4 mg/L cefotaxime at 37 °C for 24 h. All colonies were isolated and purified. A total of 75 cefotaxime-resistant *E. coli* strains were recovered from Lingbao (n=10), Luoyang (n=7), Yiluo River (n=10), Jiaozuo (n=1), Qin River (n=4), Xinxiang (n=11), the water source in Zhengzhou City (n=17), and Puyang (n=15). All strains underwent polymerase chain reaction (PCR) detection of CTX-M group 9 genes and antibiotic susceptibility testing by disk diffusion methods as previously reported (6, *8*–*9*). We selected 23 *E. coli* isolates for whole-genome sequencing (WGS) based on their diverse antibiotic resistance profiles (Supplementary Table S2, available at https://weekly.chinacdc.cn/), ensuring representation of the range of resistance patterns observed. Additionally, we downloaded 167 *E. coli* genomes from the National Center for Biotechnology Information (NCBI) database (CTX-M-14-producing *E. coli*, n=162) and the EnteroBase database (*E. coli* ST6802, n=5) for comparative phylogenetic analysis.

WGS of 23 *E. coli* strains was performed using the Illumina NovaSeq PE150 platform (Sinobiocore Biotechnology Co., Ltd., Beijing, China). The genome sequences were deposited in the NCBI database under accession number PRJNA1306565. The assembled contig files were uploaded to the Centre for Genomic Epidemiology (CGE) platform (http://www.

genomicepidemiology.org/) for screening of ARGs, virulence factors (VFs), and plasmid replicon types, as well as multilocus sequence typing (MLST) analysis. Single nucleotide polymorphisms (SNPs) were determined on the CGE platform, and the SNP-based phylogenetic tree was visualized in iTOL online. The complete genome multilocus sequence typing (cgMLST) analysis was conducted using PubMLST (https://pubmlst.org/) and R (Version 4.4.1, R Foundation for Statistical Computing, Vienna, Austria). The cgMLST-based minimum spanning tree was generated using GrapeTree (Version 1.5.0, University of Melbourne, Melbourne, Australia).

The *bla*$_{\text{CTX-M-G9}}$ gene was ubiquitously detected across all sampling sites in the Yellow River, its tributaries, and the associated water source (Figure 1A). Relative abundance of *bla*$_{\text{CTX-M-G9}}$ was significantly higher during the dry season (10^{-5}-10^{-3} copies/16S rDNA) compared to the flat season (10^{-6}-10^{-4} copies/16S rDNA) (Figure 1B), with peak levels observed in the water source during the dry season. Antibiotic susceptibility testing results for all 75 cefotaxime-resistant *E. coli* isolates are presented in Supplementary Table S2. Among these isolates, 98.7%

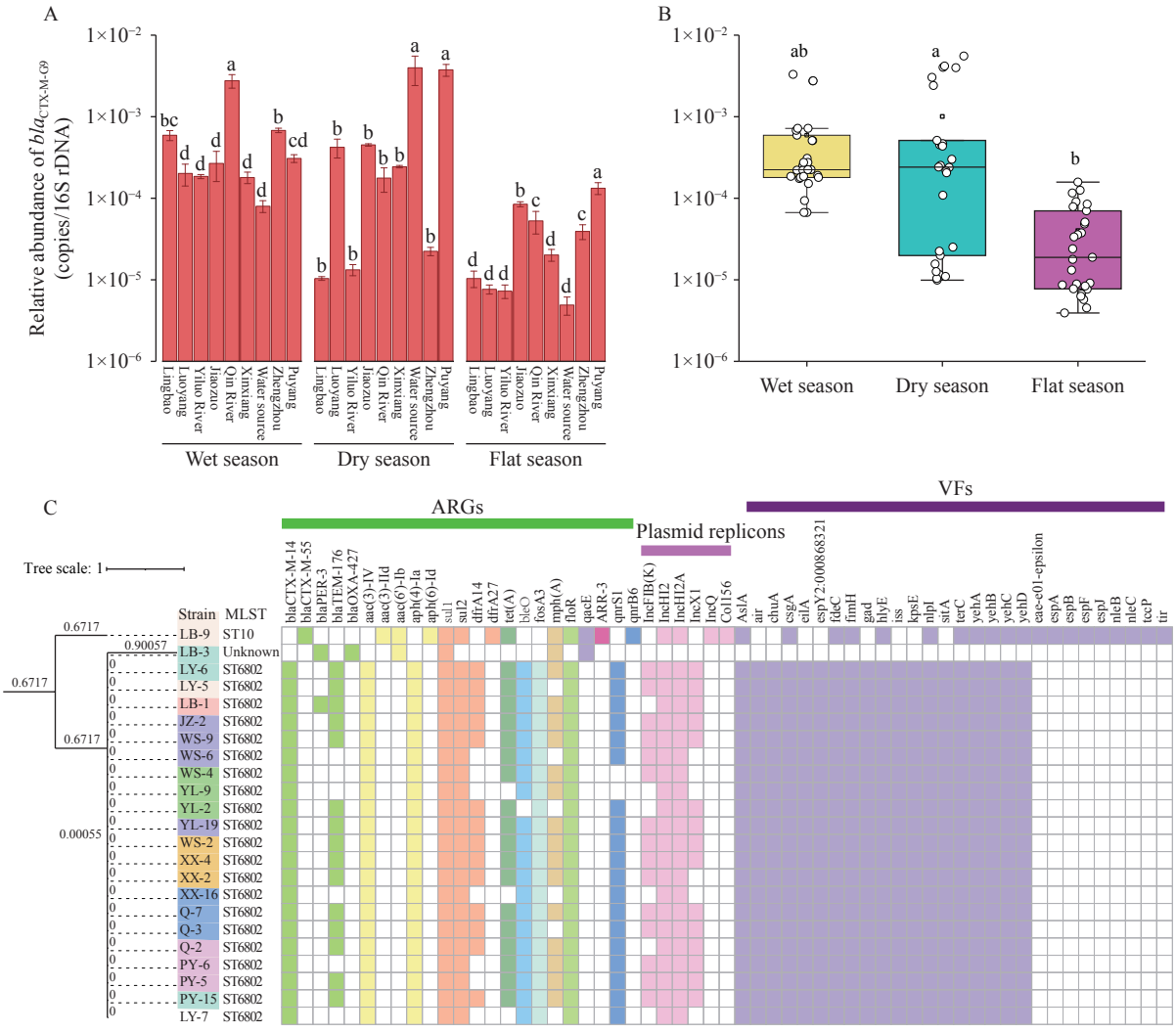

FIGURE 1. Prevalence of the *bla*$_{\text{CTX-M-G9}}$ gene and CTX-M-producing *E. coli* in the Yellow River and associated source water. Relative abundance of *bla*$_{\text{CTX-M-G9}}$ across different (A) cities and (B) seasons. (C) SNP-based phylogenetic tree of 23 CTX-M-producing *E. coli* isolates, displaying associated antibiotic resistance genes, virulence factors, and plasmid replicon types.
Note: For (A) and (B), one-way analysis of variance (ANOVA) with Tukey's *post-hoc* tests was employed to assess significant differences among groups.
Abbreviation: LB=Lingbao City; LY=Luoyang City; JZ=Jiaozuo City; XX=Xinxiang City; PY=Puyang City; WS=water source in Zhengzhou City; Q=Qin River; YL=Yiluo River; ARGs=antibiotic resistance genes; VFs=virulence factors; MLST=multilocus sequence typing; SNP=single nucleotide polymorphism.

(*n*=74) harbored the *bla*$_{\text{CTX-M-14}}$ genotype and demonstrated multidrug resistance phenotypes, with 78.7% (*n*=59) exhibiting resistance to seven or more of the tested antibiotics. Whole-genome sequencing revealed that 21 of 23 *E. coli* strains belonged to sequence type (ST) 6802, all of which carried *bla*$_{\text{CTX-M-14}}$ (Figure 1C). These ST6802 strains co-harbored 8–13 additional ARGs, 19 VFs, and two to four plasmid replicons (IncFIB, IncHI2, IncHI2A, and IncX1). SNP-based phylogenetic analysis demonstrated zero to four SNP differences among all ST6802 isolates, confirming clonal dissemination of ST6802 throughout the Yellow River. Moreover, during the dry season, *bla*$_{\text{CTX-M-G9}}$ abundance exhibited strong correlations with the plasmid replicons IncHI2 (R^2=0.86), IncHI2A (R^2=0.75), IncX1 (R^2=0.83), and IncFIB (R^2=0.67) in the Yellow River, providing additional evidence for clonal ST6802 spread (Figure 2).

Genome analysis identified 47 distinct STs among the 185 CTX-M-14-producing *E. coli* isolates examined (23 isolates from this study and 162 publicly available CTX-M-14-producing *E. coli* genomes), which were broadly distributed across human, animal, and environmental sources (Figure 3A and 3B). *E. coli* ST6802 has been previously detected in livestock and poultry feces, wild animals, animal-derived food products, anaerobic digestion systems, wastewater, and river water; however, no human isolates have been reported to date. cgMLST and SNP-based phylogenetic analyses demonstrated that the ST6802 isolates from this study were closely related to those recovered from anaerobic digestion systems treating pig manure, exhibiting 0–35 SNP differences (Figure 3C and 3D). Notably, ST6802 isolates from the drinking water source displayed zero SNP differences from the *E. coli* strain EFF60 (SAMN22853575) isolated from an anaerobic digestion system in China. These findings indicate environmental dissemination of CTX-M-14-producing *E. coli* ST6802 from a One Health perspective.

DISCUSSION

Understanding the occurrence and genetic characteristics of ESBL-producing *E. coli* in the Yellow River is essential for tracking the origin and dissemination of clinically relevant antimicrobial

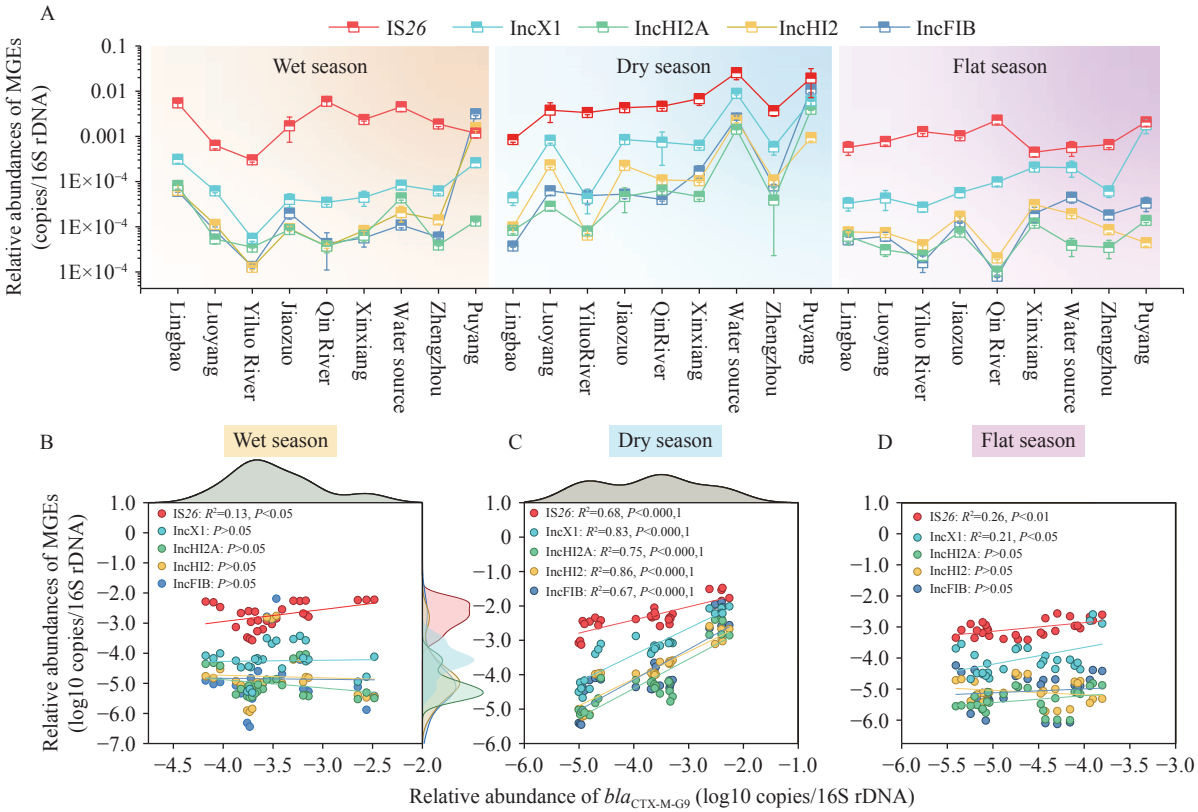

FIGURE 2. Relative abundances of plasmids and IS*26* carried by *E. coli* ST6802 in (A) the Yellow River and their correlations with *bla*$_{\text{CTX-M-G9}}$ during the (B) wet, (C) dry, and (D) flat seasons.

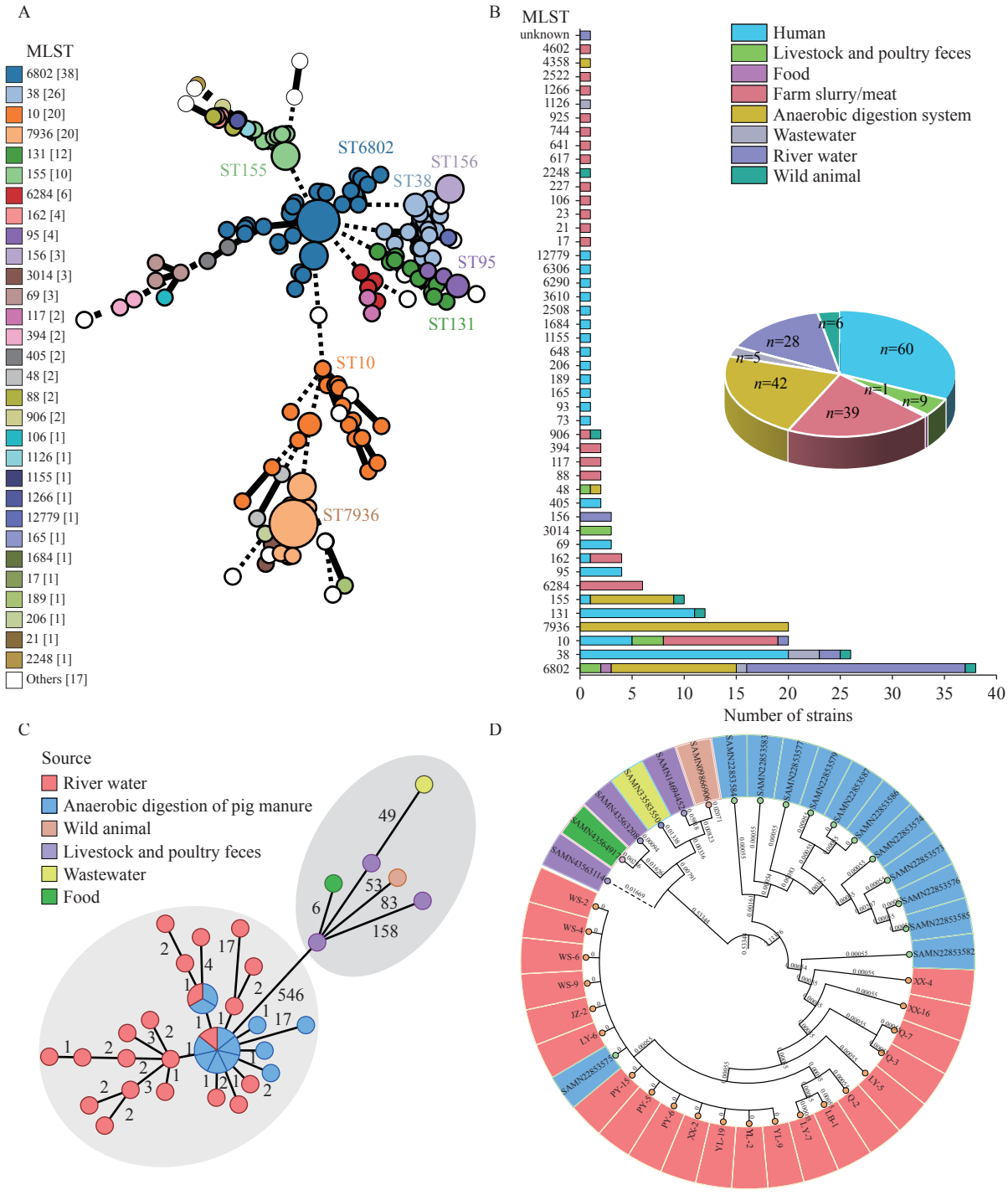

FIGURE 3. Genome-based phylogenetic analysis of CTX-M-14-producing *E. coli* and *E. coli* ST6802 from Yellow River water in this study, NCBI, and EnteroBase databases. (A) cgMLST-based minimum spanning tree of 190 *E. coli* isolates from diverse sources, comprising 185 CTX-M-14-producing *E. coli* and 5 *E. coli* ST6802 isolates. (B) Distribution of multilocus sequence types (MLSTs) among the 190 *E. coli* strains across different sources. (C) cgMLST-based minimum spanning tree of 39 ST6802 isolates from various sources. (D) SNP-based phylogenetic tree of 39 ST6802 isolates.

resistance in surface waters. This study investigated the abundance of the CTX-M group 9-type ESBL gene *bla*$_{\text{CTX-M-G9}}$ in the Yellow River across three seasons at nine sampling sites. We further characterized the genomic features of the dominant CTX-M-14-producing *E. coli* during the dry season and identified potential contamination sources through comparative genomic analysis. Our findings reveal critical insights into the environmental transmission pathways of ESBL-producing *E. coli* from a One Health

perspective, demonstrating both the necessity of continuous ESBL surveillance in the Yellow River and the urgent need to prevent environmental dissemination of ESBL-producing *E. coli* from animal sources.

Despite significant progress in China over recent decades in regulating antibiotic use in livestock and in reducing environmental ARG dissemination (*10*–*11*), $bla_{\text{CTX-M-G9}}$ was detected in all water samples, with significantly a higher relative abundance during the dry season compared to the flat season. This seasonal pattern aligns with a previous study that reported peak ARG abundance in the Yellow River during winter (*12*). Three factors likely contribute to this observation. First, reduced water volume during the dry season concentrates ARGs. Second, increased antibiotic prescriptions for seasonal epidemic diseases during winter months elevate ARG abundance in aquatic environments through wastewater discharge (*13*). Third, low winter temperatures may slow microbial community turnover, favoring the survival and proliferation of specific ESBL-producing *E. coli* clones. Consistent with a previous report (*14*), Puyang City exhibited the highest $bla_{\text{CTX-M-G9}}$ abundance during both dry and flat seasons, likely reflecting its intensive livestock and poultry farming operations.

The number of cefotaxime-resistant *E. coli* isolates varied substantially across sampling sites. The water source (n=17) and the Puyang section (n=15) yielded the highest numbers of isolates, consistent with the elevated spatial abundance of the $bla_{\text{CTX-M-G9}}$ gene observed during the dry season (Figure 1A). These findings reflect the spatial distribution patterns of cefotaxime-resistant *E. coli* across the study region. Notably, only a single *E. coli* strain was isolated from the Jiaozuo section, likely due to either the selectivity constraints of the culture medium employed or the presence of alternative bacterial hosts harboring $bla_{\text{CTX-M-G9}}$.

The predominant genotype among cefotaxime-resistant *E. coli* from the Yellow River and its water source was $bla_{\text{CTX-M}}$. The emergence and dissemination of specific *E. coli* clones represent a key mechanism driving the spread of $bla_{\text{CTX-M}}$ genes. For instance, Falgenhauer et al. (*15*) documented the emergence of an *E. coli* ST949 clone harboring chromosomal $bla_{\text{CTX-M-15}}$ in German surface waters. In contrast, $bla_{\text{CTX-M-14}}$ typically resides on diverse plasmids, and CTX-M-14-producing *E. coli* in Chinese surface waters have demonstrated considerable genetic diversity, with no single clonal group predominating (*16*). This diversity is evident in Figure 3A, where the 167 CTX-M-14-producing *E. coli* strains retrieved from public databases belonged to 47 distinct ST types, underscoring the broad host range of $bla_{\text{CTX-M-14}}$. However, our study revealed a notable exception: the *E. coli* ST6802 clone carrying $bla_{\text{CTX-M-14}}$ was detected at all sampling sites across multiple cities, suggesting widespread clonal dissemination.

The ST6802 isolates exhibited fewer than four SNP differences from one another, with highly similar ARG profiles, plasmid replicons, and VF patterns, confirming clonal dissemination. To validate this finding, we quantified the IncHI2, IncHI2A, IncX1, and IncFIB plasmids within ST6802, along with the IS*26* element, which typically flanks $bla_{\text{CTX-M-14}}$, in Yellow River samples. As anticipated, $bla_{\text{CTX-M-G9}}$ demonstrated strong correlations with these plasmids during the dry season, most notably with the IncHI2 plasmid (R^2=0.86). This correlation likely reflects the location of $bla_{\text{CTX-M-14}}$ on the IncHI2 plasmid in *E. coli* ST6802, as we previously reported (*6*). Remarkably, the ST6802 isolates harbored 19 distinct VF types, predominantly associated with adhesion and biofilm formation (fimH, csgA, fdeC, and yehA-D), iron acquisition (chuA and sitA), toxin production (hlyE), serum resistance (iss and kpsE), virulence gene expression (eilA), and stress response (gad, nlpI, and terC). The eilA gene has been identified in enteroaggregative *E. coli* strains that cause both acute and chronic diarrhea (*17*). The presence of VFs mediating bacterial adhesion and biofilm formation likely enhances the survival and environmental persistence of ST6802 isolates in the Yellow River ecosystem.

E. coli ST6802 has been documented in diverse sources globally, including chicken feces in China, a silver gull in Australia, wastewater in the United States, chicken and poultry products in Canada, and anaerobic digestion systems treating pig manure in China (Supplementary Table S3, available at https://weekly.chinacdc.cn/). Both cgMLST and SNP-based phylogenetic analyses demonstrated that the ST6802 isolates from this study were genetically identical to *E. coli* strain EFF60 (SAMN22853575) from an anaerobic digestion system and closely related to isolates from livestock and poultry feces. In contrast, these isolates showed substantial phylogenetic divergence from ST6802 strains recovered from urban wastewater. These findings strongly support an animal origin for *E. coli* ST6802 and its subsequent environmental dissemination. The zero-SNP difference

between ST6802 isolates from river water and anaerobic digestion systems is particularly striking, as it underscores the public health risk posed by transmission of animal-origin-resistant bacteria into aquatic environments. This transmission pathway — from animal feces through aquatic environments to potential human exposure — identifies critical intervention points for preventing cross-environmental spread of antibiotic resistance.

Although ST6802 has not been detected in human clinical samples, the IncHI2 plasmid harboring $bla_{\text{CTX-M-14}}$ within *E. coli* ST6802 demonstrates broad host range, exceptional conjugative transferability, and remarkable genetic stability (*6*). These characteristics position ST6802 isolates as critical vectors for $bla_{\text{CTX-M-14}}$ dissemination across bacterial populations. Moreover, the co-occurrence of multiple virulence factors in *E. coli* ST6802 amplifies concerns regarding its environmental persistence and spread throughout the Yellow River system, presenting substantial public health risks. The potential for this multidrug-resistant, virulent clone to establish itself in drinking water sources and irrigation systems warrants immediate attention and enhanced monitoring strategies.

This study advances beyond previous investigations of ESBL-producing *E. coli* in animal manure waste treatment systems (*6*) by tracing the transmission pathways of animal-origin ST6802 isolates into aquatic environments through integrated whole-genome sequencing and phylogenomic analysis of 167 publicly available *E. coli* genomes from diverse animal, human, and environmental sources. These findings underscore the critical need for sustained surveillance programs and stringent source control measures to interrupt the transmission of ESBL-producing *E. coli* from agricultural settings to natural water systems. Furthermore, comprehensive public education initiatives regarding antibiotic resistance are essential to mobilize broader societal engagement and support for antimicrobial stewardship efforts.

Conflicts of interest: No conflicts of interest.

Funding: Supported by the National Key Research and Development Program of China (2022YFC3204703), the Natural Science Foundation of Henan Province of China (242300420335), and the Specialized Project of High-level Talents in Henan Agricultural University (30501469; 30501989).

doi: 10.46234/ccdcw2025.244

[#] Corresponding author: Yu Zhang, zhangyu@rcees.ac.cn.

[1] College of Life Sciences, Henan Agricultural University, Zhengzhou City, Henan Province, China; [2] Key Laboratory of Environmental Aquatic Chemistry, State Key Laboratory of Regional Environment and Sustainability, Research Center for Eco-Environmental Sciences, Chinese Academy of Sciences, Beijing, China; [3] College of Forestry, Henan Agricultural University, Zhengzhou City, Henan Province, China; [4] University of Chinese Academy of Sciences, Beijing, China.

Submitted: September 21, 2025
Accepted: November 09, 2025
Issued: November 14, 2025

REFERENCES

1. Zhang C, Fu XH, Liu YQ, Zhao H, Wang GQ. Burden of infectious diseases and bacterial antimicrobial resistance in China: a systematic analysis for the global burden of disease study 2019. Lancet Reg Health West Pac 2024;43:100972. https://doi.org/10.1016/j.lanwpc.2023.100972.
2. Puspandari N, Sunarno S, Febrianti T, Febriyana D, Saraswati RD, Rooslamiati I, et al. Extended spectrum beta-lactamase-producing *Escherichia coli* surveillance in the human, food chain, and environment sectors: tricycle project (pilot) in Indonesia. One Health 2021;13:100331. https://doi.org/10.1016/j.onehlt.2021.100331.
3. Bevan ER, Jones AM, Hawkey PM. Global epidemiology of CTX-M β-lactamases: temporal and geographical shifts in genotype. J Antimicrob Chemother 2017;72(8):2145 – 55. https://doi.org/10.1093/jac/dkx146.
4. Miao ZM, Li S, Wang L, Song WG, Zhou YF. Antimicrobial resistance and molecular epidemiology of ESBL-producing *Escherichia coli* isolated from outpatients in town hospitals of Shandong Province, China. Front Microbiol 2017;8:63. https://doi.org/10.3389/fmicb.2017.00063.
5. Jia PY, Zhu Y, Li X, Kudinha T, Yang Y, Zhang G, et al. High prevalence of extended-spectrum beta-lactamases in *Escherichia coli* strains collected from strictly defined community-acquired urinary tract infections in adults in China: a multicenter prospective clinical microbiological and molecular study. Front Microbiol 2021;12:663033. https://doi.org/10.3389/fmicb.2021.663033.
6. Tian TT, Dai ST, Liu DJ, Wang Y, Qiao W, Yang M, et al. Occurrence and transfer characteristics of $bla_{\text{CTX-M}}$ genes among *Escherichia coli* in anaerobic digestion systems treating swine waste. Sci Total Environ 2022;834:155321. https://doi.org/10.1016/j.scitotenv.2022.155321.
7. Zhang QQ, Ying GG, Pan CG, Liu YS, Zhao JL. Comprehensive evaluation of antibiotics emission and fate in the river basins of China: source analysis, multimedia modeling, and linkage to bacterial resistance. Environ Sci Technol 2015;49(11):6772 – 82. https://doi.org/10.1021/acs.est.5b00729.
8. Yang QX, Tian TT, Niu TQ, Wang PL. Molecular characterization of antibiotic resistance in cultivable multidrug-resistant bacteria from livestock manure. Environ Pollut 2017;229:188 – 98. https://doi.org/10.1016/j.envpol.2017.05.073.
9. Liu JF, Hao DM, Ding XY, Shi MZ, Wang QJ, He HX, et al. Epidemiological investigation and β-lactam antibiotic resistance of *Riemerella anatipestifer* isolates with waterfowl origination in Anhui Province, China. Poult Sci 2024;103(4):103490. https://doi.org/10.1016/j.psj.2024.103490.
10. Zhao Q, Jiang ZN, Li T, Cheng M, Sun HY, Cui MQ, et al. Current status and trends in antimicrobial use in food animals in China, 2018-2020. One Health Adv 2023;1(1):29. https://doi.org/10.1186/s44280-023-00029-5.
11. Han ZM, Zhang Y, Yang M. Deterring the transmission of AMR in the environment: a Chinese perspective. In: Mothadaka MP, Ravishankar

CN, Vaiyapuri M, Bhatia R, Jena J, Badireddy MR, editors. Handbook on antimicrobial resistance. Singapore: Springer. 2023; p. 1-15. http://dx.doi.org/10.1007/978-981-16-9723-4_52-1.
12. Yu QL, Feng TS, Yang JW, Su WH, Zhou R, Wang YJ, et al. Seasonal distribution of antibiotic resistance genes in the Yellow River water and tap water, and their potential transmission from water to human. Environ Pollut 2022;292:118304. https://doi.org/10.1016/j.envpol.2021.118304.
13. Caucci S, Karkman A, Cacace D, Rybicki M, Timpel P, Voolaid V, et al. Seasonality of antibiotic prescriptions for outpatients and resistance genes in sewers and wastewater treatment plant outflow. FEMS Microbiol Ecol 2016;92(5):fiw060. https://doi.org/10.1093/femsec/fiw060.
14. Zhang SH, Yang GL, Zhang YY, Yang C. High-throughput profiling of antibiotic resistance genes in the Yellow River of Henan Province, China. Sci Rep 2024;14(1):17490. https://doi.org/10.1038/s41598-024-68699-8.
15. Falgenhauer L, Nieden AZ, Harpel S, Falgenhauer J, Domann E. Clonal CTX-M-15-producing *Escherichia coli* ST-949 are present in German surface water. Front Microbiol 2021;12:617349. https://doi.org/10.3389/fmicb.2021.617349.
16. Liu HX, Zhou HC, Li QF, Peng Q, Zhao Q, Wang J, et al. Molecular characteristics of extended-spectrum β-lactamase-producing *Escherichia coli* isolated from the rivers and lakes in Northwest China. BMC Microbiol 2018;18(1):125. https://doi.org/10.1186/s12866-018-1270-0.
17. de Carvalho MPN, Fernandes MR, Sellera FP, Lopes R, Monte DF, Hippólito AG, et al. International clones of extended-spectrum β-lactamase (CTX-M)-producing *Escherichia coli* in peri-urban wild animals, Brazil. Transbound Emerg Dis 2020;67(5):1804 – 15. https://doi.org/10.1111/tbed.13558.

SUPPLEMENTARY MATERIALS

SUPPLEMENTARY TABLE S1. Primers used for quantitative polymerase chain reaction quantification of ARGs and MGEs.

Genes	Primers	Size (bp)	Reference	GenBank
$bla_{CTX-M-G9}$	F: ACCAATGATATTGCGGTGAT R: CTGCGTTCTGTTGCGGCT Probe: 6FAM-TCGTGCGCCGCTG-MGBNFQ	85	(*1*)	–
IS*26*	F: AGGAGATGCTGGCTGAACG R: GGCAAAGATCGGAAGGGTT	100	This study	NZ_CP130155.1
IncFIB	F: CCTTTGGTCTCGCTCTGGAA R: CGGATTTGACTCCCGTCGTT	105	This study	JN233704
IncHI2	F: GGCCAGTACATCCAACGGAA R: ACCAGAGAAGCCGGGATTTG	97	This study	BX664015
IncHI2A	F: CTTTAAGTGCTGGCTCGGGA R: TGCACCAGATGCGTTACTGT	228	This study	BX664015
IncX1	F: ATGGGCTGTATTCTGGCTGG R: TCAGCCAGCAGTCCCAAAAT	132	This study	EU370913

Abbreivation: ARGs=antibiotic resistance genes; MGEs=mobile genetic elements.

SUPPLEMENTARY TABLE S2. Antibiotic resistance profiles of 75 *Escherichia coli* isolates collected during the dry season.

Strain	$bla_{CTX-M-G9}$	Antibiotics											No. of drugs
		AMC	AMP	CTX	FEP	GEN	KAN	TET	CIP	ERY	SXT	CHL	
LB-1	+	R	R	R	R	S	S	S	I	R	R	S	6
LB-2	+	R	R	R	I	S	S	R	R	R	S	S	6
LB-3	+	R	R	R	R	S	I	S	I	R	S	S	5
LB-4	+	R	R	R	I	S	S	R	I	R	R	S	6
LB-6	+	R	R	R	I	R	S	R	I	R	S	S	6
LB-7	+	R	R	R	I	R	I	I	I	R	R	S	6
LB-8	+	R	R	R	I	S	S	R	I	R	R	S	6
LB-9	-	R	R	R	R	R	I	R	I	R	R	R	9
LB-10	+	R	R	R	I	R	S	S	R	R	R	S	7
LB-11	+	R	R	R	I	S	S	R	R	R	R	S	7
LY-1	+	R	R	R	R	I	S	R	I	R	R	R	8
LY-3	+	R	R	R	R	I	S	R	I	R	R	I	7
LY-4	+	R	R	R	I	S	S	R	I	R	R	R	7
LY-5	+	R	R	R	R	I	S	R	I	R	R	R	8
LY-6	+	R	R	R	R	S	S	R	I	R	R	R	8
LY-7	+	R	R	R	R	I	S	R	I	R	R	R	8
LY-8	+	R	R	R	R	I	S	R	I	R	R	R	8
YL-1	+	R	R	R	I	R	S	S	I	R	S	S	5
YL-2	+	R	R	R	R	S	S	R	I	R	R	R	8
YL-3	+	R	R	R	I	R	S	S	R	R	R	S	7
YL-9	+	R	R	R	R	R	S	R	I	R	R	I	8
YL-11	+	R	R	R	R	S	S	S	I	I	S	S	4
YL-12	+	R	R	R	I	I	I	R	I	R	R	R	7
YL-15	+	R	R	R	I	S	S	S	I	I	S	S	3
YL-18	+	R	R	R	R	S	S	S	I	I	S	S	4
YL-19	+	R	R	R	R	S	S	R	I	R	R	I	7
YL-20	-	R	R	R	R	I	S	R	I	R	R	I	7

Continued

Strain	$bla_{CTX-M-G9}$	Antibiotics											No. of drugs
		AMC	AMP	CTX	FEP	GEN	KAN	TET	CIP	ERY	SXT	CHL	
JZ-2	+	R	R	R	I	S	S	S	I	R	I	S	4
Q-2	+	R	R	R	R	R	S	R	I	R	R	I	8
Q-3	+	R	R	R	R	R	I	R	I	R	R	R	9
Q-4	+	R	R	R	R	R	S	R	I	R	R	I	8
Q-7	+	R	R	R	R	R	I	R	I	R	R	I	8
XX-1	+	R	R	R	I	S	S	R	I	R	R	R	7
XX-2	+	R	R	R	R	S	S	R	I	R	R	R	8
XX-3	+	R	R	R	I	S	S	R	I	R	R	R	7
XX-4	+	R	R	R	R	I	S	R	I	R	R	I	7
XX-9	+	R	R	R	I	I	S	R	I	R	R	I	6
XX-10	+	R	R	R	I	I	S	R	I	R	R	R	7
XX-11	+	R	R	R	I	S	S	R	I	R	R	R	7
XX-13	+	R	R	R	I	S	S	R	I	R	R	R	7
XX-14	+	R	R	R	R	I	S	R	I	R	R	I	7
XX-16	+	R	R	R	R	S	S	R	I	R	R	R	8
XX-17	+	R	R	R	R	S	S	R	I	R	R	I	7
WS-1	+	R	R	R	R	S	S	R	I	R	R	R	8
WS-2	+	R	R	R	R	R	S	R	I	R	R	R	9
WS-3	+	R	R	R	R	S	S	R	I	R	R	R	8
WS-4	+	R	R	R	R	I	S	R	I	R	R	R	8
WS-5	+	R	R	R	I	S	S	R	I	R	R	R	7
WS-6	+	R	R	R	R	I	S	R	I	R	R	R	8
WS-7	+	R	R	R	R	I	I	R	I	R	R	I	7
WS-8	+	R	R	R	R	I	S	R	I	R	R	R	8
WS-9	+	R	R	R	R	S	R	I	R	R	R	R	9
WS-11	+	R	R	R	R	R	I	R	I	R	R	R	9
WS-12	+	R	R	R	R	R	S	R	I	R	R	I	8
WS-13	+	R	R	R	R	I	S	R	I	R	R	R	8
WS-14	+	R	R	R	R	I	S	R	I	R	R	R	8
WS-15	+	R	R	R	R	R	I	R	I	R	R	R	9
WS-16	+	R	R	R	R	R	S	R	I	R	R	R	9
WS-17	+	R	R	R	S	S	S	S	I	R	I	R	5
WS-18	+	R	R	R	I	S	S	R	I	R	R	I	6
PY-1	+	R	R	R	R	I	S	R	I	R	R	I	7
PY-2	+	R	R	R	I	S	S	R	I	R	R	R	7
PY-3	+	R	R	R	R	I	S	R	I	R	R	I	7
PY-4	+	R	R	R	I	I	S	R	I	R	R	I	6
PY-5	+	R	R	R	R	I	S	R	I	R	R	R	8
PY-6	+	R	R	R	R	I	I	R	I	R	R	R	8
PY-7	+	R	R	R	I	I	S	R	I	R	R	R	7
PY-9	+	R	R	R	R	S	S	R	I	R	R	I	7

Continued

Strain	$bla_{CTX-M-G9}$	Antibiotics											No. of drugs
		AMC	AMP	CTX	FEP	GEN	KAN	TET	CIP	ERY	SXT	CHL	
PY-10	+	R	R	R	R	I	S	R	I	R	R	R	8
PY-11	+	R	R	R	I	I	S	R	I	R	R	R	7
PY-12	+	R	R	R	R	R	S	R	I	R	R	I	8
PY-13	+	R	R	R	R	S	S	R	S	R	R	R	8
PY-14	+	R	R	R	I	I	S	R	I	R	R	R	7
PY-15	+	R	R	R	R	S	S	R	I	R	R	R	8
PY-16	+	R	R	R	R	I	S	R	I	R	R	R	8
Sum	74	75	75	75	48	17	1	63	5	72	66	41	

Note: Strains displayed in bold font were selected for whole-genome sequencing analysis. Different background colors represent different levels of drug resistance: red represents resistant, pink represents intermediate, and white represents susceptible."+" indicates positive PCR detection results for $bla_{CTX-M-G9}$. "-" indicates negative PCR detection results for $bla_{CTX-M-G9}$.

Abbreviations: LB=Lingbao City; LY=Luoyang City; JZ=Jiaozuo City; XX=Xinxiang City; PY=Puyang City; WS=water source in Zhengzhou City; Q=Qin River; YL=Yiluo River ; AMC=amoxicillin-clavulanic acid; AMP=ampicillin; CTX=cefotaxime; FEP=cefepime; GEN=gentamicin; KAN=kanamycin; TET=tetracycline; CIP=ciprofloxacin; ERY=erythromycin; SXT=sulfamethoxazole; CHL=chloramphenicol.

SUPPLEMENTARY TABLE S3. Genomic characteristics of *E. coli* ST6802 isolates from different sources.

Strain	ST	Source	ARG profiles	VFs	Plasmid replicons	GenBank accession number	References/ Database
E. coli ZB8C2M	6802	Chicken feces, Guangzhou, China	$bla_{CTX-M-55}$, *aac(3)*, *aadA*, *aph(3')*, *aph(6)*, *ARR*, bla_{NDM-5}, bla_{OXA}, bla_{TEM}, *cat*, *cmlA1*, *floR*, *dfrA*, *fosA3*, *mph*, *erm*, *qnr*, *sul*, *tet*	air, chuA, eilA, sitA, gad, kpsE, kpsMII_K5, terC, traT	IncFIB, IncFII, IncHI2, IncN, IncQ1, IncX1, p0111	SAMN14694452	NCBI
ESC_JA8833AA	6802	Wild animal, Silver Gull, Australia	bla_{CMY-2}, bla_{TEM-1C}, *sitABCD*	aslA, air, astA, chuA, cia, csgA, eilA, espY2, fdeC, fimH, gad, hha, hlyE, hra, kpsE, kpsMII_K5, nlpI, sitA, terC, traT, yehA, yehB, yehC, yehD, yghJ	IncI1-I(Alpha)	SAMN09866906	EnteroBase
ESC_DB8730AA	6802	Environment, wastewater, United States	*sitABCD*	aslA, air, astA, chuA, csgA, eilA, espY2, fdeC, fimH, hha, hlyE, kpsE, kpsMII_K5, nlpI, sitA, terC, yehA, yehB, yehC, yehD, yghJ	IncI1-I(Alpha)	SAMN33583550	EnteroBase
ESC_NB8187AA	6802	Poultry, chicken, Canada	*sitABCD*, *tetA*	aslA, air, chuA, cma, csgA, cvaC, eilA, espY2, fdeC, fimH, hha, hlyE, hlyF, iroN, iss, kpsE, kpsMII_K5, nlpI, ompT, sitA, terC, traJ, traT, yehA, yehB, yehC, yehD, yghJ	ColpVC, IncFIB, IncFII	SAMN43563114	EnteroBase
ESC_NB8461AA	6802	Food, chicken, Canada	bla_{CMY-2}, *sitABCD*, *tet(B)*	aslA, air, anr, chuA, cia, csgA, cvaC, eilA, espY2, etsC, fdeC, fimH, gad, hha, hlyE, hlyF, iroN, iss, iucC, iutA, kpsE, kpsMII_K5, mchF, nlpI, ompT, sitA, terC, traJ, traT, tsh, yehA, yehB, yehC, yehD, yghJ	Col440II, IncFIA, IncFIB, IncFIC, IncI1-I, p0111	SAMN43563208	EnteroBase
ESC_NB8748AA	6802	Poultry, poultry, Canada	bla_{CMY-2}, *sitABCD*, *tet(B)*	aslA, air, anr, chuA, cia, csgA, cvaC, eilA, espY2, etsC, fdeC, fimH, gad, hha, hlyE, hlyF, iroN, iss, iucC, iutA, kpsE, kpsMII_K5, mchF, nlpI, ompT, sitA, terC, traJ, traT, tsh, yehA, yehB, yehC, yehD, yghJ	Col440II, IncFIA, IncFIB, IncFIC, IncI1-I, p0111	SAMN43564917	EnteroBase
12 *E. coli* isolates	6802	Anaerobic digestion systems of pig manure, China	$bla_{CTX-M-14}$, $bla_{TEM-176}$, *aac(3)-IV*, *aph(4)-Ia*, *sul1*, *sul2*, *dfrA14*, *tet(A)*, *fosA3*, *mph(A)*, *floR*, *mdf(A)*, *qnrS1*	air, chuA, eilA, gad, iss, kpsE, sitA, terC	IncFIB, IncHI2, IncHI2A, IncX1	PRJNA777386	NCBI
21 *E. coli* isolates	6802	River water and water source, China	$bla_{CTX-M-14}$, $bla_{TEM-176}$, *aac(3)-IV*, *aph(4)-Ia*, *sul1*, *sul2*, *dfrA14*, *tet(A)*, *bleO*, *fosA3*, *mph(A)*, *floR*, *qnrS1*	aslA, air, chuA, csgA, eilA, espY2:000868321, fdeC, fimH, gad, hlyE, iss, kpsE, nlpI, sitA, terC, yehA, yehB, yehC, yehD	IncFIB, IncHI2, IncHI2A, IncX1	This study	This study

Abbreviation: ST=sequence type; ARG=antibiotic resistance gene; VFs=virulence factors.

REFERENCES

1. Zhao ZZ, Gao BQ, Henawy AR, ur Rehman A, Ren ZQ, Jiménez N, et al. Mitigating the transfer risk of antibiotic resistance genes from fertilized soil to cherry radish during the application of insect fertilizer. Environ Int 2025;199:109510. https://doi.org/10.1016/j.envint.2025.109510.

Preplanned Studies

Genomic Surveillance of *Salmonella* London and Rissen Reveals International Transmission Patterns and Expanding Antimicrobial Resistance — Shanghai Municipality, China, 2020–2024

Xueer Li[1,2]; Ling Zhong[1,3]; Yanru Liang[2]; Shuqi You[2]; Yahui Zhan[4]; Qing Cao[5]; Zhemin Zhou[6]; Lifeng Pan[2,#]; Heng Li[1,3,#]

Summary

What is already known about this topic?

Non-typhoidal *Salmonella* (NTS) represents a leading cause of foodborne gastroenteritis worldwide. The epidemiological landscape of NTS continues to evolve, with specific serotypes emerging as significant human pathogens through contaminated food products. This evolution occurs particularly within the context of globalized food supply chains and widespread antimicrobial use in agricultural settings.

What is added by this report?

This study integrated local isolates from Shanghai with global genomic data to reveal distinct international transmission patterns for *Salmonella* London and Rissen. *S.* London disseminated through historical, geographically segregated clades, whereas *S.* Rissen demonstrated recent intercontinental mixing, with Thailand identified as the primary global source. Our analysis identified high-risk plasmids harboring up to 15 resistance genes and demonstrated that Chinese isolates carried the highest antimicrobial resistance burden globally.

What are the implications for public health practice?

The global dissemination of these pathogens is directly linked to international food trade networks. Our findings necessitate a paradigm shift toward integrated global One Health surveillance that bridges human, animal, and food sectors. Implementing harmonized international policies, rigorous trade monitoring, and enhanced antimicrobial stewardship programs is essential to contain the transnational threat posed by resistant foodborne pathogens.

ABSTRACT

Introduction: Non-typhoidal *Salmonella* (NTS) represents a major global cause of foodborne illness. The emergence and worldwide dissemination of specific serotypes, including *Salmonella* London and Rissen, constitute a significant public health threat due to their escalating association with antimicrobial resistance (AMR), which compromises the effectiveness of first-line antibiotic therapies.

Methods: We performed a comprehensive genomic analysis integrating 200 local isolates collected between 2020 and 2024 from Shanghai, China, with a global dataset comprising 1,353 *S.* London and 882 *S.* Rissen genomes retrieved from EnteroBase. Through whole-genome sequencing, phylogenetic reconstruction, and AMR gene profiling, we systematically characterized the population structure, transmission dynamics, and resistance profiles of these serotypes.

Results: Phylogeographic analysis revealed contrasting dissemination patterns: *S.* London spread predominantly through historical, geographically segregated clades, whereas *S.* Rissen demonstrated recent intercontinental mixing, with Thailand identified as a primary global source. We detected high-risk plasmids harboring up to 15 resistance genes that drove elevated multidrug resistance rates in 64% of *S.* London and 59% of *S.* Rissen isolates. Notably, Chinese isolates exhibited the highest AMR burden, with clinical environments identified as critical hotspots for resistance amplification.

Conclusion: The global dissemination of *S.* London and Rissen is directly linked to international food trade networks, and their evolving AMR landscape represents a critical public health concern. These findings underscore the urgent need for integrated One Health surveillance strategies to effectively control the spread of resistant foodborne pathogens.

Non-typhoidal *Salmonella* (NTS), a leading cause of foodborne illness responsible for an estimated 90

million annual cases of acute gastroenteritis worldwide, has undergone significant epidemiological shifts in recent decades (*1*–*2*). Globalized food supply chains and extensive antimicrobial use in agriculture have driven the emergence of host-restricted serotypes such as *Salmonella* Rissen and *Salmonella* London. These serotypes have accelerated the dissemination of antimicrobial resistance (AMR) through plasmid-mediated transfer of critical resistance genes (e.g., $bla_{\text{CTX-M}}$, *mcr*-1), compromising the efficacy of first-line treatments including extended-spectrum β-lactams and fluoroquinolones (*3*–*4*).

In China, the increasing detection of *S.* London and *S.* Rissen represents a notable shift in the epidemiological landscape of foodborne illness. *S.* Rissen has gained clinical prominence in regions such as Jiangsu Province (*5*), while *S.* London has expanded beyond dairy products to diverse food and clinical sources worldwide (*6*–*7*). Despite their growing public health significance, comprehensive molecular epidemiological characterization of these serotypes remains limited.

Understanding the genomic architecture underlying the success of these emerging serotypes is crucial for informing public health interventions and antimicrobial stewardship strategies. We employed whole-genome sequencing (WGS) to systematically characterize the population genomics, virulence repertoire, and antimicrobial resistance profiles of *S.* London and *S.* Rissen. Our approach integrated local isolates from Shanghai's Pudong District with global genomic surveillance data to elucidate transmission patterns and resistance mechanisms.

We sequenced 200 *Salmonella* isolates (*S.* London and *S.* Rissen) collected in Pudong, Shanghai, between 2020 and 2024. These local isolates were integrated with publicly available genomic data retrieved from EnteroBase (version November 2023) to construct a comprehensive global dataset comprising 1,353 *S.* London genomes (spanning 24 countries, 1971–2023) and 882 *S.* Rissen genomes (spanning 27 countries, 2001–2023). Genome assembly was performed using EToKi/SPAdes (*8*), followed by gene annotation with PROKKA (*9*) and functional characterization using eggNOG-mapper. AMR genes were identified using AMRfinder, and core genome clustering data were obtained from the HierCC database. For phylogenetic reconstruction, we constructed maximum likelihood trees using IQ-TREE (*10*) after removing recombinant regions from the alignment. Temporal signal analysis using TempEst revealed a weak but significant root-to-tip correlation (R^2=0.14), which exceeded that of date-randomized controls; BactDating further confirmed the presence of a temporal signal in the dataset. Time-calibrated phylogenies were then generated using TreeTime to infer host-switching events and reconstruct geographic transmission pathways. Host-switching and transmission inferences were restricted to phylogenetic nodes supported by bootstrap values exceeding 70%.

Our genomic surveillance of 200 isolates from Pudong, Shanghai, revealed a diverse serotype distribution: *S.* Enteritidis (26.5%, *n*=53), *S.* Typhimurium (16.5%, *n*=33), *S.* London (10.5%, *n*=21), and *S.* Rissen (6.5%, *n*=13). Core genome multi-locus sequence typing (cgMLST) at the HC900 resolution (≤900 allelic distances) demonstrated distinct clustering patterns that correlated with both serotype identity and source characteristics. Typing analysis revealed distinct host associations: all *S.* London isolates belonged to ST155 and were predominantly linked to pork products (81.0%), whereas the primary food-derived serovar, *S.* Rissen (ST469), was largely isolated from pig viscera (84.6%, Figure 1A).

To contextualize our local findings, we constructed global datasets comprising 1,353 *S.* London and 882 *S.* Rissen genomes. High-resolution typing delineated two distinct global transmission paradigms and elucidated specific host adaptation patterns. The lineage HC50_37, specific to *S.* London, demonstrated clear evidence of cross-host transmission, directly linking pork products (81.0%) to clinical cases (14.3%). In parallel, HC50_142 encompassed all *S.* Rissen isolates from pig liver (46.2%) and kidney (15.4%), indicating persistent circulation within specific organ systems (Figure 1B).

Core-genome SNP phylogenies revealed distinct population structures. *S.* London stratified into four clades: a China-dominated lineage (*n*=212), a US-dominated clade (*n*=778), and two additional global lineages (Figure 2A). In contrast, *S.* Rissen exhibited significant intercontinental mixing across three primary lineages, characterized by US-mixing (*n*=366), Europe-mixing (*n*=255), and Asia-mixing clades (*n*=215, Figure 3A).

Phylogenetic analysis revealed contrasting transmission dynamics between the two serotypes. *S.* London emerged circa 1905 (HPD: 1889–1914), with subsequent divergence aligning with World War I and trade expansion; a distinct US clade formed between 1951 and 1964 (HPD: 1951–1964), coinciding with

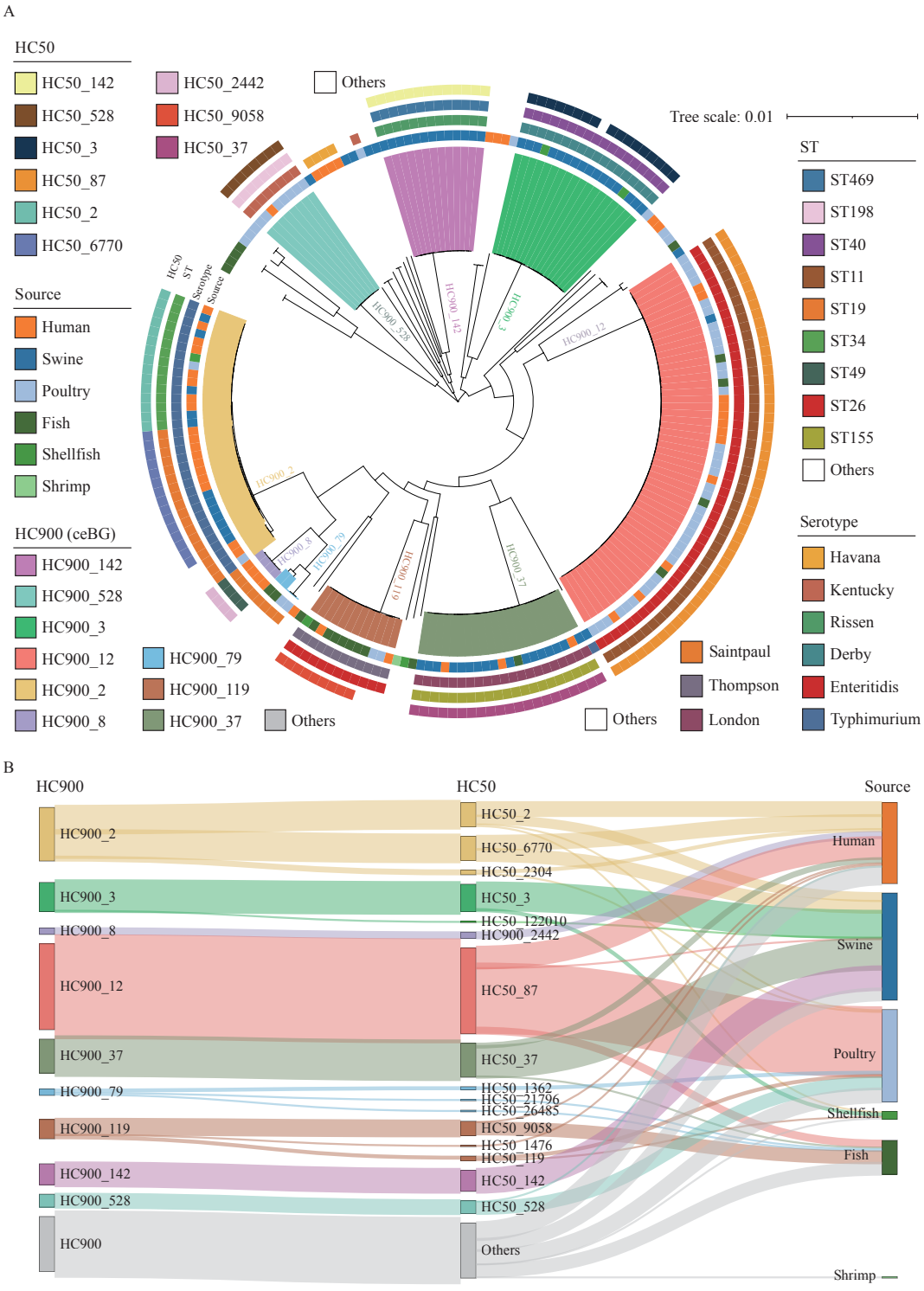

FIGURE 1. Genomic epidemiology of 200 *Salmonella* isolates from Pudong, Shanghai. (A) Maximum-likelihood phylogenetic tree of 200 *Salmonella* isolates, comprising 21 *S.* London and 13 *S.* Rissen strains, constructed through core genome multilocus sequence typing (cgMLST). (B) Sankey diagram depicting the hierarchical relationships between HC900 and HC50 clusters and their corresponding isolation sources among 200 *Salmonella* isolates from Pudong, Shanghai.
Note: For (A), the tree was visualized and annotated using the iTOL platform (https://itol.embl.de). Branch colors correspond to serotype classifications. Concentric rings (from inner to outer) represent: 1) isolation source, 2) serotype, 3) sequence type (ST), and 4) HC900 (ceBG) lineage designation. The scale bar indicates single nucleotide polymorphism (SNP) distance. For (B), flow paths connect HC900 clusters (left panel) to their constituent HC50 subclusters (middle panel) and ultimately to their respective isolation sources (right panel), emphasizing predominant epidemiological associations.

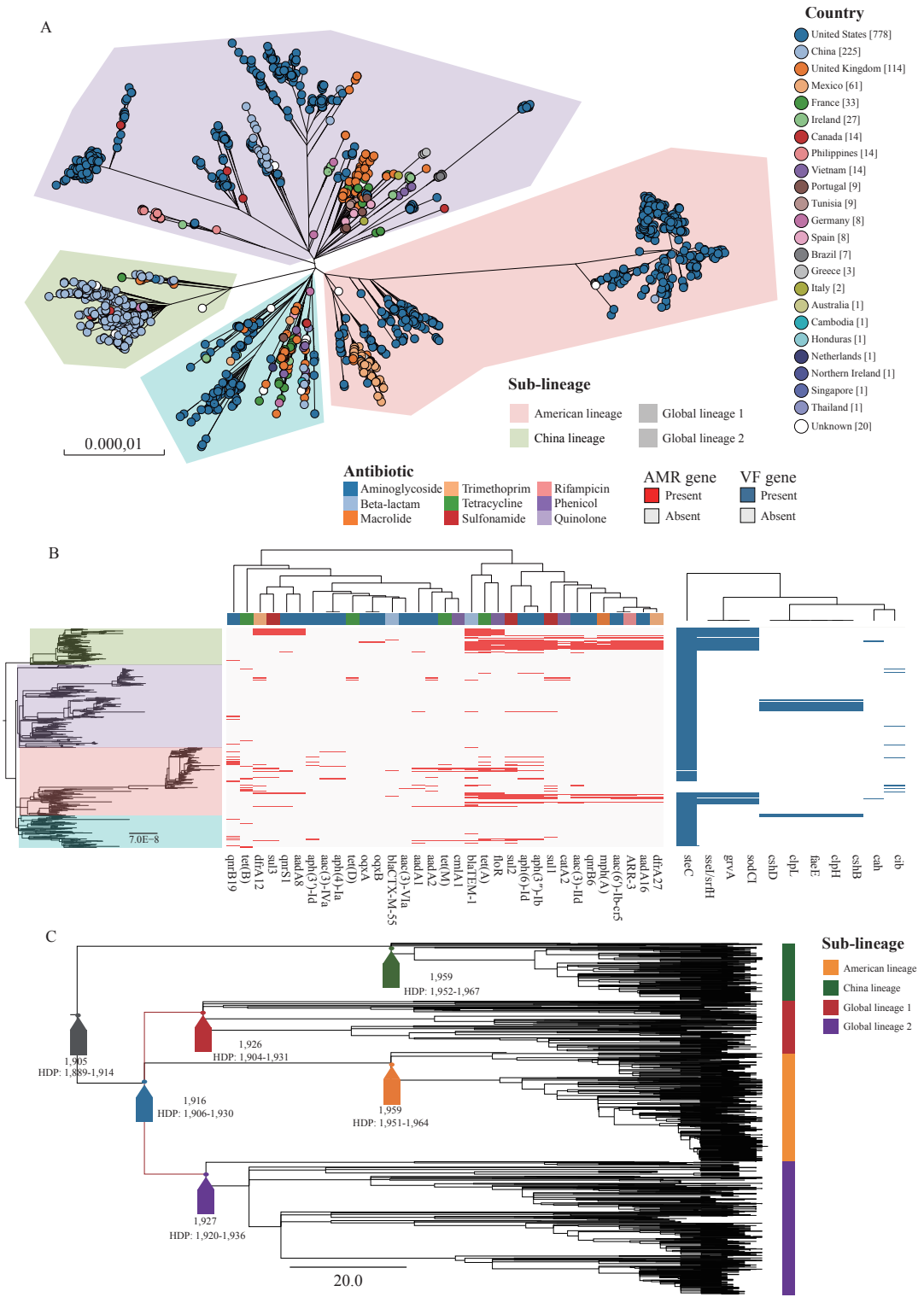

FIGURE 2. Population structure, virulence gene profiles, and antimicrobial resistance in *S*. London. (A) Minimum spanning tree derived from core genome SNP analysis of 1,353 *S*. London isolates, delineating four major phylogenetic clusters. (B) Heatmap displaying the distribution of key virulence genes across the global *S*. London collection. Blue shading indicates gene presence, while white denotes absence. (C) Chronograph depicting the estimated timing of most recent common ancestors (MRCAs) for *S*. London clades.

Note: For (C), arrows denote the MRCA for each clade, with the estimated age (in years) and 95% HPD interval displayed as text.

Abbreviation: HPD=highest posterior density; MRCA=most recent common ancestor.

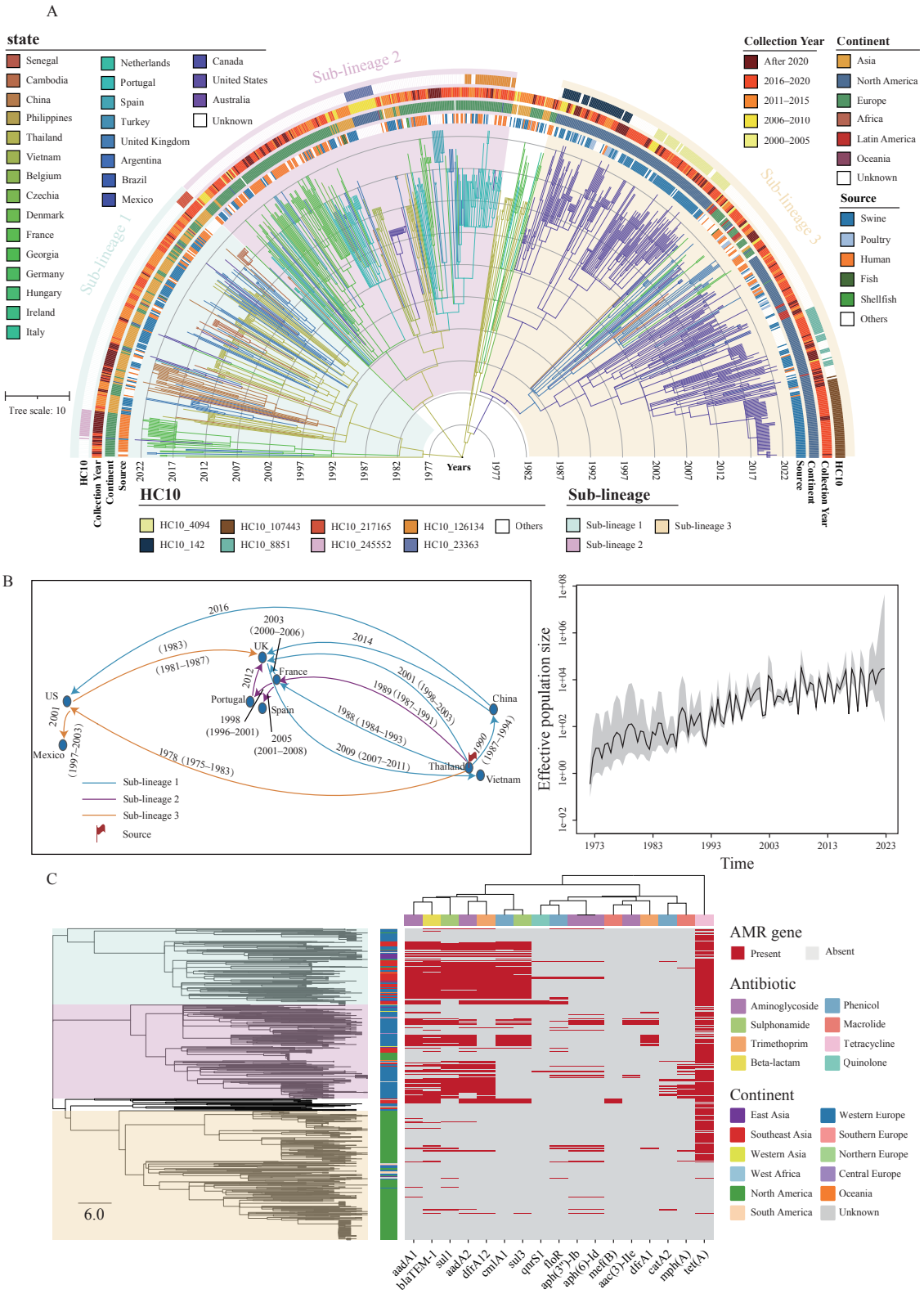

FIGURE 3. Global transmission dynamics and geographically structured antimicrobial resistance (AMR) in *S.* Rissen. (A) Phylogenetic reconstruction of 882 global *S.* Rissen isolates, annotated by continent, country, collection year, isolation source, sub-lineage, and HC10 type. (B) Reconstructed international transmission routes, illustrating inferred directionality, transmission frequency, and estimated years of cross-border dissemination events. (C) Geographic distribution of antimicrobial resistance genes throughout the global *S.* Rissen collection.

agricultural industrialization (Figure 2C). For *S.* Rissen, Thailand was identified as the predominant global source. Between 1983 and 1994, phylogenetic data indicate that Thailand exported over 200 strains, including a single event involving 117 strains to France. Europe and the United States acted as secondary hubs, with France functioning as a key redistribution center (Figure 3B). Evidence of strains being detected in the United Kingdom a decade after their inferred export illustrates the delayed and complex nature of transmission through global food chains. These transmission pathways correlate strongly with international trade in pork products.

AMR profiling revealed striking geographic disparities in resistance gene distribution. Among *S.* London isolates, we identified 75 distinct resistance genes, with 64% (308/480) exhibiting multidrug-resistance (MDR) to three or more antimicrobial categories. Chinese isolates demonstrated the highest resistance burden, with notably elevated prevalence of *tet(A)* (68.0%, 153/225), $bla_{\text{TEM-1}}$ (62.7%, 141/225), and *floR* (62.2%, 140/225) (Figure 2B). Similarly, *S.* Rissen displayed a comparable global pattern, with 59% (377/635) of isolates exhibiting MDR. Southeast Asian strains harbored the most extensive resistance gene repertoires, including the world's highest documented rates of *tet(A)* (92.4%, 134/145), *sul1* (83.4%, 121/145), and *qnrS1* (83.4%, 121/145). Notably, 18 *S.* Rissen isolates (2.0%) carried *mcr* genes, with eight originating from the United States. Although $bla_{\text{CTX-M-55}}$ and *mcr-1* were detected in genomes from the global database, both genes were absent from isolates collected in Pudong, Shanghai, China (Figure 3C).

Two high-risk plasmids were identified as key vectors facilitating the rapid dissemination of multidrug resistance. A large conjugative plasmid detected in Chinese *S.* London isolates harbored 15 resistance genes, conferring resistance to nearly all major antibiotic classes (Supplementary Figure S1A, available at https://weekly.chinacdc.cn/). More critically, a broad-host-range plasmid (GenBank: CP051314.1) was identified across multiple *Salmonella* serotypes from Shanghai, carrying essential resistance determinants including $bla_{\text{CTX-M-55}}$, *qnrS1*, and *tet(M)* (Supplementary Figure S2B). This plasmid demonstrated the highest prevalence in Chinese (n=24) and American (n=93) isolates; however, the average resistance gene load was greatest in Chinese and Mexican strains, at 8.0 and 5.8 genes per plasmid, respectively (Supplementary Figure S1C). Further investigation is required to elucidate the precise evolutionary mechanisms underlying plasmid diversification and to experimentally validate conjugation efficiency and horizontal transfer dynamics, as current findings are derived exclusively from genomic inference.

Virulence profiling revealed divergent evolutionary trajectories for *S.* London and *S.* Rissen that reflect their distinct host ranges and ecological adaptations. We identified 294 putative virulence factors in *S.* London, with the effector gene *steC* present in nearly all isolates (93.8%). Other virulence genes demonstrated marked geographic clustering patterns. The gene combination *sseI*/*srfH*, *grvA*, and *sodCI* was highly prevalent in Chinese mainland strains (87.3%) yet completely absent from Taiwanese isolates. Additionally, *clpH* predominated in UK strains (61.7%), while *cib* was enriched in US isolates (75.0%), indicating region-specific adaptive evolution (Figure 2B). A fundamental genomic distinction emerged in motility and niche adaptation capabilities. *S.* Rissen possesses a complete flagellar system, whereas *S.* London harbors a defective one due to the absence of key genes (*fliC*, *fljB*). This impaired motility likely facilitated *S.* London's adaptation to a more restricted host range, such as poultry, by favoring persistent colonization over active dissemination. In contrast, the near-universal presence of *ssek2* in *S.* Rissen (99.9%) compared to its rarity in *S.* London suggests this gene plays a critical role in survival across the diverse environmental niches and broader host range characteristic of *S.* Rissen (Figure 3C).

This study integrates genomic surveillance of *Salmonella* in Shanghai with global comparative analysis to reveal local serotype distribution and resistance profiles while elucidating the distinct transmission patterns and adaptive evolution of *S.* London and *S.* Rissen. These findings underscore the essential role of combined local-and-global perspectives in understanding bacterial pathogen dissemination.

DISCUSSION

Our study demonstrates that foodborne pathogens such as *Salmonella* London and Rissen pose significant transnational threats through their dissemination along global trade routes. The reconstruction of their intercontinental transmission networks over six decades provides conclusive genomic evidence that their spread follows patterns established by modern international trade systems. These findings underscore the need to

transition from reactive, nation-based outbreak responses to proactive, internationally coordinated genomic surveillance strategies.

The two serotypes exhibit divergent global dissemination patterns. *S.* London demonstrates a pattern of geographically isolated clades, suggesting historical introductions followed by regional establishment. In contrast, *S.* Rissen exhibits ongoing intercontinental gene flow, consistent with persistent trade-linked transmission. These distinct dispersal dynamics require tailored surveillance protocols that account for serotype-specific transmission patterns.

Phylogeographic reconstruction identifies Thailand as the primary global source for *S.* Rissen, with its decades-long intercontinental spread directly corresponding to its role as a major pork exporter. The identification of secondary transmission hubs in key European food processing centers, including France and Portugal, demonstrates that effective surveillance systems must integrate trade network data to predict and prevent cross-border transmission. Our phylogeographic analysis further revealed that the global spread of these pathogens is primarily driven by contaminated pork products, with pig viscera representing a particularly high-risk commodity. This direct association between pathogen transmission and specific trade flows emphasizes the critical need for enhanced border surveillance and harmonized international safety standards for meat products.

The identification of broad-host-range conjugative plasmids carrying up to 15 resistance genes substantially expands our understanding of antimicrobial resistance dissemination mechanisms. The co-occurrence of carbapenemase and colistin resistance genes in globally circulating strains represents a critical development in the evolution of pan-drug-resistance. The elevated resistance burden observed in human-derived isolates further indicates that clinical environments serve as evolutionary accelerators for resistance acquisition, underscoring the urgent need for enhanced antimicrobial stewardship and stringent infection control measures in healthcare settings.

Our findings underscore the need for a comprehensive global One Health surveillance framework that integrates harmonized international policies, systematic trade monitoring, and interoperable data-sharing platforms to effectively track and contain the worldwide dissemination of antimicrobial resistance and foodborne pathogens. The high prevalence of resistance to ampicillin and tetracyclines substantially undermines the effectiveness of standard empirical therapies. Notably, the potential establishment of $bla_{\text{CTX-M-55}}$ and *mcr-1* in *S.* Rissen populations threatens to generate pan-drug-resistant clones that simultaneously compromise last-resort antibiotics (*3*–*4*). These findings support a transition toward treatment strategies guided by rapid molecular diagnostics or whole-genome sequencing to ensure timely administration of effective antimicrobial agents. Implementation of integrated, real-time genomic surveillance platforms that connect human health, veterinary medicine, and food safety sectors would enable more proactive pathogen tracking and containment strategies.

This study has several limitations that warrant consideration. The absence of clinical outcome data limits our capacity to directly correlate genomic characteristics with public health consequences. Sampling biases inherent in global genome databases may result in underrepresentation of certain geographical regions or ecological niches. Furthermore, our transmission analysis relied predominantly on human and food isolates; the scarcity of comprehensive animal and environmental genomic data constrains our ability to fully reconstruct transmission pathways and identify all potential reservoirs. Future investigations should integrate clinical metadata, expand sampling efforts in underrepresented regions, and incorporate multi-sector genomic surveillance to comprehensively elucidate transmission dynamics and optimal intervention strategies.

Ethical statement: The Ethics Review Committee of the Pudong New Area Center for Disease Control and Prevention, Shanghai, reviewed and approved this study protocol. The same committee waived the requirement for informed consent.

Conflict of interest: No conflicts of interest.

Funding: Supported by the Research Project of Pudong New Area Health Commission (PW2023D-03), the Outstanding Leaders Training Program of Shanghai Pudong New Area Health Commission (PWRl2025-02), the Clinical Application and Resistance Evaluation of Antimicrobial Drugs by the National Health Commission (ECCUAEAR-2024-10), and the National Natural Science Foundation of China (82530102, 32370099).

doi: 10.46234/ccdcw2025.245

[#] Corresponding authors: Lifeng Pan, lfpan@pdcdc.sh.cn; Heng Li, hli@suda.edu.cn.

[1] Key Laboratory of Alkene-carbon Fibres-based Technology &

Application for Detection of Major Infectious Diseases, MOE Key Laboratory of Geriatric Diseases and Immunology, Cancer Institute, Suzhou Medical College, Soochow University, Suzhou City, Jiangsu Province, China; [2] Department of Microbiology, Pudong District Center for Disease Control and Prevention, Shanghai, China; [3] Department of Microbiology, School of Basic Medical Sciences, Suzhou Medical College, Soochow University, Suzhou City, Jiangsu Province, China; [4] Suzhou Center for Disease Control and Prevention, Suzhou City, Jiangsu Province, China; [5] Department of Infectious Disease, Shanghai Children's Medical Center, School of Medicine, Shanghai Jiao Tong University, Shanghai, China; [6] National Key Laboratory of Intelligent Tracking and Forecasting for Infectious Diseases, National Institute for Communicable Disease Control and Prevention, Chinese Center for Disease Control and Prevention, Beijing, China.

Submitted: October 18, 2025
Accepted: November 10, 2025
Issued: November 14, 2025

REFERENCES

1. Majowicz SE, Musto J, Scallan E, Angulo FJ, Kirk M, O'Brien SJ, et al. The global burden of nontyphoidal *Salmonella* gastroenteritis. Clin Infect Dis 2010;50(6):882 – 9. https://doi.org/10.1086/650733.
2. Kirk MD, Pires SM, Black RE, Caipo M, Crump JA, Devleesschauwer B, et al. World Health Organization estimates of the global and regional disease burden of 22 foodborne bacterial, protozoal, and viral diseases, 2010: a data synthesis. PLoS Med 2015;12(12):e1001921. https://doi.org/10.1371/journal.pmed.1001921.
3. Nang SC, Li J, Velkov T. The rise and spread of *mcr* plasmid-mediated polymyxin resistance. Crit Rev Microbiol 2019;45(2):131 – 61. https://doi.org/10.1080/1040841X.2018.1492902.
4. Crump JA, Sjölund-Karlsson M, Gordon MA, Parry CM. Epidemiology, clinical presentation, laboratory diagnosis, antimicrobial resistance, and antimicrobial management of invasive *Salmonella* infections. Clin Microbiol Rev 2015;28(4):901 – 37. https://doi.org/10.1128/cmr.00002-15.
5. Zhang K, Zhang Y, Wang ZY, Li Y, Xu HY, Jiao XN, et al. Characterization of CRISPR array in *Salmonella enterica* from asymptomatic people and patients. Int J Food Microbiol 2021;355:109338. http://dx.doi.org/10.1016/j.ijfoodmicro.2021.109338.
6. Trimoulinard A, Beral M, Henry I, Atiana L, Porphyre V, Tessier C, et al. Contamination by *Salmonella* spp. , Campylobacter spp. and Listeria spp. of most popular chicken- and pork-sausages sold in Reunion Island. Int J Food Microbiol 2017;250:68 – 74. https://doi.org/10.1016/j.ijfoodmicro.2017.03.017.
7. Xu HY, Zhang WB, Zhang K, Zhang Y, Wang ZY, Zhang W, et al. Characterization of *Salmonella* serotypes prevalent in asymptomatic people and patients. BMC Infect Dis 2021;21(1):632. https://doi.org/10.1186/s12879-021-06340-z.
8. Bankevich A, Nurk S, Antipov D, Gurevich AA, Dvorkin M, Kulikov AS, et al. SPAdes: a new genome assembly algorithm and its applications to single-cell sequencing. J Comput Biol 2012;19(5):455 – 77. https://doi.org/10.1089/cmb.2012.0021.
9. Seemann T. Prokka: rapid prokaryotic genome annotation. Bioinformatics 2014;30(14):2068 – 9. https://doi.org/10.1093/bioinformatics/btu153.
10. Nguyen LT, Schmidt HA, von Haeseler A, Minh BQ. IQ-TREE: a fast and effective stochastic algorithm for estimating maximum-likelihood phylogenies. Mol Biol Evol 2015;32(1):268 – 74. https://doi.org/10.1093/molbev/msu300.

SUPPLEMENTARY MATERIAL

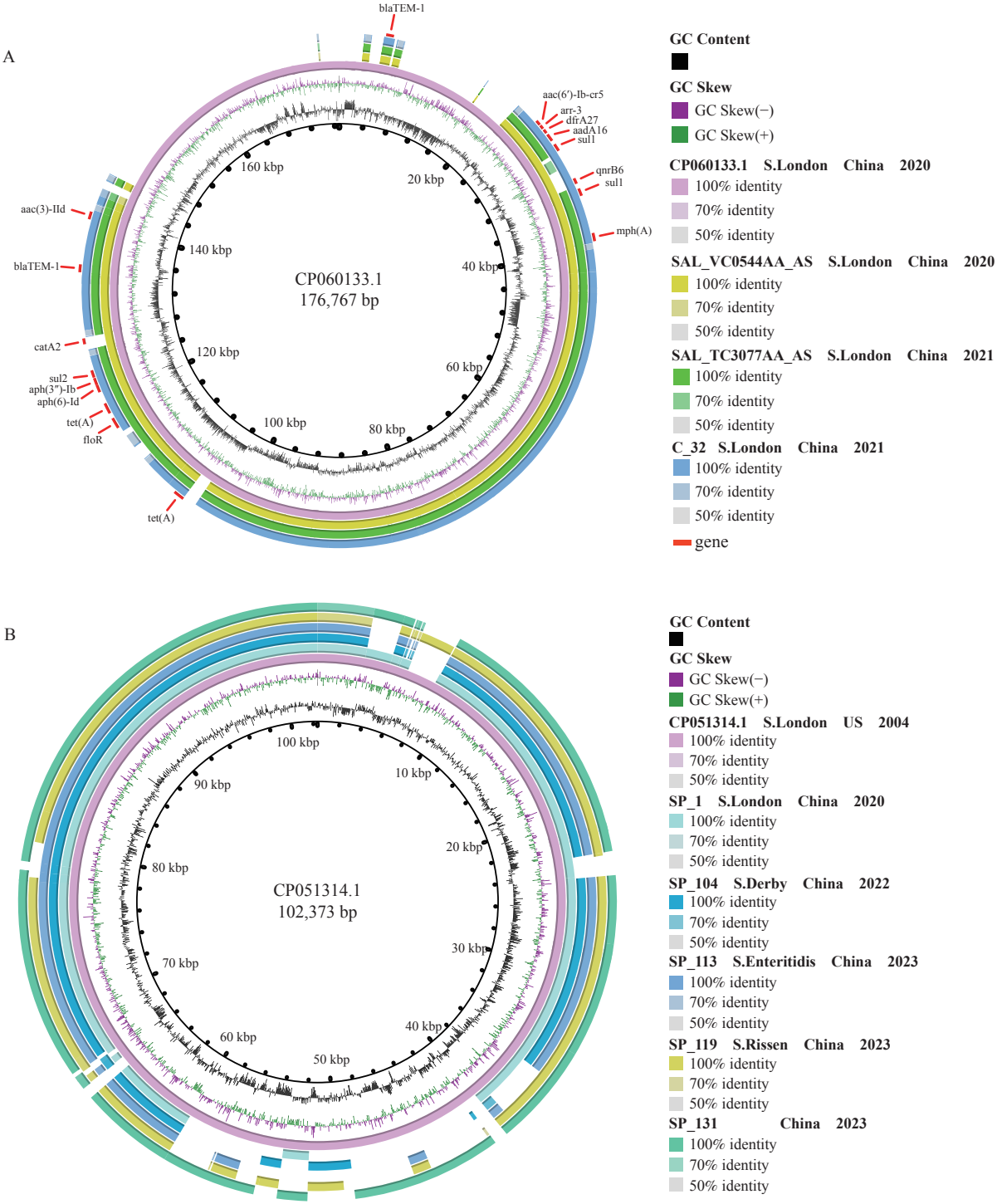

SUPPLEMENTARY FIGURE S1. Characterization of a Prominent Multidrug-Resistance Plasmid. (A) Circular map of the 176,767 bp MDR plasmid CP060133.1, displaying (from inner to outer rings): GC content, GC skew, reference sequence, and comparative alignment with related plasmids. (B) Circular map of the 102,373 bp MDR plasmid CP051314.1, displaying (from inner to outer rings): GC content, GC skew, reference sequence, and comparative alignment with related plasmids. (C) Mean number of resistance genes harbored by plasmid CP051314.1 per isolate, stratified by country of origin.
Note: For (A), Antimicrobial resistance genes are indicated by red arrows.
Abbreviation: MDR=multidrug-resistance.

Youth Editorial Board

Indexed by Science Citation Index Expanded (SCIE), Social Sciences Citation Index (SSCI), PubMed Central (PMC), Scopus, Chinese Scientific and Technical Papers and Citations, and Chinese Science Citation Database (CSCD)

The inauguration of *China CDC Weekly* is in part supported by Project for Enhancing International Impact of China STM Journals Category D (PIIJ2-D-04-(2018)) of China Association for Science and Technology (CAST).

CCDC weekly

Vol. 7 No. 46 Nov. 14, 2025

Responsible Authority
National Disease Control and Prevention Administration

Sponsor
Chinese Center for Disease Control and Prevention

Editing and Publishing
China CDC Weekly Editorial Office
No.155 Changbai Road, Changping District, Beijing, China
Tel: 86-10-63150501, 63150701
Email: weekly@chinacdc.cn

CSSN
ISSN 2096-7071 (Print)
ISSN 2096-3101 (Online)
CN 10-1629/R1